

2014

# Forensic analysis of plant based drugs of abuse by DART-MS

---

<https://hdl.handle.net/2144/15356>

*Downloaded from DSpace Repository, DSpace Institution's institutional repository*

BOSTON UNIVERSITY  
SCHOOL OF MEDICINE

Thesis

**FORENSIC ANALYSIS OF PLANT BASED DRUGS OF  
ABUSE BY DART-MS**

by

**CRYSTAL NICHOLE HART**

B.S., Southern Oregon University, 2012

Submitted in partial fulfillment of the  
requirements for the degree of  
Master of Science  
2014

© 2014 by  
CRYSTAL NICHOLE HART  
All Rights Reserved

Approved by

First Reader \_\_\_\_\_

Adam B. Hall, Ph.D.  
Instructor, Biomedical Forensic Sciences

Second Reader \_\_\_\_\_

Jason Shepard, Ph.D.  
Assistant Professor of Chemistry  
University at Albany, State University of New York

# **FORENSIC ANALYSIS OF PLANT BASED DRUGS OF ABUSE**

**BY DART-MS**

**CRYSTAL NICHOLE HART**

## **ABSTRACT**

Many plant species around the world are known to contain various psychoactive compounds. Due to their effects when consumed, many of these plants are used as a part of religious and ritualistic practices in many different cultures. As with any psychoactive compounds, these plants have the potential to be used in a recreational manner. In the United States, plant based drugs of abuse, such as marijuana, have become commonly abused substances. Although marijuana is currently regulated by the federal government, many of the plant materials containing potential drugs of abuse are not, and can be purchased legally from various online sources.

The goals of this research were to develop methods for the analysis of a wide variety of plant based drugs of abuse by Direct Analysis in Real Time – Mass Spectrometry (DART-MS) and to apply the methods in an effort to differentiate between multiple strains of a single seed species. DART is an ambient ionization technique that allows for rapid analysis of samples while eliminating the need for sample preparation considerations for many applications. Analytes of interest can be detected within the

complex plant matrix of ground up seeds, with no need for further extraction or isolation of the analytes.

For this study, fourteen different seed samples, including twelve different species, reported to have psychoactive effects on the user were obtained and analyzed. Physical examination was performed, in which average measurements were obtained to describe the length, width, thickness, and mass of each seed species, followed by analytical analysis by DART-MS.

The seeds were prepared for analysis by DART-MS by grinding to expose the middle of the seed containing the analytes of interest, and embedding the powder onto QuickStrip™ cards (IonSense, Inc.). To optimize the method for analysis, three different DART carrier gas temperatures (250°C, 300°C, and 350°C) were investigated for each seed sample by considering the signal to noise ratio, ion abundance, and presence of the analyte of interest at each source temperature using a single quadrupole mass spectrometer. The analytes detected were then subjected to MS<sup>n</sup> fragmentation in a quadrupole ion trap to confirm the identity of the analytes being detected. Fragmentation patterns were then compared to fragmentation patterns reported in the literature through methods such as chemical ionization, atmospheric pressure chemical ionization, and electrospray ionization.

Thirteen of the fourteen seed samples were known to contain compounds with psychoactive properties. One of the species contained no known hallucinogenic compounds, however it was reported to have psychoactive effects when ingested or

smoked. Protocols were developed for each sample and the identification of the analytes of interest was successful in twelve of the fourteen samples.

DART-MS is a powerful technique for the detection and identification of a variety of plant based drugs of abuse, including tetrahydrocannabinol, lysergic acid amide, and numerous others. The ability to rapidly analyze a large number of samples makes DART-MS a technique with great potential in forensic laboratory settings, such as forensic drug analysis, where case backlog is often an area of concern. The majority of the samples explored in this study are not considered common substances of abuse. However, as their abuse is becoming more common, the high throughput nature of the analytical methods and techniques discussed will become increasingly important.

## TABLE OF CONTENTS

Title Page .....	i
Copyright Page.....	ii
Reader’s Approval Page .....	iii
ABSTRACT.....	iv
LIST OF TABLES.....	xi
LIST OF FIGURES .....	xii
LIST OF ABBREVIATIONS.....	xx
1. Introduction.....	1
<i>1.1 Prevalence of Drug Use in the United States</i> .....	1
<i>1.2 Significance of Drugs of Abuse in Forensic Science</i> .....	2
<i>1.3 Classes of Drugs of Abuse</i> .....	4
<i>1.4 Goals of Thesis Research</i> .....	5
<i>1.5 Chemical Components Commonly Associated with Plants</i> .....	6
<i>1.5 Plant Based Drugs of Abuse</i> .....	7
1.5.1 <i>Anadenanthera colubrina (Cebil)</i> .....	8
1.5.1.1. Background and Traditional Uses.....	8
1.5.1.2. Reported Effects and Active Components .....	8
1.5.2 <i>Voacanga africana (Voacanga)</i> .....	10



1.5.2.1. Background and Traditional Uses.....	10
1.5.2.2. Reported Effects and Active Components .....	10
1.5.3 <i>Rivea corymbosa</i> (Ololiuqui) .....	11
1.5.3.1. Background and Traditional Uses.....	11
1.5.3.2. Reported Effects and Active Components .....	12
1.5.4 <i>Ipomoea violacea</i> (Morning Glory) .....	13
1.5.4.1. Background and Traditional Uses.....	13
1.5.4.2. Reported Effects and Active Components .....	13
1.5.5 <i>Argyreia nervosa</i> (Hawaiian Baby Woodrose).....	14
1.5.5.1. Background and Traditional Uses.....	14
1.5.5.2. Reported Effects and Active Components .....	14
1.5.6 <i>Entada rheedii</i> (African Dream Herb) .....	15
1.5.6.1. Background and Traditional Uses.....	15
1.5.6.2. Reported Effects and Active Components .....	16
1.5.7 <i>Peganum harmala</i> (Syrian Rue or Harmel).....	16
1.5.7.1. Background and Traditional Uses.....	16
1.5.7.2. Reported Effects and Active Components .....	17
1.5.8 <i>Hyoscyamus niger</i> (Black Henbane) .....	17
1.5.8.1. Background and Traditional Uses.....	17

1.5.8.2. Reported Effects and Active Components .....	18
1.5.9 Ephedra sinica (Ma-Huang).....	19
1.5.9.1. Background and Traditional Uses.....	19
1.5.9.2. Reported Effects and Active Components .....	19
1.5.10 Mucuan pruriens (Cowage) .....	20
1.5.10.1. Background and Traditional Uses.....	20
1.5.10.2. Reported Effects and Active Components .....	21
1.5.11 Argemone mexicana (Mexican Poppy) .....	21
1.5.11.1. Background and Traditional Uses.....	21
1.5.11.2. Reported Effects and Active Components .....	22
1.5.12 Celastrus paniculatus (Intellect Tree) .....	23
1.5.12.1. Background and Traditional Uses.....	23
1.5.12.2. Reported Effects and Active Components .....	23
1.6 Direct Analysis in Real Time – Mass Spectrometry (DART-MS) .....	24
2. Materials and Methods.....	28
2.1 Materials.....	28
2.2 Physical Characterization of Seed Samples .....	29
2.3 DART-MS Method Development for Plant Based Drugs of Abuse.....	30
2.3.1 Sample Preparation.....	30

2.3.2 DART Source Temperature Profile .....	30
2.3.3 Fragmentation .....	32
2.4 Identification .....	33
3. Results and Discussion .....	34
3.1 Physical Characterization .....	34
3.2 DART Source Temperature Profiles .....	40
3.3 MS <sup>2</sup> Fragmentation Data .....	65
4. Conclusion .....	92
5. Future Directions .....	93
LIST OF ABBREVIATED JOURNAL TITLES .....	95
REFERENCES .....	98
CURRICULUM VITAE .....	107

## **LIST OF TABLES**

Table 1. Quadrupole mass spectrometer and DART parameters for the DART source temperature profile.....	31
Table 2. Ion trap MS Parameters used throughout the fragmentation experiments.....	33
Table 3. Summary of physical measurements of each seed.....	39
Table 4. Summary of data collection and conclusions for each seed type. ....	91

## LIST OF FIGURES

Figure 1. Chemical Structure of Bufotenine.	9
Figure 2. Structures of other tryptamine compounds reportedly found in the seeds of the cebil plant.	10
Figure 3. Structure of Voacamine, the main compound responsible for psychoactive effects of Voacanga Africana seeds.	11
Figure 4. Structures of additional psychoactive compounds reported to be found in the seeds of the Voacanga Africana plant.	11
Figure 5. Ergot alkaloids: ergine, ergometrine, and ergosinine commonly found in lolium seeds.	13
Figure 6. Additional ergot alkaloids found in seeds of Hawaiian baby woodrose seeds.	15
Figure 7. Structures of psychoactive compounds reported to be in Syrian rue seeds.	17
Figure 8. Psychoactive compounds found in henbane seeds, atropine and scopolamine.	19
Figure 9. Structures of compounds reported to be present in Ephedra sinica plant material.	20
Figure 10. Structures of compounds of interest reported to be present in cowage seeds.	21
Figure 11. Structures of compounds reported to be found in the seeds and seed oil of the Mexican poppy plant.	23
Figure 12. Structures of possible alkaloids found in Intellect tree seeds, although no scientific evidence was found to support the existence of these compounds in the seeds.	24
Figure 13. DART schematic of gas flow through the source to create metastable species. Photo provided courtesy of IonSense, Inc.	25

## **LIST OF FIGURES, CONTINUED**

- Figure 14. DART Quick Strip™ card in metal holder. Image courtesy of Drew Horsley. 27
- Figure 15. Linear Rail Enclosure attached between MS inlet (left of image) and DART ionization source (right of image) with Quick Strip™ card in holder. Image courtesy of Drew Horsley. 27
- Figure 16. Diagram of Quickstrip used to perform temperature profiles for each seed. 32
- Figure 17. Images of seeds analyzed. A) Cebil seeds, B) Voacanga seeds, C) Morning Glory seeds, and D) Syrian Rue seeds 35
- Figure 18. Images of seeds analyzed. A) Henbane seeds, B) Ololiuqui seeds, and C) *Ephedra sinica* seeds. 36
- Figure 19. Images of seeds analyzed. A) African Dream Herb seed, B) Cowage seeds, C) Mexican Poppy seeds, D) Intellect Tree seeds. 37
- Figure 20. Three different strains of Hawaiian Baby Woodrose seeds. A) Ghana Strain, B) Hawaiian Strain, C) Indian Strain. 38
- Figure 21. A) Total Ion Chromogram of crushed cebil seeds at 250°C, 300°C, and 350°C. The split in the peaks represents two different spaces on the QuickStrip™ being passed in front of the DART source. Mass spectral data collected during DART source temperature profiles for the analysis of crushed cebil seeds at B) 250°C, C) 300°C, and D) 350°C. 42
- Figure 22. Mass spectral data collected during DART source temperature profiles for the analysis of crushed voacanga seeds at A) 250°C, B) 300°C, and C) 350°C. 44

## **LIST OF FIGURES, CONTINUED**

- Figure 23. Mass spectral data collected during DART source temperature profiles for the analysis of crushed ololiuqui seeds at A) 250°C, B) 300°C, and C) 350°C. 46
- Figure 24. Mass spectral data collected during DART source temperature profiles for the analysis of crushed morning glory seeds at A) 250°C, B) 300°C, and C) 350°C. 48
- Figure 25. Mass spectral data collected during DART source temperature profiles for the analysis of crushed Syrian rue seeds at A) 250°C, B) 300°C, and C) 350°C. The MS data inserted in the top right corner is zoomed in on the region from 210 to 220 $m/z$  to show the ions of interest. 49
- Figure 26. Mass spectral data collected during DART source temperature profiles for the analysis of crushed African Dream Herb seeds at A) 250°C, B) 300°C, and C) 350°C. 51
- Figure 27. Mass spectral data collected during DART source temperature profiles for the analysis of crushed Cowage seeds at A) 250°C, B) 300°C, and C) 350°C. 53
- Figure 28. Mass spectral data collected during DART source temperature profiles for the analysis of crushed Henbane seeds at A) 250°C, B) 300°C, and C) 350°C. 54
- Figure 29. Mass spectral data collected during DART source temperature profiles for the analysis of crushed Hawaiian Baby Woodrose Hawaiian strain seeds at A) 250°C, B) 300°C, and C) 350°C. 56
- Figure 30. Mass spectral data collected during DART source temperature profiles for the analysis of crushed Hawaiian Baby Woodrose Indian Strain seeds at A) 250°C, B) 300°C, and C) 350°C. 57

## **LIST OF FIGURES, CONTINUED**

- Figure 31. Mass spectral data collected during DART source temperature profiles for the analysis of crushed Hawaiian Baby Woodrose Ghana Strain seeds at A) 250°C, B) 300°C, and C) 350°C. 59
- Figure 32. Mass Spectral data collected with a DART source temperature 350°C for Hawaiian Baby Woodrose A) Hawaiian Strain, B) Indian Strain, and C) Ghana Strain. 60
- Figure 33. Mass spectral data collected during DART source temperature profiles for the analysis of crushed Intellect Tree seeds at A) 250°C, B) 300°C, and C) 350°C. 61
- Figure 34. Mass spectral data collected during DART source temperature profiles for the analysis of crushed Ephedra Sinica seeds at A) 250°C, B) 300°C, and C) 350°C. 63
- Figure 35. Mass spectral data collected during DART source temperature profiles for the analysis of crushed Mexican Poppy seeds at A) 250°C, B) 300°C, and C) 350°C. 64
- Figure 36. MS<sup>2</sup> fragmentation data of  $m/z$  205 for crushed cebil seeds with a normalized collision energy of 25%. 65
- Figure 37. Suggested fragmentation pattern of bufotenine by electrospray ionization – ion trap mass spectrometry as suggested by McClean et al.<sup>23</sup> 66
- Figure 38. MS<sup>2</sup> fragmentation data of  $m/z$  337 for crushed *Voacanga africana* seeds with a normalized collision energy of 32%. 67
- Figure 39. MS<sup>2</sup> fragmentation data of  $m/z$  353 for crushed *Voacanga africana* seeds with a normalized collision energy of 30%. 68
- Figure 40. MS<sup>2</sup> fragmentation data of  $m/z$  369 for crushed *Voacanga africana* seeds with a normalized collision energy of 30%. 68



## LIST OF FIGURES, CONTINUED

- Figure 41. MS<sup>2</sup> fragmentation data of *m/z* 268 for crushed ololiuqui seeds with a normalized collision energy 38%. 69
- Figure 42. Suggested fragmentation of ergine as reported by Lehner et al.<sup>70</sup>. 69
- Figure 43. MS<sup>2</sup> fragmentation data of *m/z* 268 for crushed morning glory seeds with a normalized collision energy of 30%. 70
- Figure 44. MS<sup>2</sup> fragmentation data of *m/z* 326 for crushed morning glory seeds with a normalized collision energy of 32%. 71
- Figure 45. Suggested fragmentation pattern for ergometrine (*m/z* 326) to form fragments at *m/z* 223 and 208. 71
- Figure 46. MS<sup>2</sup> fragmentation data of *m/z* 213 for crushed Syrian rue seeds with normalized collision energy of A) 55% and B) 60%. 72
- Figure 47. Suggested fragmentation of harmine. The loss of the methyl group to form a hydroxyl substituent would result in a fragment at *m/z* 198, likely associated with the formation of harmol through demethylation. 72
- Figure 48. MS<sup>2</sup> fragmentation data of *m/z* peak at 215 for crushed Syrian rue seeds with normalized collision energy of A) 55% and B) 60%. 74
- Figure 49. Suggested fragmentation of harmaline. The loss of the methyl group to form a ketone would result in a fragment at *m/z* 200. Alternatively, rearrangement resulting in the loss of a CH<sub>3</sub>CN would result in a compound responsible for *m/z* 174. Both fragments have been shown in previous studies to be related to the metabolism of harmaline. 74

## **LIST OF FIGURES, CONTINUED**

- Figure 50. MS<sup>2</sup> fragmentation data of *m/z* 116 for crushed African Dream herb seeds with normalized collision energy of A) 45% and B) 50%. 76
- Figure 51. Suggested fragmentation pattern of proline (*m/z* 116) to form fragments at *m/z* 70 and 46. 76
- Figure 52. MS<sup>2</sup> fragmentation data of *m/z* 142 for crushed African Dream herb seeds with normalized collision energy of 50%. 77
- Figure 53. MS<sup>2</sup> fragmentation data of *m/z* 116 for crushed cowage seeds with normalized collision energy of 45%. 78
- Figure 54. MS<sup>2</sup> fragmentation data of *m/z* 198 for crushed cowage seeds with normalized collision energy of 55%. 79
- Figure 55. Suggested fragmentation of L-dopa, resulting in [M+H]<sup>+</sup> fragments of *m/z* 181 and 152. 79
- Figure 56. MS<sup>2</sup> fragmentation data of *m/z* 298 for crushed cowage seeds with normalized collision energy of 50%. 80
- Figure 57. MS<sup>2</sup> fragmentation data of *m/z* 290 for crushed henbane seeds with normalized collision energy of 57%. 81
- Figure 58. Suggested fragmentation of atropine to form fragments at *m/z* 124 and 166. Only the fragment at *m/z* 124 is observed in this study. 81
- Figure 59. MS<sup>2</sup> fragmentation data of *m/z* 308 for crushed henbane seeds with normalized collision energy of 57%. 82

## **LIST OF FIGURES, CONTINUED**

- Figure 60. MS<sup>2</sup> fragmentation data of  $m/z$  128 for crushed ephedra seeds with normalized collision energy of 57%. 83
- Figure 61. MS<sup>2</sup> fragmentation data of  $m/z$  332 for crushed ephedra seeds with normalized collision energy of 55%. 83
- Figure 62. MS<sup>2</sup> fragmentation data of  $m/z$  peak at 334 for crushed Mexican poppy seeds with normalized collision energy of 50%. 84
- Figure 63. Suggested fragmentation of dihydrosanguinarine to form a fragment with  $m/z$  319 through the loss of a methyl group. 85
- Figure 64. MS<sup>2</sup> fragmentation data of  $m/z$  319 for crushed Mexican poppy seeds with normalized collision energy of 55%. 85
- Figure 65. MS<sup>2</sup> fragmentation data of  $m/z$  534 for crushed Intellect tree seeds with normalized collision energy of 50%. 86
- Figure 66. MS<sup>2</sup> fragmentation data of  $m/z$  524 for crushed Intellect tree seeds with normalized collision energy of 55%. 86
- Figure 67. MS<sup>2</sup> fragmentation data of  $m/z$  268 for crushed Hawaiian Baby Woodrose (Hawaiian strain) seeds with normalized collision energy of 50%. 87
- Figure 68. MS<sup>2</sup> fragmentation data of  $m/z$  326 for crushed Hawaiian Baby Woodrose (Hawaiian strain) seeds with normalized collision energy of 55%. 88
- Figure 69. MS<sup>2</sup> fragmentation data of  $m/z$  268 for crushed Hawaiian Baby Woodrose (Indian strain) seeds with normalized collision energy of 53%. 89

### **LIST OF FIGURES, CONTINUED**

- Figure 70. MS<sup>2</sup> fragmentation data of  $m/z$  326 for crushed Hawaiian Baby Woodrose (Indian strain) seeds with normalized collision energy of 55%. 89
- Figure 71. MS<sup>2</sup> fragmentation data of  $m/z$  268 for crushed Hawaiian Baby Woodrose (Ghana strain) seeds with normalized collision energy of 55%. 90

## **LIST OF ABBREVIATIONS**

% w/w	Percent weight per weight
5-MeO-MPI	5-methoxy- <i>N</i> -methyl-( $\alpha$ - <i>N</i> -trimethylene)tryptamine
CE	Collision Energy
DART	Direct Analysis in Real Time
DMT	<i>N,N</i> -dimethyltryptamine
FBI	Federal Bureau of Investigation
FDA	Food and Drug Administration
GC-MS	Gas chromatography-Mass spectrometry
L-dopa	L-3,4-dihydroxyphenylalanine
LRE	Linear rail enclosure
LSA	Lysergic acid amide
LSD	Lysergic acid diethylamide
<i>m/z</i>	Mass to charge ratio
MS	Mass Spectrometry
MS <sup>n</sup>	Tandem Mass Spectrometry
NFLIS	National Forensic Laboratory Information System
NMT	<i>N</i> -methyltryptamine
NSDUH	National Survey on Drug Use and Health
SAMHSA	Substance Abuse and Mental Health Services Administration

THC	Tetrahydrocannabinol
TIC	Total Ion Chromogram
TOF	Time of Flight
U.S.	United States
UCR	Uniform Crime Report

## **1. Introduction**

Psychoactive substances have long been an important aspect of many cultures, both spiritually and religiously. Many of those substances eventually make their way into the hands of individuals who treat them differently than their traditional use. In the United States (U.S.) today, many teenagers and young adults turn to illicit drugs to fulfill some part of their life. Many of these drugs include substances that were originally used in other parts of the world for very different reasons, such as religious or ceremonial purposes, including communicating with the supernatural or deceased individuals<sup>1</sup>. Many individuals use drugs for reasons such as peer pressures, to escape from reality, or as a form of entertainment. Since the 1960's drug use in the U.S. has become an issue of concern and continues to increase in popularity<sup>2</sup>.

### ***1.1 Prevalence of Drug Use in the United States***

The National Survey on Drug Use and Health (NSDUH) is administered annually by the Substance Abuse and Mental Health Services Administration (SAMHSA). NSDUH/SAMHSA collects data on drug use through annual interviews, with approximately 67,500 individuals aged 12 and older. In 2012, it was estimated that about 9.2% of the population (23.9 million Americans) were current drug users, meaning that they admitted to consuming at least one illicit substance within the month prior to the survey<sup>3</sup>. Illicit drugs included any psychoactive substance used for non-medical purposes, such as marijuana, hashish, cocaine (including crack cocaine), heroin, hallucinogens, inhalants, and prescription drugs<sup>3</sup>. Hallucinogens, which are found naturally in plants,

were reported by the National Forensic Laboratory Information System (NFLIS) to represent 4% of all reported drug cases in 2012<sup>4</sup>.

Drug use is a common feature when analyzing crime statistics in the U.S. A substantial number of crimes are committed while under the influence of drugs or to enable a drug habit. According to a special report by the Bureau of Justice in 2006, about one third of state and one quarter of federal prisoners in 2004 had committed their crimes while under the influence of drugs; these numbers have essentially remained unchanged since 1997<sup>5</sup>. Additionally, approximately 21% of state prisoners and 55% of federal prisoners were incarcerated due to violations of drug laws, such as drug possession, distribution, or trafficking<sup>5</sup>.

### ***1.2 Significance of Drugs of Abuse in Forensic Science***

Testing for drugs of abuse is a significant area in forensic science. The Federal Bureau of Investigation (FBI) Uniform Crime Report (UCR) estimated that in the U.S., approximately 1,841,200 arrests for drug violations occurred in 2007<sup>6</sup>. Once an arrest is made, it is the responsibility of investigators to prove that the drug violation is accurate and just. One important aspect of proof is to demonstrate that the offender was in possession of a controlled substance. Although field tests are oftentimes performed before the arrest is made, such tests are considered preliminary, and confirmatory testing in a forensic laboratory must be conducted to verify the presence of a controlled substance.



According to a survey of Crime Laboratory Drug Chemistry and Controlled Substances sections conducted by NFLIS in 2013, there were 163,806 drug cases backlogged during 2012<sup>7</sup>. A backlogged case was defined as one that had not been analyzed for 30 days or more since the evidence was submitted to the lab. About 90% of all state and local forensic laboratories in the U.S. participated in the survey; federal forensic laboratories were not included. Additionally, about one third of the labs reported that they had seen an increase in total drug cases compared to the previous year. While a number of factors contributed to the increased backlog, including a decrease in the number of analysts and an increase in the total number of cases, the survey reported that 61% of laboratories cited sudden increases in emerging drugs as a primary reason for the increase. Emerging drugs are defined as any substance, controlled or uncontrolled, that had first been detected in the laboratories within the last five years. Additionally, emerging drugs oftentimes require the development of new testing methods, which was reported by about 14% of laboratories to also be contributing to the backlog<sup>7</sup>. Many of these emerging drugs are uncontrolled substances, not subject to any legal regulations or consequences. Uncontrolled substances were identified by about 86% of laboratories<sup>7</sup>. Although there are no criminal consequences associated with the possession of an uncontrolled substance; testing of such compounds takes up time and resources. With emerging drugs continually presenting themselves in the community, forensic labs need to obtain standards and validate new procedures with limited resources to devote to such challenges. Obtaining standards and validating procedures were reported as the most important issues regarding the testing of emerging drugs by 92% and 66% of state and

local labs, respectively<sup>7</sup>. As seen in the NFLIS data, drug use is prevalent in the U.S., and new compounds and substances continue to be introduced into the community.

### ***1.3 Classes of Drugs of Abuse***

Drugs of abuse can be divided into three classifications: synthetic, semi-synthetic, and natural. Synthetic drugs are those that are manufactured in a laboratory and are synthesized to mimic the effects of other drugs. Examples of synthetic drugs are synthetic cannabinoids such as K2, Spice, and “bath salts”<sup>8,9</sup>. Synthetic cannabinoids and other synthetic drugs such as bath salts/cathinones became popular, in part, because they were seen as a legal alternative to marijuana and other drugs while still providing the same high. Often, these compounds are labeled and sold as “not for human consumption” so that they can avoid the regulations set forth by the Food and Drug Administration (FDA)<sup>5</sup>. As regulations expand to include new variations of synthetic drugs, the manufacturers of these compounds make slight chemical changes, resulting in the creation of analogs and by inclusion of various functional groups, allowing the new drugs to stay just out of reach of the laws restricting them. The Controlled Substance Analogue Enforcement Act of 1986 originally sought to deal with this issue by defining a controlled substance analogue as a compound with a chemical structure that is “substantially similar to the chemical structure of a controlled substance”<sup>10</sup>. In 2012, Congress passed the Synthetic Drug Abuse Prevention Act of 2012, which added synthetic drugs to schedule I of the Controlled Substances Act<sup>11</sup>. However, the efforts by these manufacturers exploit the ambiguity of what can be considered an analog and represents a major concern of

enforcement agencies to overcome the legal challenges to demonstrate illegality.

Semi-synthetic drugs contain compounds that are found in nature but are then chemically processed to make them more potent, increase the ability for the compounds to be absorbed into the body, or improve the way in which the compound is metabolized. The two most common examples are heroin and cocaine. Both drugs are synthesized from naturally occurring plant material. Heroin is derived from opium in *Papaver somniferum*, which is a member of the poppy family and cocaine is derived from the leaves of the South American *Erythroxylon coca* plant<sup>12</sup>.

Natural drugs include compounds that occur in nature and are pharmacologically active in their natural state. Most natural drugs can be classified as hallucinogens. Common examples of natural drugs are marijuana, salvia, psilocin/psilocybin, dimethyltryptamine (DMT) and salvia.

#### ***1.4 Goals of Thesis Research***

The two main goals of this research were to develop analytical methods for the analysis and identification of potential plant based drugs of abuse using Direct Analysis in Real Time – Mass Spectrometry (DART-MS) and to determine whether three types of seeds from different strains of the same plant species could be differentiated from one another. The ability to detect the drug analytes of interest within the plant based matrix was investigated while minimizing the sample preparation and time required for the complete analysis of a sample. Although methods were developed for each of the samples, identification was only possible within twelve of the plant matrices.

### ***1.5 Chemical Components Commonly Associated with Plants***

Plant material represents an extremely complex matrix. Plants can contain thousands of diverse compounds, including many different alkaloids, amino acids, amines, proteins, glycosides, phenolics, volatile oils, and polysaccharides<sup>13</sup>. Although different species of plants contain unique chemical components, many compounds are common among all plants. Many of these compounds are essential for plant growth, reproduction, and protection. Although the relative concentration of each component may vary from seed to seed, all seeds need some combination of these compounds to function. The main function of plant seeds is reproduction<sup>14</sup>. In addition, seeds are able to store fats, oils, waxes, sterols, glycolipids, phospholipids, and fat-soluble vitamins which provide the plant with energy, aid in the structural composition of the cell membranes, and participate in cell signaling<sup>13</sup>. Each plant species may differ in the exact chemical composition found in the seeds, however, the chemical composition may also be influenced by the season, parent plant, temperature, soil nutrients, and water availability<sup>13</sup>.

Although slight differences may be detectable in the exact composition of common compounds that could be useful for larger concerns such as species differentiation, the focus of this study was on development of a rapid screening method for detection of emerging, natural psychoactive compounds and the detection of potential drugs of abuse present within the seeds. The analytes of interest for each species is discussed in the following section.

### ***1.5 Plant Based Drugs of Abuse***

Many plants contain potential drugs of abuse. As previously mentioned, marijuana is the most commonly used drug in the U.S. However, many other plants containing psychoactive compounds have not yet been widely abused or regulated. In recent years, *Salvia divinorum*, or salvia, has gained popularity in the U.S.<sup>15</sup>. The plant grows naturally in the tropical rainforests of Mexico, and the Mazatec Indians of Oaxaca, have used the leaves as a part of various rituals for their hallucinogenic properties<sup>16,17</sup>. In the U.S., salvia is not currently regulated under the Controlled Substances Act. However, as of 2010, many states had passed laws controlling the plant<sup>18</sup>.

The internet has become an area of significant interest when it comes to information about psychoactive plants and drug use. Many websites are available to the public that allow users to ask questions and discuss individual experiences with the substances. Many of the websites also discuss where and how to obtain the plant materials. In 2008, Hoover et al. performed an internet based study on salvia and found that half of the websites investigated were either selling *S. divinorum* or were linked to other sites that were selling the plant. The study also found that about 78% of the sites were advocating for the use of the drug, often with false information about its use<sup>19</sup>, which can have detrimental effects on the public as the websites are often used as a guide for new users. As the availability and effectiveness of other plants containing psychoactive compounds become better known in the U.S., it is likely that the pattern seen with the use of salvia will be seen with other plants as well.

### *1.5.1 Anadenanthera colubrina (Cebil)*

#### 1.5.1.1. Background and Traditional Uses

*Anadenanthera colubrina*, also known as cebil, is a tree that grows in South American countries such as Brazil, Argentina, Bolivia, Brazil, Paraguay, and Peru. It is very closely related to the *Anadenanthera peregrina* tree, which is referred to as Yopo<sup>20</sup>. Cebil trees produce flat seed pods that appear gray to black in color which break open to expose three to ten reddish-brown flat seeds.

Many different cultures have reported using the plant seeds in various ways to fulfill their needs<sup>21,1</sup>. Traditionally, cebil and yopo seeds are used to produce a snuff which can then be smoked or inhaled through the nose. The seeds have also been used as enemas in many cases<sup>21,1</sup>. The use of an enema in this case was not only for medicinal or therapeutic reasons, but as a way to alter the users state of mind and provide a connection with the supernatural<sup>1</sup>. One group of shamans, the Mataco, prefer to smoke the roasted seeds, believing that smoking the seeds allows them to experience other realities<sup>22</sup>.

#### 1.5.1.2. Reported Effects and Active Components

The seeds of this plant have been reported for use to induce rapid intoxication and instantaneous visual and auditory sensations that are associated with direct communication with the spirit animals, deceased individuals, or other supernatural sensations<sup>1</sup>. The experience is generally very short, about 20-30 minutes<sup>22</sup>, but it can affect different individuals in vastly different ways, including the intensity and

psychoactive effects experienced. Today, cebil is still used as part of shamanistic rituals, however it is also often used recreationally in South American cultures<sup>1</sup>.

The hallucinogenic properties of cebil seeds have been reported to be due to a number of compounds. The main psychoactive ingredient is bufotenine (5-hydroxy-*N,N*-dimethyltryptamine), and it has been reported that the cebil seeds may contain up to 4% bufotenine by weight<sup>16</sup>. Bufotenine, shown in Figure 1, is a tryptamine alkaloid that is found in the skin of some toads<sup>23</sup>, mushrooms<sup>24</sup>, plants<sup>25</sup>, and mammals<sup>26</sup>. It is a hallucinogenic serotonin analog and has been widely studied by many researchers. Although some studies have shown that the seeds contain only bufotenine, there are studies showing that other derivatives such as *N,N*-dimethyltryptamine (DMT), *N*-methyltryptamine (NMT), and 5-methoxy-*N*-methyl-( $\alpha$ ,*N*-trimethylene)tryptamine (5-MeO-MPMI) may be present<sup>16,1</sup>. The structures are shown in Figure 2.

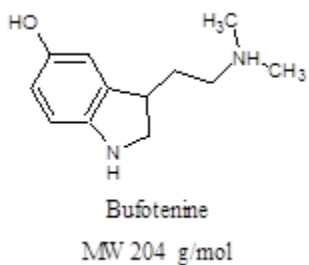


**Figure 1. Chemical Structure of Bufotenine.**

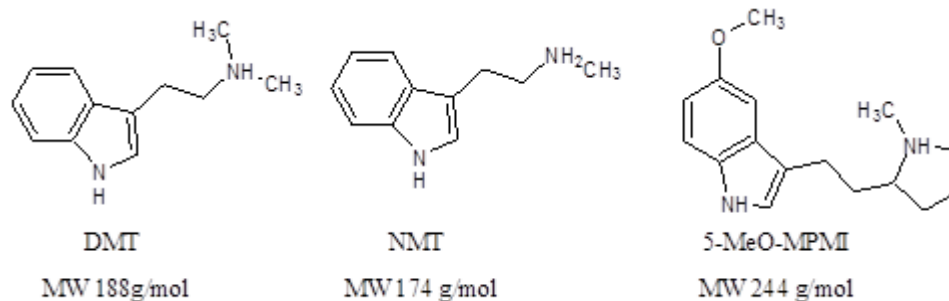


**Figure 2. Structures of other tryptamine compounds reportedly found in the seeds of the cebil plant.**

### 1.5.2 *Voacanga africana* (*Voacanga*)

#### 1.5.2.1. Background and Traditional Uses

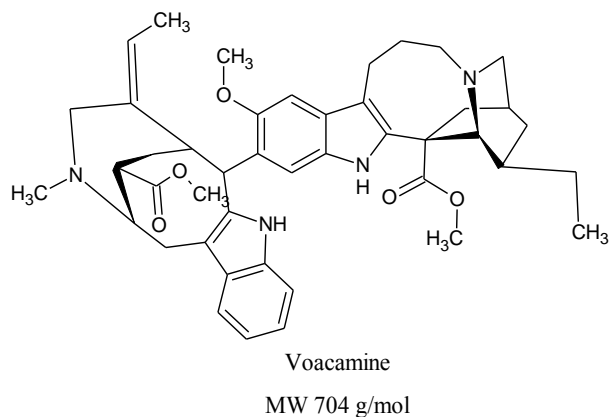
*Voacanga africana* is a tropical tree indigenous to Africa. It has been reported that this tree and many other varieties of the *Voacanga* genus have been used as hallucinogens, aphrodisiacs, and medicines<sup>16</sup>. In some parts of Africa, the bark of the plant is used to aid in hunting by providing a stimulating experience for the hunters<sup>22</sup>. In other places across Africa, reported reasons for use range from its potent aphrodisiac effects to a substitute for marijuana<sup>22</sup>. The *Voacanga* plant is known to play an important role when it comes to the ritualistic practices in African cultures, but not many details are known about the specific uses of the plant<sup>22</sup>.

#### 1.5.2.2. Reported Effects and Active Components

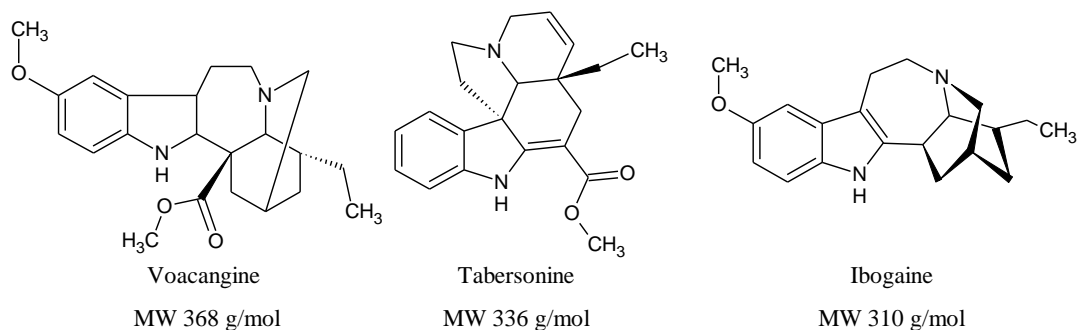
The bark and seeds of the *Voacanga* plant contain up to 10% indole alkaloids, which are linked to enhancing visionary experiences. The main active ingredient in the seeds and the bark is voacamine, shown in Figure 3. The seeds also contain ibogaine, voacamine-*N*-oxide, voacangine, and significant amounts of tabersonine as shown in



Figure 4<sup>27,28</sup>. Tabersonine is readily converted to vincamine derivatives which are shown to improve performance in animals with cognitive dysfunctions<sup>29,30</sup>.



**Figure 3. Structure of Voacamine, the main compound responsible for psychoactive effects of Voacanga Africana seeds.**



**Figure 4. Structures of additional psychoactive compounds reported to be found in the seeds of the Voacanga Africana plant.**

### 1.5.3 *Rivea corymbosa* (*Ololiuqui*)

#### 1.5.3.1. Background and Traditional Uses

The *Rivea corymbosa* vine is a part of the morning glory family known as Convolvulaceae<sup>22</sup>. Many plant species are very closely related to ololiuqui, but only a few of them have been studied. The plant is believed to have originated in tropical

regions of Mexico, but is now common in Cuba, the West Indies, the Gulf Coast of North America, the Philippines, and Central America<sup>22</sup>.

Although the use of the ololiuqui plant for ritualistic and medical purposes can be traced back to the 1500's, it was not until 1940 that the botanical identity of the plant was clarified<sup>16,22</sup>. Up until that point, it was believed that the ololiuqui plant was related to the poppy species due to its narcotic properties<sup>22</sup>. Today, the seeds of the plant are present in many cultures for purposes of divination and witchcraft<sup>16</sup>.

#### 1.5.3.2. Reported Effects and Active Components

The ololiuqui seeds have been reported to contain various ergot alkaloids, including, but not limited to lysergic acid amide (LSA), or ergine, and lysergic acid hydroxyethylamide<sup>16</sup>. Ergot alkaloids are compounds that are similar in structure and activity to the hallucinogenic lysergic acid diethylamide, or LSD. LSD was discovered when Albert Hofmann, the chemist synthesizing the compound, accidentally ingested it and experienced a distortion of reality, in which he saw intense colors, unusual images, and a disconnect with time and dimension<sup>31</sup>.

Ergot alkaloids all have the same moiety and vary in the substituents. The three main compounds known to be present in ololiuqui seeds are ergine, ergometrine, and ergosinine and are shown in Figure 5. Although these compounds are common in morning glory species, there are many more ergot alkaloids that could be present<sup>16</sup>.

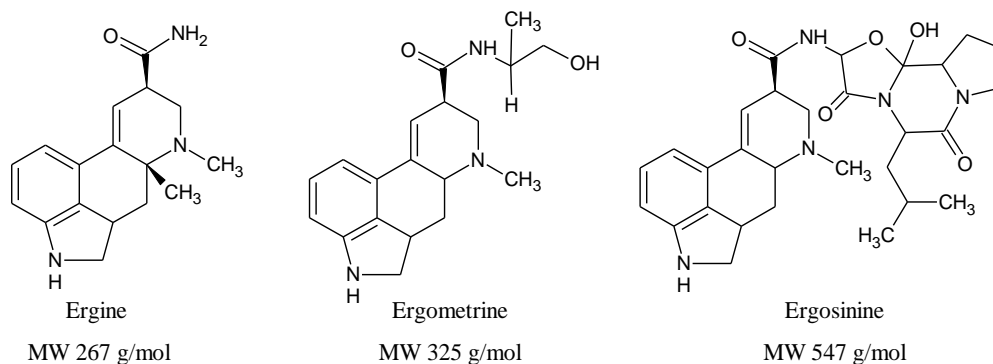


**Figure 5. Ergot alkaloids: ergine, ergometrine, and ergosinine commonly found in ololiuqui seeds.**

#### 1.5.4 *Ipomoea violacea* (Morning Glory)

##### 1.5.4.1. Background and Traditional Uses

The morning glory plant originated in the tropics of Mexico, but is now common around the world<sup>22</sup>. Although it has not been scientifically proven, the morning glory plant is likely the same plant that the Aztec people called *tlitiltzin*, which has been used in divinations and healing rituals since the late 16<sup>th</sup> century<sup>22</sup>. Traditionally, a dosage consisted of 26 seeds ground up before being mixed with water. This process is believed to allow the seeds to “speak”<sup>22</sup>. Although many different cultures reported using the plant materials in religious rituals for its psychoactive properties, the intended outcome is very similar among all of them.

##### 1.5.4.2. Reported Effects and Active Components

Various parts of the morning glory plant possess psychoactive components. The leaves and seeds contain ergot alkaloids such as ergine and many ergine derivatives such as ergometrine, ergosinine, elymoclavine, chanoclavine and hydroxyethylamide<sup>22</sup>.

The psychoactive components of morning glory seeds are very similar to that of the ololiuqui seeds. The structures for ergine, ergometrine, and ergosinine, which are reported to be present in morning glory seeds, can be seen in Figure 5 in the Ololiuqui section.

#### *1.5.5 Argyreia nervosa (Hawaiian Baby Woodrose)*

##### 1.5.5.1. Background and Traditional Uses

The Hawaiian Baby Woodrose plant originated in India, but is now common in the Pacific Islands. The plant is a perennial vine that produces purple colored flowers and fruits containing smooth, brown seed capsules, each with up to four seeds<sup>22</sup>. In India, the plant material has been used medicinally since Ancient times. Although there are no documented traditional uses for the plant material, the seeds and roots of the Hawaiian Baby Woodrose plant are reported to contain psychoactive materials<sup>22</sup>. Additionally, there have been reports of individuals using the plant material as an alternative to marijuana or other intoxicating substances. For example, in Australia today, the seeds are regularly used recreationally as a psychedelic<sup>22</sup>.

##### 1.5.5.2. Reported Effects and Active Components

The Hawaiian Baby Woodrose seeds contain about 0.3% ergot alkaloids, making it the most potent of all vines containing drugs<sup>22</sup>. Many alkaloids have been identified as constituents of the seeds, including but not limited to ergine, isoergine, chanoclavine, elymoclavine, lysergol, ergometrine (ergonovine), and ergometrine<sup>22,32</sup>. Due to the similarities in the compounds present in the Hawaiian Baby Woodrose seeds, morning

glory seeds, and lolium seeds, the effects due to consumption of the seeds was expected to be similar<sup>33</sup>. The structures of ergine, ergometrine, and ergosinine are shown previously in Figure 5. Structures of lysergic acid and lysergol are shown in Figure 6.

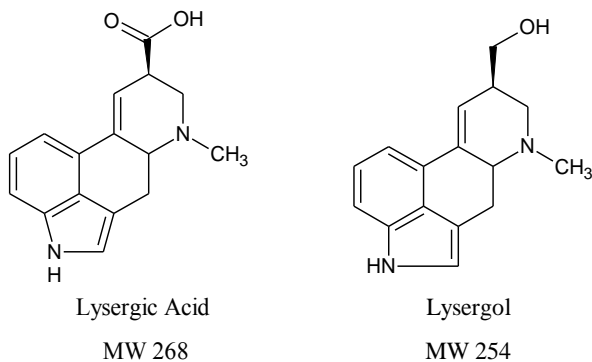


**Figure 6. Additional ergot alkaloids found in seeds of Hawaiian baby woodrose seeds.**

#### *1.5.6 Entada rheedii (African Dream Herb)*

##### 1.5.6.1. Background and Traditional Uses

The African Dream Herb is a climbing vine that is native to tropical regions such as the coastlines of Madagascar, Southern African, Asia, and Australia<sup>34</sup>. The plant is most known for the large seeds that it produces. The seed pods can grow to be over 5 feet long and each pod contains 12 or more seeds. The seeds are round with a diameter of approximately 2 inches. Each seed is protected by a thick, dark brown casing containing a lighter brown seed that is hollow in the center. Traditionally, the African Dream Herb has been used for many centuries by tribes for its medicinal healing properties; although, reports do not indicate the specific effects or traditional practices. In South Africa, the plant is used to induce vivid dreams that were believed to be a way to communicate with the spiritual world.

#### 1.5.6.2. Reported Effects and Active Components

Very little scientific research has been done on the active components of the African Dream Herb seeds. Based on studies of the *Entada* species, the plant likely contains psychoactive alkaloids, phenylacetic acid derivatives, and essential oils<sup>35</sup>, but no scientific reports were found to suggest any specific compounds present in the African Dream Herb seeds. Based on anecdotal sources, the seeds are generally believed to aid in sleep that allows the user to experience more vivid dreams and provide an increased level of awareness during REM sleep, allowing a more lucid dream experience.

Based on several recent studies, components within the seeds have begun to be investigated, but none of them are being studied as a possible source for hallucinogenic properties<sup>34,36</sup>. Currently, studies are focusing on the tryptophan derivatives in the plant and their effect on cell viability and HIV infections<sup>34</sup> and the antiproliferative and antioxidant properties of triterpene saponins found in the *Entada rheedii* plant<sup>36</sup>.

#### *1.5.7 Peganum harmala (Syrian Rue or Harmel)*

##### 1.5.7.1. Background and Traditional Uses

*Peganum harmala* is a plant that grows in many parts of the world, including the eastern Mediterranean region, Mongolia, Manchuria, Yemen, the Negev Desert, and parts of California<sup>22</sup>. The Syrian rue plant has traditionally been used by cultures in the Middle East, Central Asia and South America for ritualistic and medicinal purposes<sup>22,37</sup>. In ancient literature, the plant was referred to as peganon, likely after the word Pegasus from Greek mythology<sup>22</sup>. Syrian rue was also a sacred plant in the Middle East, where it is stated in

the Koran that, “every root, every leaf of harmel, is watched over by an angel who waits for a person to come in search of healing”<sup>22,38</sup>. In North Africa, the seeds are used as incense, in which the smoke is inhaled to cure headaches and other diseases<sup>22,37,38</sup>.

#### 1.5.7.2. Reported Effects and Active Components

Syrian rue seeds contain psychoactive compounds, specifically the  $\beta$ -carbolines harmine and harmaline shown in Figure 7. Harmine is reported to make up about 4.3% weight/weight (w/w) of the dry seeds, and harmaline is 5.6% (w/w)<sup>38</sup>. Harmol, harmalol, and ibogaine have also been reported as being components of the seeds<sup>37,38</sup>. Ingestion of the seeds is reported to cause improved imagination and dream-like effects.

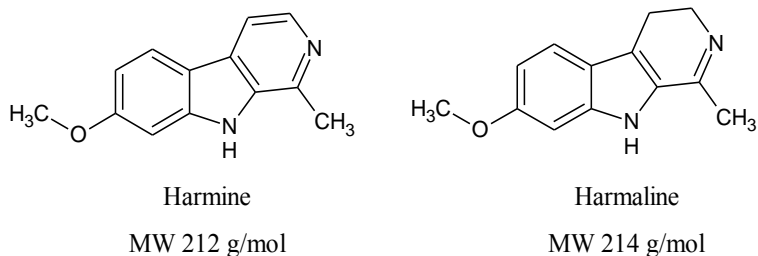


**Figure 7. Structures of psychoactive compounds reported to be in Syrian rue seeds.**

### *1.5.8 Hyoscyamus niger (Black Henbane)*

#### 1.5.8.1. Background and Traditional Uses

Black henbane grows naturally in Scandinavia, North America, and Australia and is distributed throughout the world, including Europe, Asia, and North Africa<sup>22,39</sup>. The plant has been used for medicinal purposes since ancient times. Henbane is a member of the Nightshade family, which is often associated with witchcraft in Europe<sup>16</sup>. In Persia,

the plant was called banha, which is the term often associated with psychoactive plants, including marijuana<sup>22</sup>. Reportedly, a Persian prince drank a mixture of henbane and wine and experienced three days of deep sleep while his soul experienced religious travels<sup>22</sup>. Henbane also played an important role in the ritualistic practices of the Vikings and multiple cases have been reported in which the seeds were recovered from graves of Vikings<sup>22</sup>. Overall, the plant has a long history of practice for purposes of inebriation related to witchcraft and superstition<sup>16</sup>.

#### 1.5.8.2. Reported Effects and Active Components

The primary active ingredients in henbane are hyoscyamine, atropine, and scopolamine, shown in Figure 8<sup>16,22,39,40</sup>. Hyoscyamine is an isomer of atropine and is not shown. Each of these compounds is found throughout the entire plant, although they are reported to be most highly concentrated in the seeds and roots<sup>16</sup>. Atropine and scopolamine are different than most hallucinogens because they are extremely toxic, causing temporary anterograde amnesia while under the influence<sup>16,41</sup>. Henbane intoxication generally results in pressure headaches, blurred and distorted vision, and visual hallucinations. The user often experiences hallucinations related to taste and smell as well<sup>16</sup>.



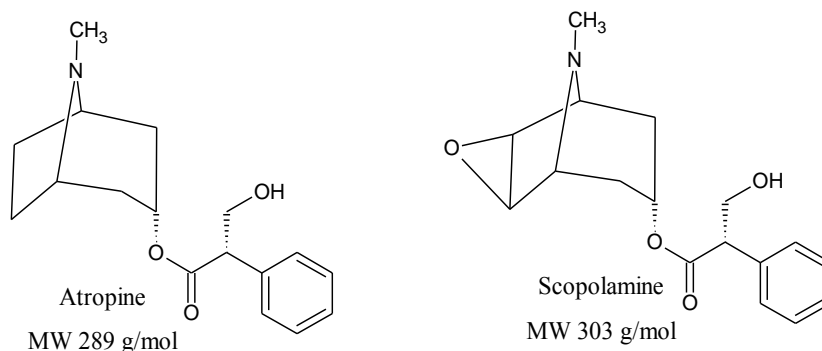


**Figure 8. Psychoactive compounds found in henbane seeds, atropine and scopolamine.**

### 1.5.9 *Ephedra sinica* (Ma-Huang)

#### 1.5.9.1. Background and Traditional Uses

*Ephedra sinica* is a perennial plant native to northern China and grows at altitudes of almost 5,000 feet<sup>22</sup>. Traditionally, the Chinese have used the plant material to treat asthma, diseases of the lungs and bladder, fevers, headache, and hayfever<sup>22</sup>. The Chinese and Mongolian shamans used ma-huang for magical, medicinal, and ritualistic purposes<sup>22</sup>, but no scientific sources were found to describe the specific details of how it was used. In recent years, the plant was distributed throughout the world to be used in dietary supplements, but was banned by the FDA for use in supplements in the U.S. in 2004<sup>22,42</sup>. In addition to use in supplements, the plant material is still used in tonics and aphrodisiacs due to its stimulating effects<sup>22</sup>.

#### 1.5.9.2. Reported Effects and Active Components

Of all the ephedra species, *Ephedra sinica* has the highest alkaloid content. The dried plant material contains up to 2.5% alkaloids including ephedrine, pseudoephedrine, and norephedrine<sup>22,42</sup>. The structure of each compound is shown in Figure 9. Ephedrine

is the most abundant compound and accounts for up to 60% of the total alkaloid content in the plant<sup>42</sup>. Many studies have been conducted to investigate different aspects of ephedrine including its stimulating effects, potential for use as a precursor to methamphetamine, and performance enhancing properties within the athletic community<sup>43,44</sup>. Consumption of the plant material results in constricted blood vessels and increased pulse, causing a stimulating effect. Although studies state that the dried plant material and stems possess psychoactive properties, no reports address any psychoactive alkaloids in the seeds<sup>22,42</sup>.

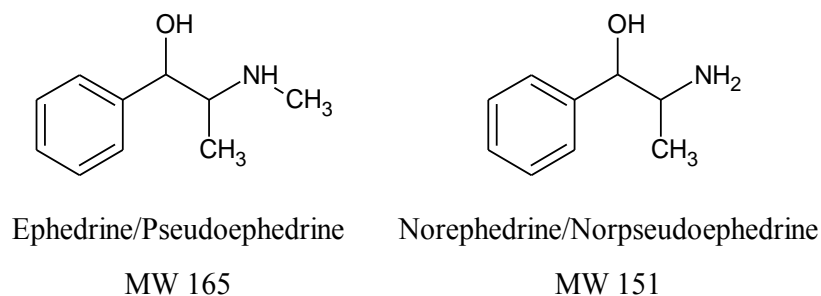


**Figure 9. Structures of compounds reported to be present in *Ephedra sinica* plant material.**

#### *1.5.10 Mucuan pruriens (Cowage)*

##### 1.5.10.1. Background and Traditional Uses

Cowage can be found throughout the world in areas near forests and oceans in Africa, Asia, and Central and South America<sup>45,22</sup>. Many cultures use the seeds or seed powder for different purposes including the prevention of eye inflammation in infants, to increase semen production, to remove venom after a scorpion bite, to treat nervous disorders, or to remove parasites from the body<sup>11,22</sup>. In addition to consumption for their

therapeutic properties, the seeds are also consumed as a source of nutrients by poor populations in Africa and Asia<sup>46</sup>.

#### 1.5.10.2. Reported Effects and Active Components

Cowage seeds are reported to contain DMT, bufotenine, serotonin, and L-3,4-dihydroxyphenylalanine (L-dopa)<sup>22</sup>. DMT and bufotenine produce psychoactive effects including hallucinations and a sense of euphoria, but DMT must be consumed in combination with a monoamine oxidase inhibitor in order for it to be active<sup>47</sup>. L-dopa, which is the precursor to dopamine and has been shown in numerous studies to aid in the treatment of Parkinson's disease<sup>45,48</sup>. The structures of DMT and L-dopa are shown in Figure 10.

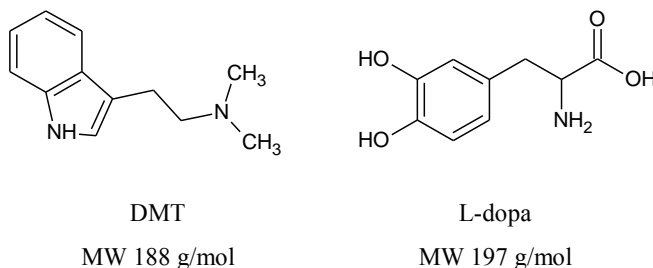


**Figure 10. Figures of compounds of interest reported to be present in cowage seeds.**

#### *1.5.11 Argemone mexicana (Mexican Poppy)*

##### 1.5.11.1. Background and Traditional Uses

The Mexican poppy is a plant that grows to about three feet in height and produces several small black seeds contained within the fruit<sup>22</sup>. The leaves, flowers, capsules, and dried latex contain psychoactive ingredients, although the plants' use for its

psychoactive properties is unknown<sup>22</sup>. Limited research was found to suggest the psychoactive use of the seeds, but they were associated with the underworld by the Aztecs and were used in various rituals<sup>22</sup>. The plant has been utilized as a “nourishment of the dead” in some cultures, including the Aztecs and other Mesoamerican people, and food for various ceremonies was often prepared using portions of the Mexican poppy plant<sup>22</sup>. The plant has also been used by various cultures for medicinal practices. For example, in Peru, muscle pain is treated with a plaster made from the plant<sup>22</sup>.

#### 1.5.11.2. Reported Effects and Active Components

Very little research has been done on the effects of the plant material, especially the seeds. The seeds have been reported to produce an effect similar to that of cannabis<sup>49</sup>. Additionally, reports in Mexico state that smoking the dried leaves of the plant produces an aphrodisiac and euphoric effect<sup>22</sup>. Specifically, the seeds contain berberine and protopine<sup>22,49</sup>, which may be responsible for the effects noted upon consumption. The oils obtained from the seeds also contain the compounds sanguinarine and dihydrosanguinarine<sup>49,50</sup>. The structures of all compounds of interest are shown in Figure 11.

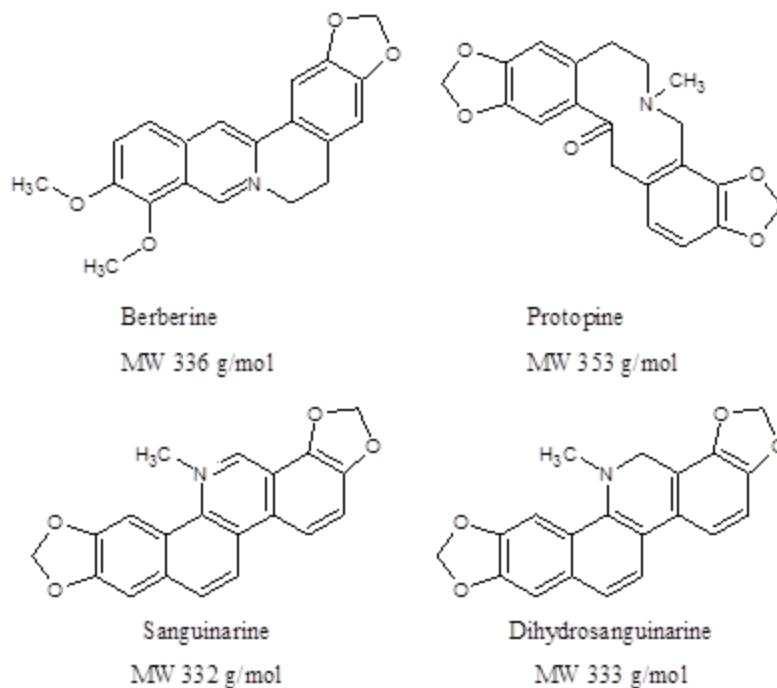


**Figure 11. Figures of compounds reported to be found in the seeds and seed oil of the Mexican poppy plant.**

#### 1.5.12 *Celastrus paniculatus* (Intellect Tree)

##### 1.5.12.1. Background and Traditional Uses

The intellect tree is a plant that is native to Southern Asia. Although there is limited research describing the plant or its use, reports suggest that the plant was used to improve memory<sup>51,52</sup> and treat various diseases such as epilepsy, insomnia, rheumatism, gout, and dyspepsia<sup>53</sup>. Specific details describing the practices were not found.

##### 1.5.12.2. Reported Effects and Active Components

Many studies have indicated the use of the seed and flower extracts to improve the memory and learning abilities in mice and as a source of anti-inflammatory and

analgesic properties<sup>51,54</sup>. No studies were found to suggest a specific compound that may be responsible for the properties observed; although there are various anecdotal reports available online suggesting the psychoactive effects of consuming the seeds. In addition, a webpage entitled “Entheology Preserving Ancient Sacred Knowledge” has a page dedicated to describing the seeds. The site states that the seeds contain up to 50% oils, which contain active alkaloids including celastrine and paniculatin<sup>55</sup>. No studies were found to suggest the properties of either compound. The structure of each compound is shown in Figure 12.

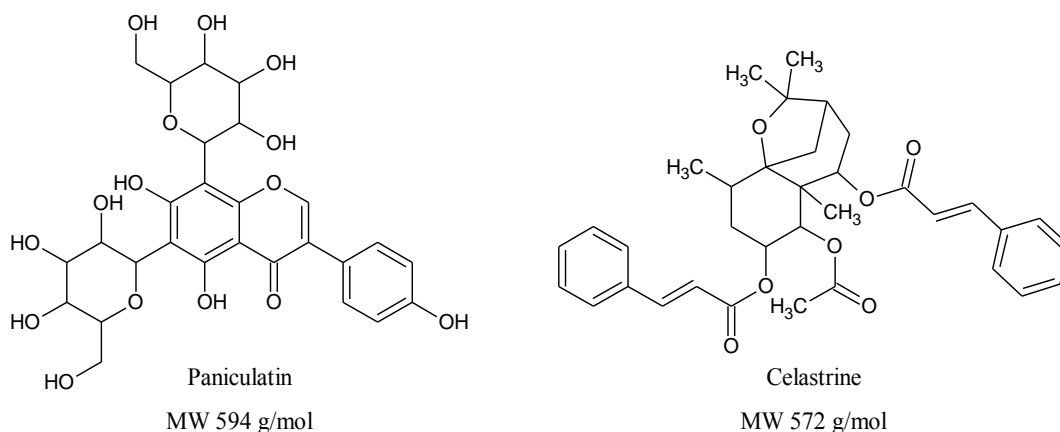


**Figure 12. Structures of possible alkaloids found in Intellect tree seeds, although no scientific evidence was found to support the existence of these compounds in the seeds.**

### 1.6 Direct Analysis in Real Time – Mass Spectrometry (DART-MS)

Direct analysis in real time (DART) is an ambient ionization technique that allows for high-throughput analysis of a wide variety of samples and analytes. Since its invention in 2003, DART has been applied to a wide variety of applications, including but not limited to analysis of controlled substances<sup>56,57</sup>, synthetic cannabinoids<sup>58</sup>,

chemical warfare agents<sup>59,60</sup>, pesticides on produce and food products<sup>61,62</sup>, and food quality based on oil content<sup>63</sup>.

The DART ionization source consists of a carrier gas inlet, glow discharge region, grounded perforated electrode, a grid electrode, gas heater region, and a ceramic insulator cap at the atmospheric exit, as shown in Figure 13.

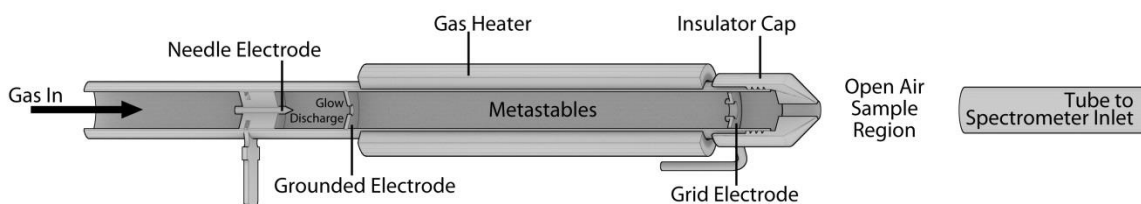
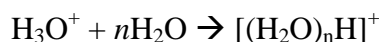


**Figure 13. DART schematic of gas flow through the source to create metastable species. Photo provided courtesy of IonSense, Inc.**

The gas, often helium or nitrogen, enters the DART source where it is introduced to an electric potential, creating ions, electrons, and excited state metastable species. The gas then continues through the source where a counter electrode is used to remove all ions, leaving only the metastable species. The metastable species then travel into a region of the DART source where they can be heated before exiting through the final grid voltage and the insulator cap into the ambient atmosphere<sup>64</sup>. Once the metastable species are exposed to the open atmosphere, a series of competing mechanisms take place through which ionization occurs<sup>65</sup>. One reaction that occurs is the ionization of water vapor in the air through Penning ionization and the creation of a protonated water cluster and a hydroxyl radical, as shown in  $\text{He}^* + \text{H}_2\text{O} \rightarrow \text{H}_3\text{O}^+ + \text{OH}^- + \text{He}$

Equation 1. Penning ionization occurs with any compound present in the

atmosphere that has an ionization energy that is lower than the internal energy of the excited metastable<sup>65</sup>.



Once the water clusters in the atmosphere are protonated, proton transfer to the sample (M) will occur if the analyte has a ionization potential greater than that of the water cluster<sup>65</sup>, resulting in the formation of an  $[\text{M}+\text{H}]^+$  species, as shown in Equation 2. Although it is also possible to observe hydride abstraction of electrophilic species to form negative ions<sup>65</sup>, negative ion mode was not investigated in this study.

Equation 2

Two advantages of DART are that it requires little to no sample preparation and ionization occurs in the open atmosphere<sup>64,66</sup>. Solid, liquid, or gas samples can be analyzed directly by placing the sample in the open air sample region between the DART source and the mass spectrometer. Depending on the specific application of the analysis, many different sample introduction methods are available, including sampling apparatus's for tablets<sup>57</sup>, glass capillaries<sup>67</sup>, TLC plates<sup>68</sup>, tweezers<sup>67</sup>, and sorbent swabs<sup>61</sup>. One method of introducing the sample was developed by IonSense, Inc. (Saugus, MA), in which a linear rail enclosure (LRE) is fitted into the open air gap between the DART and mass spectrometer. A consumable metal mesh Quick Strip<sup>TM</sup> is then placed into a metal holder in the LRE and can be passed in front of the DART source in an automated manner, allowing for rapid analysis of multiple samples in a short



period of time. The consumable Quick Strip™ and LRE set-up are shown in Figure 14 and Figure 15.

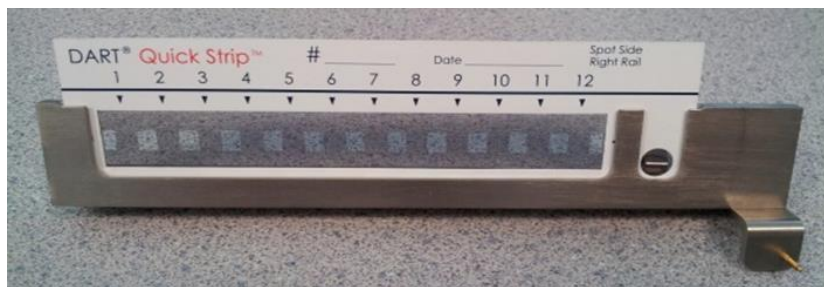


**Figure 14. DART Quick Strip™ card in metal holder. Image courtesy of Drew Horsley.**

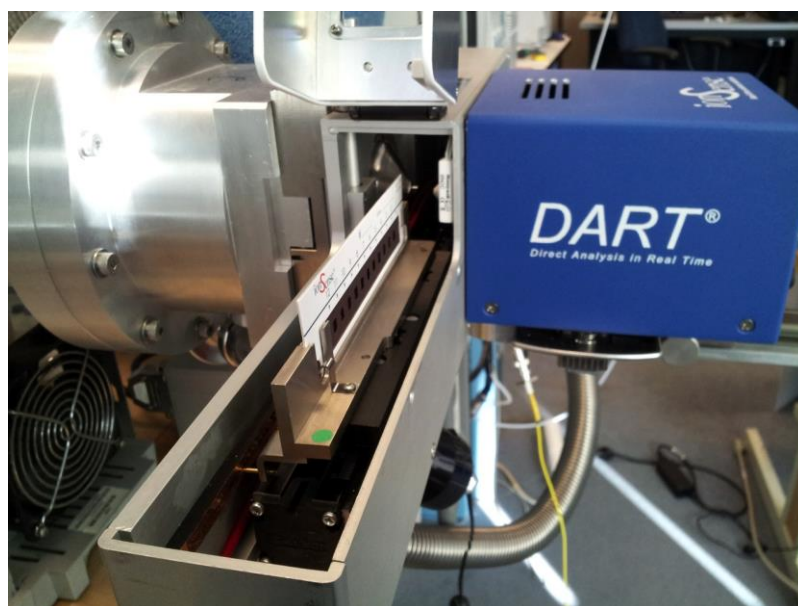


**Figure 15. Linear Rail Enclosure attached between MS inlet (left of image) and DART ionization source (right of image) with Quick Strip™ card in holder. Image courtesy of Drew Horsley.**

Although not a requirement, the most common position of the DART source relative to the mass spectrometer (MS) inlet is directly in-line, which allows the carrier gas to travel from the source, interact with the sample, and continue into the inlet of the MS. The DART source can be coupled to various MS instruments including time of flight

(TOF)<sup>62,68,69</sup>, quadrupole mass spectrometers<sup>70</sup>, and quadrupole ion trap mass spectrometers<sup>23,62</sup>. DART allows for ionization and fragmentation patterns similar to those commonly observed when using soft ionization techniques such as atmospheric pressure chemical ionization and electrospray ionization.

## **2. Materials and Methods**

### **2.1 Materials**

Fourteen different samples including twelve different species of plant seeds were obtained from various online sources including shamansgardern.com, bouncingbearbotanicals.com, and ethnobotanicals.com. The seeds analyzed in this study were *Anadenanthera colubrine* (Cebil), *Voacanga africana* (Voacanga), *Rivea corymbosa* (Ololiuqui), *Ipomoea violacea* (Morning Glory), *Peganum harmala* (Syrian Rue), *Entada rheedii* (African Dream Herb), *Argyreia nervosa* (Hawaiian baby woodrose), *Hyoscyamus niger* (Henbane), *Ephedra sinica* (Ma huang), *Mucuna pruriens* (Cowage), *Argemone mexicana* (Mexican Poppy), and *Celastrus paniculatus* (Intellect tree). Three strains of Hawaiian baby woodrose were obtained from a single online source in an attempt to conduct studies that would allow an analyst to differentiate between the strains by chemical components unique to each strain.

Each seed was prepared through the use of a mortar and pestle and a Bertin Technologies Minilys Homogenizer (France) prior to analysis with a DART ionization source (IonSense, Inc. Saugus, MA) coupled to a modified single quadrupole mass analyzer by Agilent Technologies with Enhanced MSD ChemStation E.02.02.1431 data

analysis software by Agilent Technologies. Additional information was obtained through analysis with a DART ionization source coupled to a Finnigan quadrupole ion trap mass analyzer followed by data analysis with XCaliber<sup>TM</sup> Qual Browser 2.2 by Thermo Fisher Scientific.

## **2.2 Physical Characterization of Seed Samples**

Each seed type was characterized by taking digital photographs, followed by physical measurements including average mass, length, width, and thickness. Some of the seeds were too small to measure with digital calipers and physical measurements of the length, width, and thickness were not obtained. For the remaining seeds, random samples of fifteen seeds were measured using a digital caliper. Each of the 15 seeds was weighed using an analytical balance (Denver Instrument). From the recorded measurements, the average and standard deviation for each seed was calculated.

For the seeds that were not measured with calipers, average mass determinations were the only physical measurements collected. An average mass was determined by weighing 25 seeds in triplicate. For each trial, the average mass of a single seed was calculated. The average masses determined in the three trials were then averaged and a standard deviation was determined based on the data from all three trials.

## **2.3 DART-MS Method Development for Plant Based Drugs of Abuse**

### *2.3.1 Sample Preparation*

In order to provide a representative sample of each seed, multiple seeds were ground with a mortar and pestle. Once the seeds were crushed, they were placed into small plastic tubes containing metal balls ranging in size from 5/32 to 1/8 inches to be used in the homogenizer. Each sample was then homogenized on the medium speed setting for approximately one minute. Once the samples were homogenized, the powders were removed from the plastic tubes and placed into individual labeled black top vials.

To prepare the samples for analysis by DART-MS, a small amount of the powder was placed onto a Quickstrip™ (IonSense, Inc., Saugus MA, USA) to create an approximately 3mm square sample area. The powder was then ground into the mesh using a metal spatula to ensure the sample was embedded into the mesh. The Quickstrip™ was then tapped against the table to remove any excess loose powder before being placed into the LRE for analysis.

### *2.3.2 DART Source Temperature Profile*

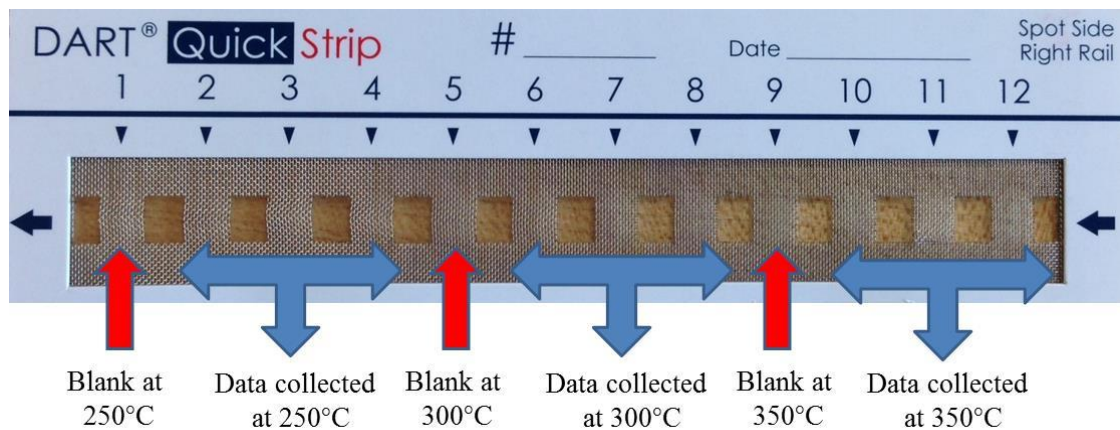
**In order to determine the optimal source temperature for each seed sample, a temperature profile was collected for each sample using the DART/single mass analyzer. The analysis was performed in positive mode using helium as the gas. The parameters for the experiment can be seen in**

Table 1.

**Table 1. Quadrupole mass spectrometer and DART parameters for the DART source temperature profile.**

Capillary Inlet	78.8 V
Skimmer Focus	60.0 V
Skimmer	12.0 V
Ion Guide Offset	8.3 V
Ion Guide Exit Lens	5.9 V
MSD Focus Lens	-299.0 V
MSD Quad Entrance Lens	-27.0 V
RF Voltage	480 V
Capillary Temperature	150°C
Grid Voltage	250 V
DART Source Temperature	250°C, 300°C, 350°C
Linear Rail Speed	0.8 mm/s

Three samples were analyzed at each temperature (250°C, 300°C, 350°C) and an average was taken of the resulting spectra for comparison to determine the optimal source temperature. The analysis at all three temperatures was performed using samples on a single QuickStrip™, with a space on the mesh between each temperature to serve as a blank. An example of this set-up is shown in Figure 16. The optimal source temperature was determined based on the abundance of the ions of interest for each sample, the amount of noise, and the abundance of any other ions present in the spectra.



**Figure 16. Diagram of Quickstrip used to perform temperature profiles for each seed.**

### 2.3.3 Fragmentation

After the optimal source temperature was determined and the ions of interest were identified, more information was necessary before identification could be made, based on SWGDRUG guidelines as to what is required for a confirmatory identification. Using the DART/quadrupole ion trap, MS<sup>2</sup> fragmentation was performed on the molecular ions of interest to obtain fragmentation patterns for each compound. The MS parameters used are shown in .

Table 2.

**Table 2. Ion trap MS Parameters used throughout the fragmentation experiments.**

MS Capillary Temperature	200°C
MS Voltage	15 V
Multipole 1 Offset	-6.8 V
Lens Voltage	23.00 V
Multipole 2 Offset	-8.0 V
Multipole RF Amplitude	400 V
Entrance Lens Voltage	-46 V
Electron Multiplier Voltage	-1090.0 V

The DART source was set at the optimal temperature determined for each sample and the percent collision energy (CE) used to induce MS<sup>n</sup> fragmentation was varied to determine the optimal CE for each compound of interest.

Data was collected at multiple CE percentages and the optimal value was determined when the most abundant fragment ion occurred without complete loss in

abundance of the parent ion. The structure of the compound was studied in an attempt to understand where the resulting fragments were likely originating. The fragmentation patterns observed were also compared to patterns reported in the literature.

## **2.4 Identification**

Based on the data collected, the major compounds present in each sample were identified through analysis of the fragmentation patterns along with the compounds that were reported to be present in each of the plant seeds. In some cases, past studies were able to provide known fragmentation patterns for the compounds suspected to be present in the seed samples. In cases where no studies could be found discussing fragmentation, suggestions were made as to the source of each fragment observed based on the structure of the compound of interest. Although identifications were made for each sample, no standards were analyzed to confirm the results.

## **3. Results and Discussion**

### **3.1 Physical Characterization**

Digital photographs were taken of each seed for visual comparison and identification of macroscopic details for the entire seed. The photos of each seed type are shown in Figure 17, Figure 18, Figure 19, and Figure 19 Figure 20. A scale with centimeter measurements was included in each of the photographs for a reference. The cebil seeds (Figure 17A) were flat, circular black seeds with a thin, smooth outer shell. The voacanga seeds (Figure 17B) were oblong and brown with a noticeable node at each end. The



surface of the seeds was rough and textured. The morning glory seeds (Figure 17C) were black and oblong with a defined ridge running along the length of the seed on one side. The Syrian rue seeds (Figure 17D) were very small, irregular in shape, and brown in color.

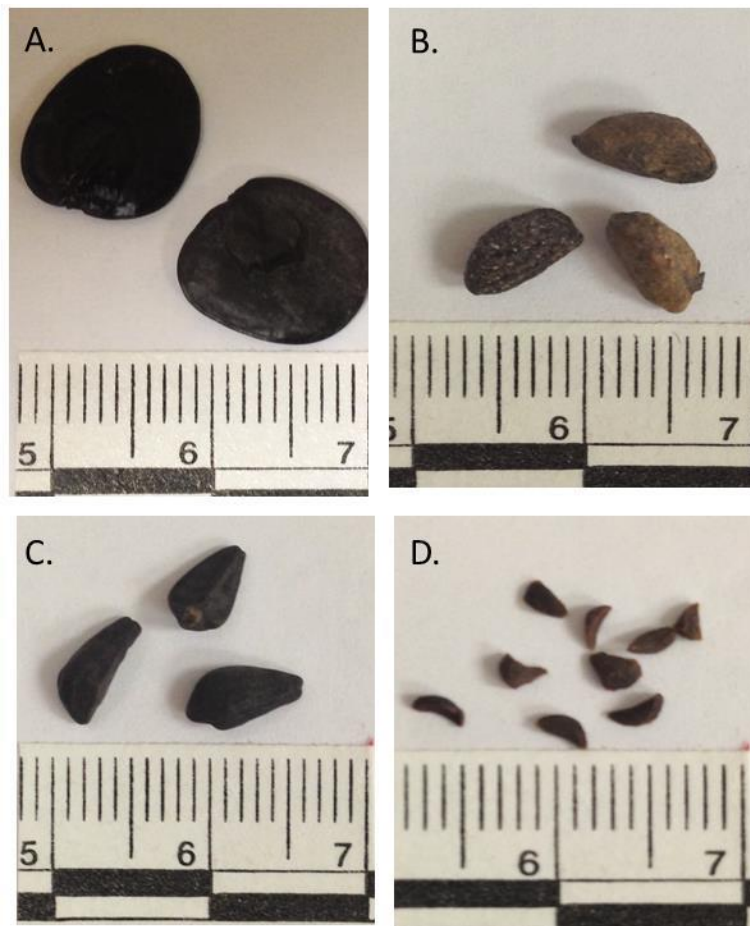


**Figure 17. Images of seeds analyzed. A) Cebil seeds, B) Voacanga seeds, C) Morning Glory seeds, and D) Syrian Rue seeds**

The henbane seeds (Figure 18A) were very small, round, and light brown in color. No physical measurements other than weight were able to be obtained for the

henbane seeds. The ololiuqui seeds (Figure 18B) were light brown and oval in shape with a width and thickness that were very similar. The *Ephedra sinica* seeds (Figure 18C) were very dark, almost black in color. The seeds were mostly flat with smooth surfaces.

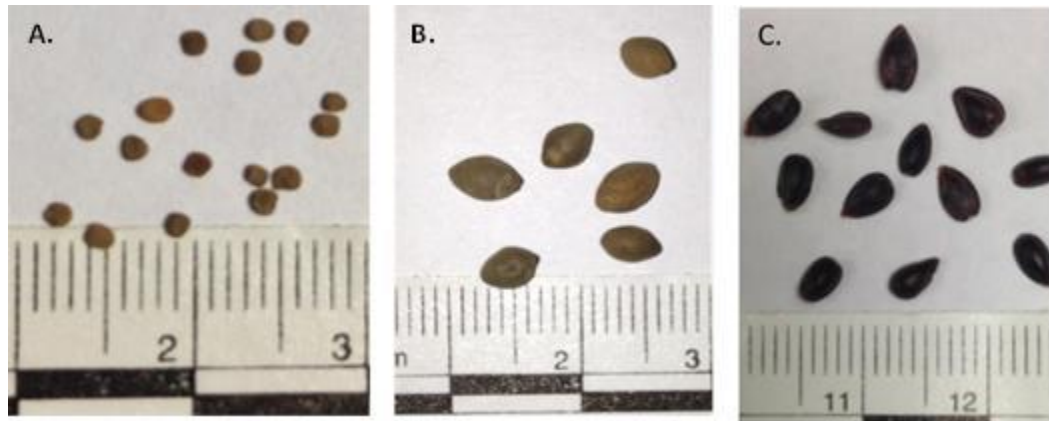


**Figure 18. Images of seeds analyzed. A) Henbane seeds, B) Ololiuqui seeds, and C) *Ephedra sinica* seeds.**

The African dream herb seeds (Figure 19A) were very large in comparison to the other seeds examined. The seeds were circular with a smooth dark brown to black outer covering. When opened, the seeds were hollow in the center. The cowage seeds (Figure 19B) were also oval in shape and dark colored in color. The color ranged from a mix of black and brown to solid black. On one edge of the seed, there was a small brown layer, likely the location in which the seed was connected to the plant. The Mexican poppy seeds (Figure 19C) were very small, round black seeds that came to a point at one edge. No physical measurements other than weight were able to be obtained for the Mexican poppy seeds. The Intellect tree seeds (Figure 19D) were round in shape with a two splits in the middle, dividing the seed into three sections. They were a reddish-brown color.

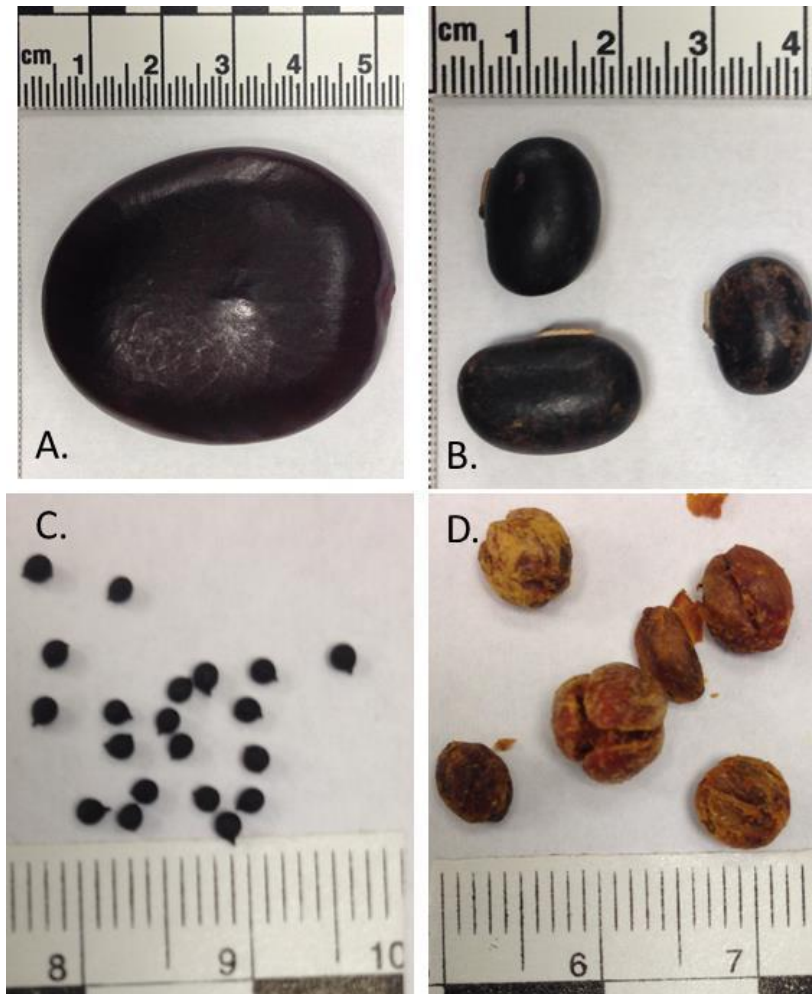


**Figure 19. Images of seeds analyzed. A) African Dream Herb seed, B) Cowage seeds, C) Mexican Poppy seeds, D) Intellect Tree seeds.**

The three strains of Hawaiian Baby Woodrose seeds were visually different. The Ghana strain (Figure 20A) appeared more light brown to orange in color while the Hawaiian (Figure 20B) and Indian strain (Figure 20C) are more of a darker brown to gray color. The visible differences may be due to the environments in which they were obtained, including differences in soil composition and moisture content. Although the seeds were sold under the label of Hawaiian, Ghana, or Indian strain the environmental conditions or specific origins of each seed was unknown.

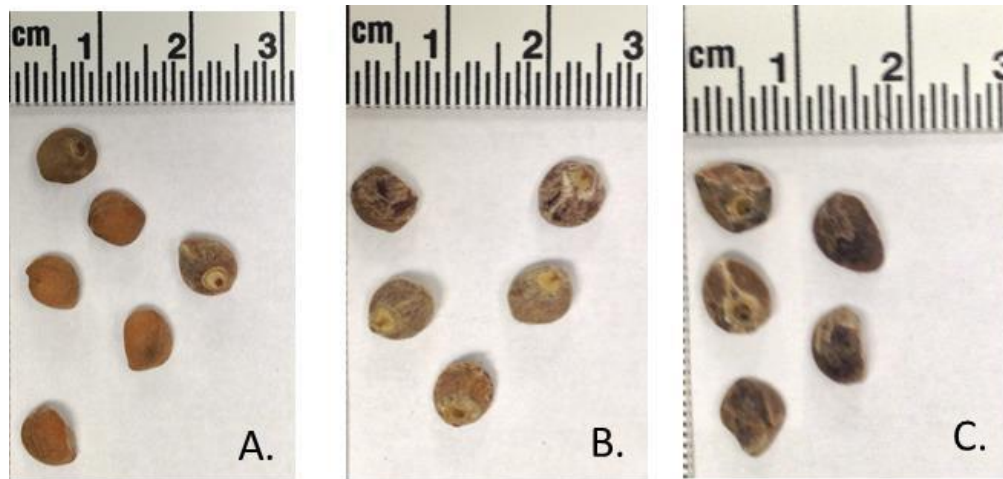


**Figure 20. Three different strains of Hawaiian Baby Woodrose seeds. A) Ghana Strain, B) Hawaiian Strain, C) Indian Strain.**

The seeds were physically measured using digital calipers. The length and width were determined based on nodes at either end of the seed. The length was measured from the node to the opposite side. The width was measured at approximately half way between the node and the end of the seed. The thickness of the seed was measured by placing the caliper on the front and back of the seed and measuring at the same point on the seed that the width was taken, as this was approximately the middle of the seed. Each seed was also weighed individually using an analytical balance to obtain a mass in grams. Once all fifteen seeds were measured, the average and standard deviation were calculated.

The seeds examined as part of this study ranged in size from approximately 0.77 mg to 20515 mg. With the exception of the voacanga, intellect tree, and ephedra sinica seeds, the mass of each seed had a standard deviation of less than 20%, with several being less than 10%. The length of the seeds measured ranged from approximately 2.86

to 39.34 mm with standard deviations of 4.8% to 17.5%. The width of the seeds measured ranged from approximately 3.34 to 44.31 mm with standard deviations of 4% to 11.6%. The thickness of the seeds measured ranged from approximately 1.44 to 18.63 mm with standard deviations less than 20% with the exception of the Intellect tree seeds which had a standard deviation of 32.6%.

A summary of the average and standard deviations calculated for each seed type is shown in Table 3.

**Table 3. Summary of physical measurements of each seed.**

Sample	Average Mass (mg)	Average Length (mm)	Average Width (mm)	Average Thickness (mm)
Yopo Seed	99.66 ± 15.52	12.13 ± 0.71	10.52 ± 0.83	1.44 ± 0.21
Voacanga Africana Seed	39.18 ± 10.68	7.15 ± 0.65	3.97 ± 0.31	3.16 ± 0.32
Ololiuqui Seed	3.34 ± 0.18	4.80 ± 0.35	3.34 ± 0.17	3.35 ± 0.23
Morning Glory Seed	34.65 ± 7.00	6.43 ± 0.92	3.52 ± 0.29	2.50 ± 0.50
Syrian Rue Seed*	2.28 ± 0.14	---	---	---
African Dream Herb	20515 ± 2590	39.34 ± 3.27	44.31 ± 2.97	18.63 ± 1.66
Cowage	1463 ± 233	12.28 ± 0.72	17.73 ± 1.06	9.36 ± 0.72
Hawaiian Baby Woodrose - Hawaii	104.58 ± 7.29	6.25 ± 0.33	7.02 ± 0.28	4.61 ± 0.33
Hawaiian Baby Woodrose - Ghana	108.79 ± 8.53	5.85 ± 0.62	6.80 ± 0.35	4.68 ± 0.31
Hawaiian Baby Woodrose - Indian	97.43 ± 14.39	6.18 ± 0.30	7.76 ± 0.49	4.40 ± 0.37
Henbane*	0.77 ± 0.01	---	---	---
Intellect Tree	42.77 ± 15.87	4.63 ± 0.81	6.01 ± 0.70	3.47 ± 1.31
Ephedra sinica	9.92 ± 2.18	2.86 ± 0.27	5.00 ± 0.51	1.65 ± 0.15
Mexican Poppy Seed*	2.04 ± 0.15	---	---	---

(\* indicates that three measurements were taken of 25 seeds at once and an average was calculated based on that value. This was done for very small seeds)

### 3.2 DART Source Temperature Profiles

For each sample, data was collected while the DART source temperature was varied. Data was collected at 250°C, 300°C, and 350°C and comparisons were made between the quality of the spectra as well as the relative abundance of the ions of interest. Unlike typical GC data, there is no separation of the components within a sample. Rather than obtaining a chromatogram, the analysis results in a plot of ion abundance as a function of time in minutes, also known as a Total Ion Chromogram (TIC). In Figure 21A, each peak represents a point in time where the ion abundance showed a significant increase. This correlates with the time in which a crushed cebil seed sample was ionized by DART and carried into the mass spectrometer for detection. The separation between peaks can vary based on the sample introduction method, including the speed of the linear rail which is carrying the sample into the ionization region. For all of the experiments in this study, the linear rail was set to proceed at 0.8 mm/s to ensure baseline resolution of each sample being analyzed.

Due to variations in ion intensity based on precise placement of the sample on the QuickStrip™ relative to the DART and the detector, averages were taken by measuring from the start of the peak, where signal increased above the baseline, to the end of the peak, where signal decreased into the baseline. Figure 21B-D shows the data collected for crushed cebil seeds at the three different carrier gas temperatures. The data is an average of three trials all analyzed on a single QuickStrip™. The analyte of interest in cebil seeds is bufotenine which would exhibit an  $[M+H]^+$  peak at  $m/z$  205. With a DART source

temperature of 300°C, the peak at  $m/z$  205 had the greatest abundance at approximately 120,000 counts. As the source temperature increased or decreased, the abundance of the  $m/z$  205 peak decreased. The optimal source temperature for the analysis of cebil seeds was determined to be 300°C, and was utilized later for future fragmentation experiments. The detection of a peak at  $m/z$  205 was used as a presumptive positive identification of bufotenine.

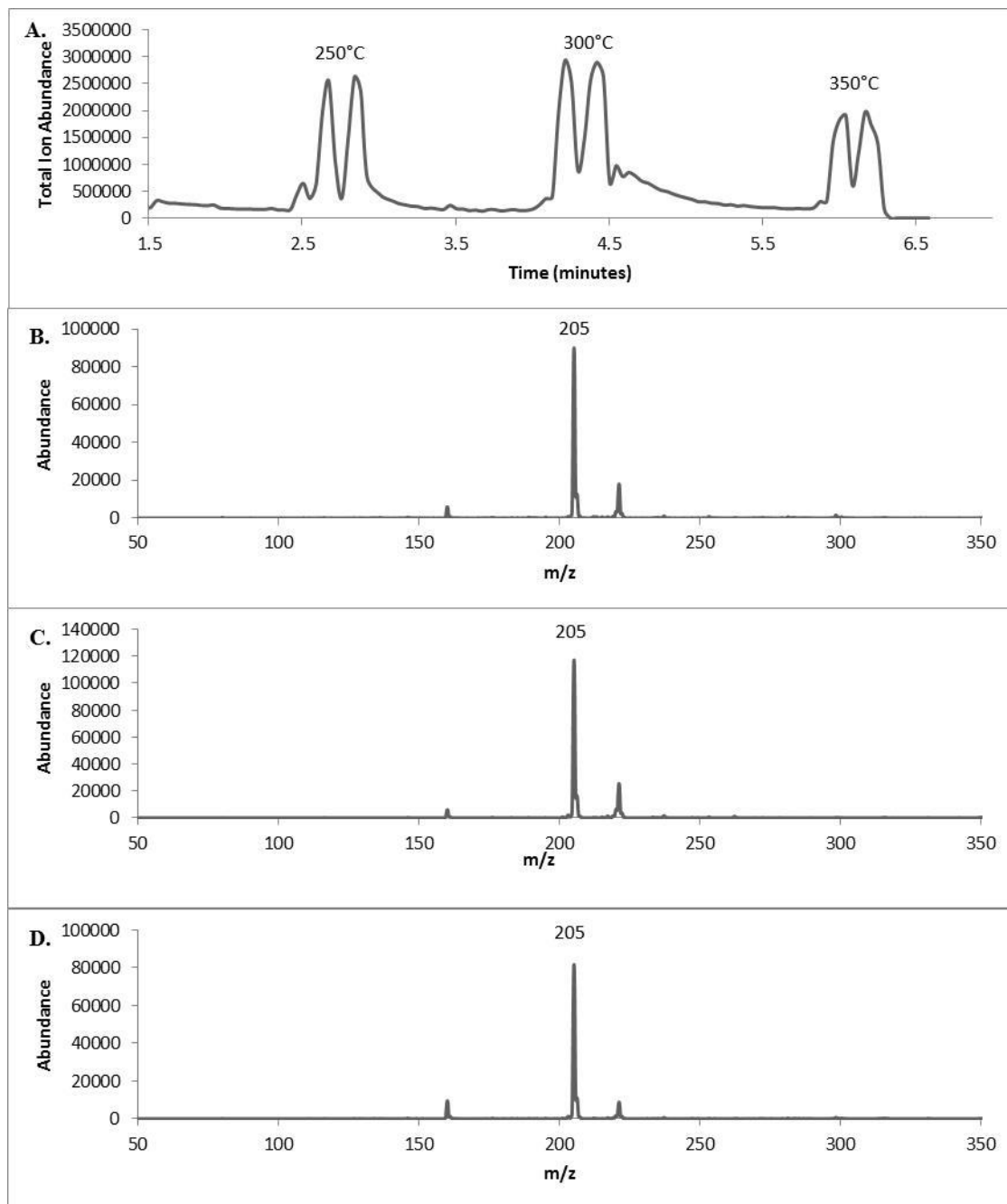


**Figure 21. A) Total Ion Chromogram of crushed cebil seeds at 250°C, 300°C, and 350°C. The split in the peaks represents two different spaces on the QuickStrip™ being passed in front of the DART source. Mass spectral data collected during DART source temperature profiles for the analysis of crushed cebil seeds at B) 250°C, C) 300°C, and D) 350°C.**



The analysis of *Voacanga africana* seeds produced very similar results with a source temperature of 300 and 350°C. The main ions of interest for these seeds were voacamine, voacangine, tabersonine, and ibogaine which have  $[M+H]^+$  values of  $m/z$  705, 369, 337, and 311, respectively. **Error! Reference source not found.** Although the TIC is not shown, the total abundance of ions remained approximately the same as the source temperature is increased from 250°C to 300°C and tended to decrease at 350°C. Ion abundance may be an important trend to note, but the mass spectral data must be considered, as the total abundance of ions does not necessarily correlate to the ions of interest present, and ion abundance can vary greatly with DART. Differences in background noise and the signal to noise ratio must be considered in order to determine the optimal source temperature for *Voacanga*. As can be seen in Figure 22, the abundance of the peak at  $m/z$  337 is the most abundant peak at all three source temperatures. At 300°C, the abundance of  $m/z$  337 is the greatest and the peak at  $m/z$  369 is present. In addition, a peak at  $m/z$  353 is present. Although this could not be associated with any compounds known to be main components in the seeds, the ion may be due to akuammidine, which has a molecular weight of 352 g/mol. Akuammidine is not well documented as being a component of *Voacanga Africana* seeds; however it is reported to be a compound in other *Voacanga* species<sup>71</sup>. The optimal source temperature for *Voacanga* was determined to be 300°C, although 250°C was sufficient to ionize the analytes of interest. The two additional peaks in the spectrum collected with a source temperature of 250°C could not be associated with any known compounds. Although voacamine and ibogaine are also present in the *Voacanga africana* seeds, no ions were

detected that could be associated with either of the compounds. The absence of expected compounds may be due to the inability of DART to ionize these compounds, or the compounds may have been present in such low concentrations that they were not detected using this method. It is also possible that voacamine and ibogaine were not present in the sample.

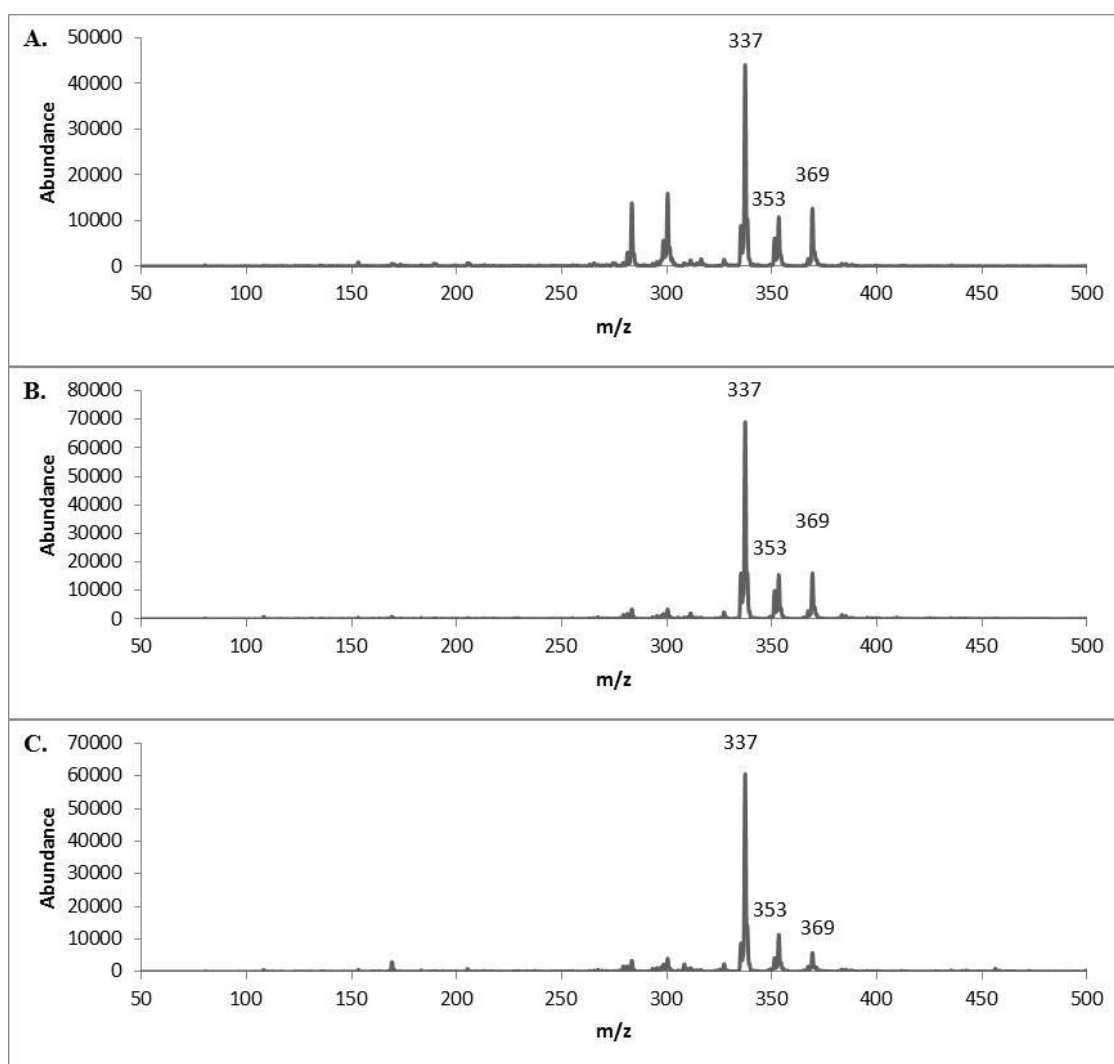


**Figure 22. Mass spectral data collected during DART source temperature profiles for the analysis of crushed voacanga seeds at A) 250°C, B) 300°C, and C) 350°C.**

The main ion of interest in ololiuqui seeds was ergine which has an  $[M+H]^+$  value of  $m/z$  268 and ergometrine which would produce a peak at  $m/z$  326. As shown in Figure 23, the ion at  $m/z$  268 was most abundant relative to other ions when the source temperature was set to 350°C. Also, as the source temperature was increased, other ions that were present at the lower source temperature became less apparent.

Even as the source temperature was adjusted, no peak at  $m/z$  326 was detected. The absence may be due to a low concentration or absence of ergometrine in the sample of seeds analyzed, or that the analyte is unable to be ionized by DART within the specific plant matrix. Although the specifics of the exact plant matrix are unknown, many compounds have the ability to suppress the ionization of compounds that would ionize in alternative settings. Ion suppression effects are observed when there are analytes that are preferentially excited by the DART source, reducing the ability of the analyte of interest to be detected. Smaller molecular weight compounds may be suppressed by larger compounds, and polar compounds are more susceptible to ion suppression effects<sup>72,73</sup>. Experiments could be designed in which the analyte of interest is isolated from the plant matrix and then analyzed. The ion abundance should increase as there are no matrix effects limiting the detection of the ions.

Although the identity of the other peaks is unknown, the detection and identification of ergine is essential for the purposes of drug identification in a forensic setting.

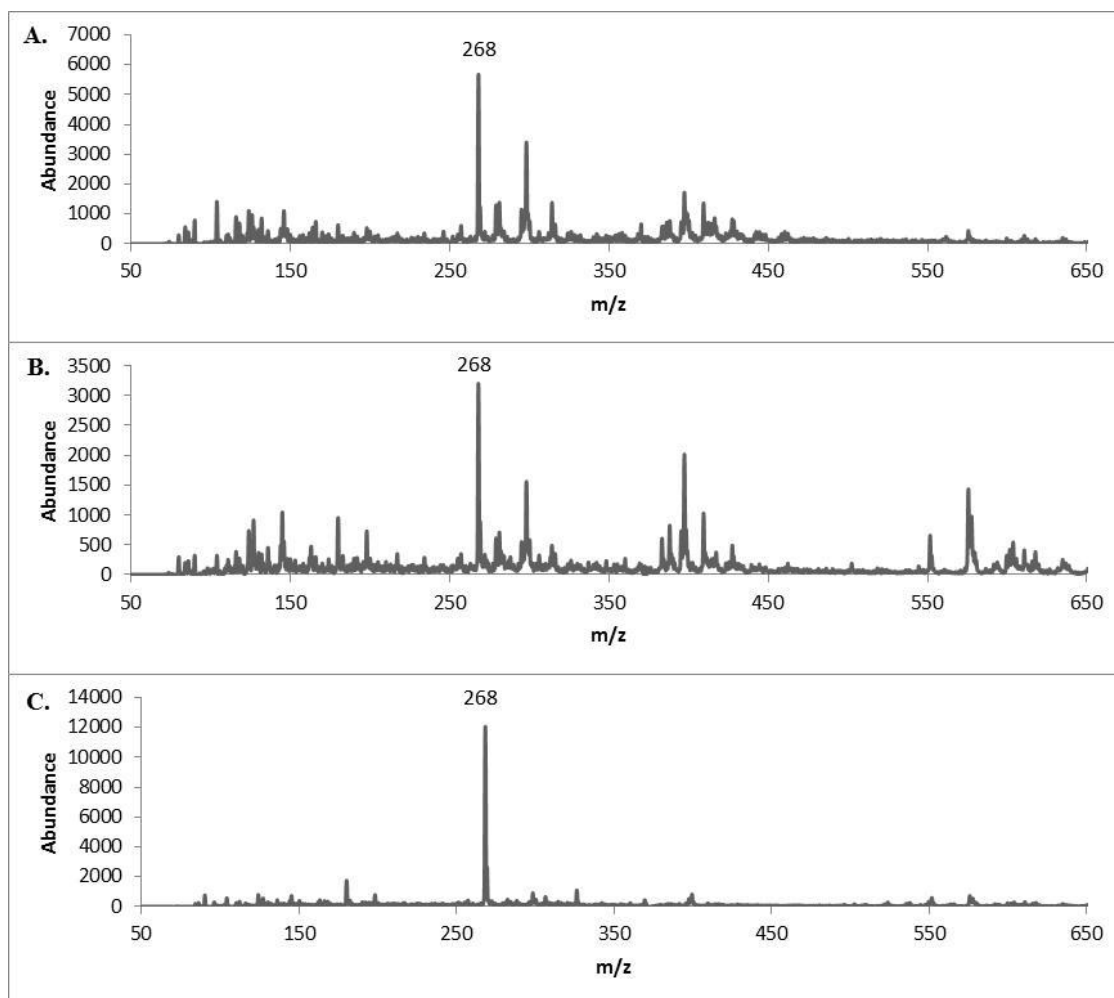


**Figure 23. Mass spectral data collected during DART source temperature profiles for the analysis of crushed ololiuqui seeds at A) 250°C, B) 300°C, and C) 350°C.**

Similar to ololiuqui seeds, the main ions of interest for morning glory seeds were ergine and ergometrine/ergonovine which have  $[M+H]^+$  values of  $m/z$  268 and 326, respectively. As shown in Figure 24, the ion at  $m/z$  268 was present at all three temperatures, but was most abundant when the source temperature was 350°C. The ion at  $m/z$  326 was not distinguishable from the baseline until the source temperature reached 350°C. At lower source temperatures, the mass spectrum contained a significant number

of peaks whose identities were unknown, indicating that there are other compounds present in the seeds that ionize more readily than what is suspected to be ergometrine. This may be useful in species determination or aiding in the determination of origin, but not for the purpose of identifying potential drugs of abuse. Not only does ergometrine become present when the source temperature reaches 350°C, the number of other ions present decreases, making the ions of interest more apparent, which may be due to the lack of thermal stability of the compounds as the carrier gas temperature was increased. The optimal source temperature for the analysis of morning glory seeds was determined to be 350°C even though an ion at  $m/z$  359 becomes apparent and cannot be associated with a specific analyte present in the seeds.

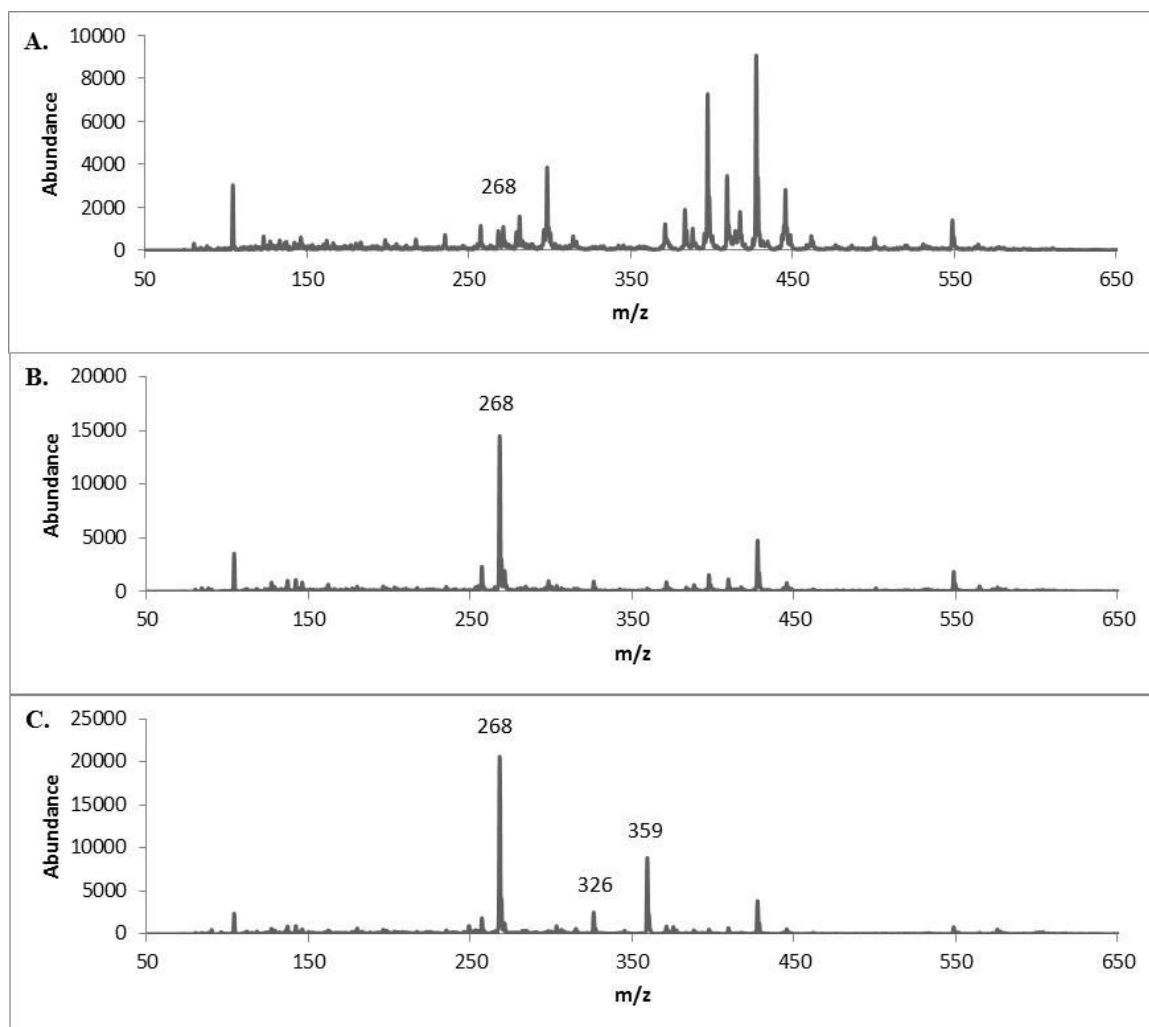


**Figure 24. Mass spectral data collected during DART source temperature profiles for the analysis of crushed morning glory seeds at A) 250°C, B) 300°C, and C) 350°C.**

Syrian rue seeds contain harmine and harmaline which have  $[M+H]^+$  values of  $m/z$  213 and 215, respectively. As shown in Figure 25, peaks at  $m/z$  213 and 215 were present at all three source temperatures, indicating that the compounds ionize relatively easily by DART. Also, it can be noted that as the source temperature increased, the abundance of harmine in comparison to harmaline decreased. Although harmaline is known to be

oxidized to form harmine in the presence of heat<sup>74</sup>, no explanation for the reverse reaction was found. Due to the drastic decrease in the abundance of the peak at  $m/z$  213, the optimal source temperature for analysis of Syrian rue seeds was determined to be 250°C. Like with many of the other samples, peaks are present that cannot be associated with any known components of the seed.

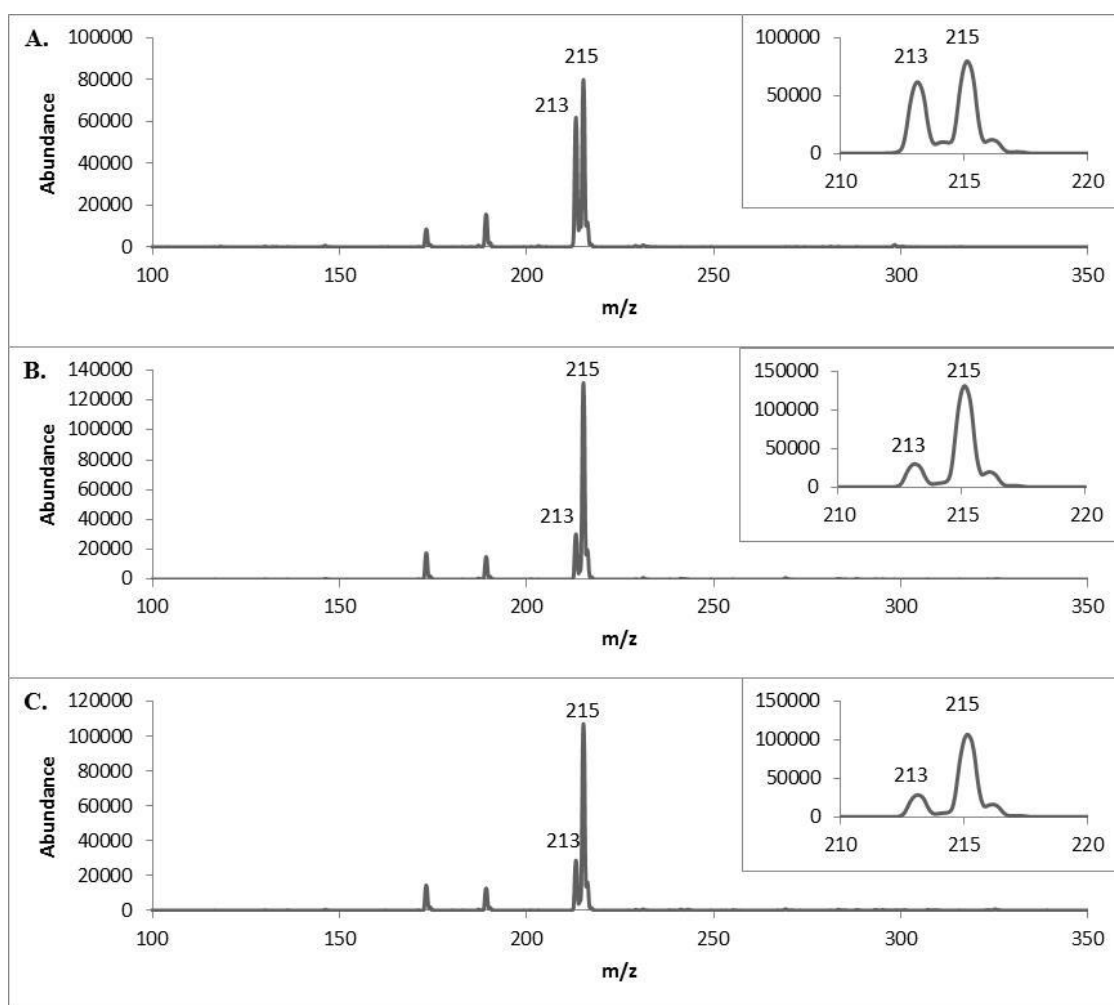


**Figure 25.** Mass spectral data collected during DART source temperature profiles for the analysis of crushed Syrian rue seeds at A) 250°C, B) 300°C, and C) 350°C. The MS data inserted in the top right corner is zoomed in on the region from 210 to 220 $m/z$  to show the ions of interest.

The African dream herb seeds were unique in that no compounds of interest were known before analysis. Determination of the optimal source temperature in this case was based on the signal to noise ratio as well as the abundance of the ions that were most prominent in the spectra. Based on the analysis of previous samples and studies, any hallucinogenic compounds present at significant concentrations would be among the most abundant ions produced. As shown in Figure 26, the peak at  $m/z$  142 was seen at all temperatures in relatively high abundances. Additionally, a peak at  $m/z$  116 was present at all three source temperatures. Because these peaks were seen at all three source temperatures and were the most abundant ions in each of the spectra, remainder of the analysis was focused on the identification of the ions. Therefore, the optimal source temperature for the analysis of African dream herb seeds was 300°C, assuming  $m/z$  142 and 116 were the ions of interest. Upon further investigation on common components in plant materials, proline was reported to oftentimes accumulate in the seeds<sup>75</sup>. Proline is an amino acid with a molecular weight of 115g/mol, which would exhibit an  $[M+H]^+$  peak at 116g/mol<sup>76</sup>. Further testing would be necessary to confidently identify proline within the African dream herb samples.



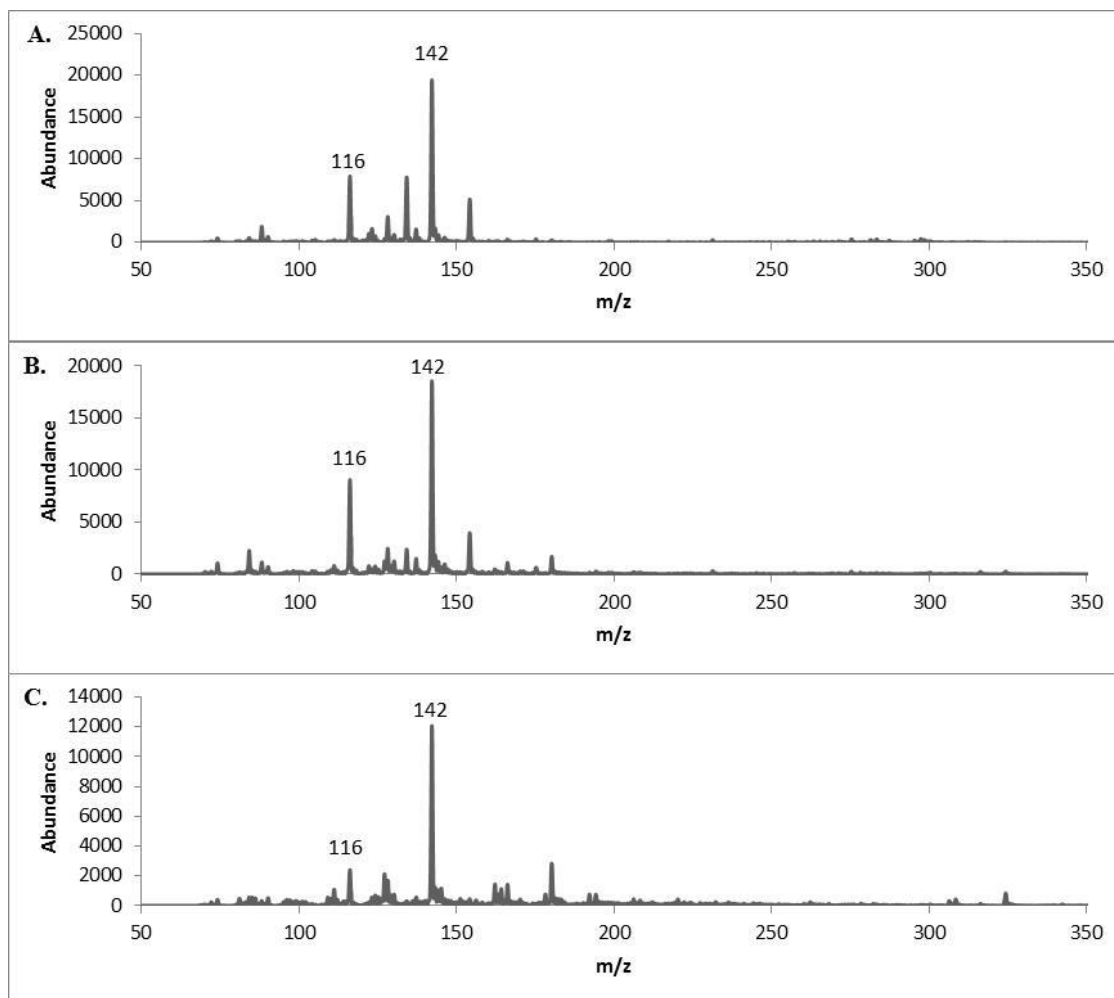


**Figure 26. Mass spectral data collected during DART source temperature profiles for the analysis of crushed African Dream Herb seeds at A) 250°C, B) 300°C, and C) 350°C.**

Cowage seeds reportedly contain a variety of compounds including DMT, L-dopa, serotonin, and nicotine. Each of these would result in  $[M+H]^+$  values of  $m/z$  189, 198, 177, and 163, respectively. As can be seen in Figure 27, when the source temperature was 250°C, the most abundant peaks occurred at  $m/z$  116 and 298. As the source temperature increased, the peak at  $m/z$  116 became the only ion present, which may indicate ion suppression or that the other compounds are not as thermally stable as

the source temperature is increased. The species at  $m/z$  116 may ionize so readily that it does not allow the other analytes of interest to be observed. At this point, the identity of this ion is unknown; however, as discussed above, it may be due to proline accumulation in the seeds<sup>75</sup>. Another possibility is that the ions of interest in cowage seeds are not readily ionizable by DART given the complex plant matrix. Identification of the other analytes of interest may have been possible by first preparing a sample extract in methanol to remove the analytes from the plant matrix, but this was not done in this thesis, as the goal was to minimize the sample preparation requirements.

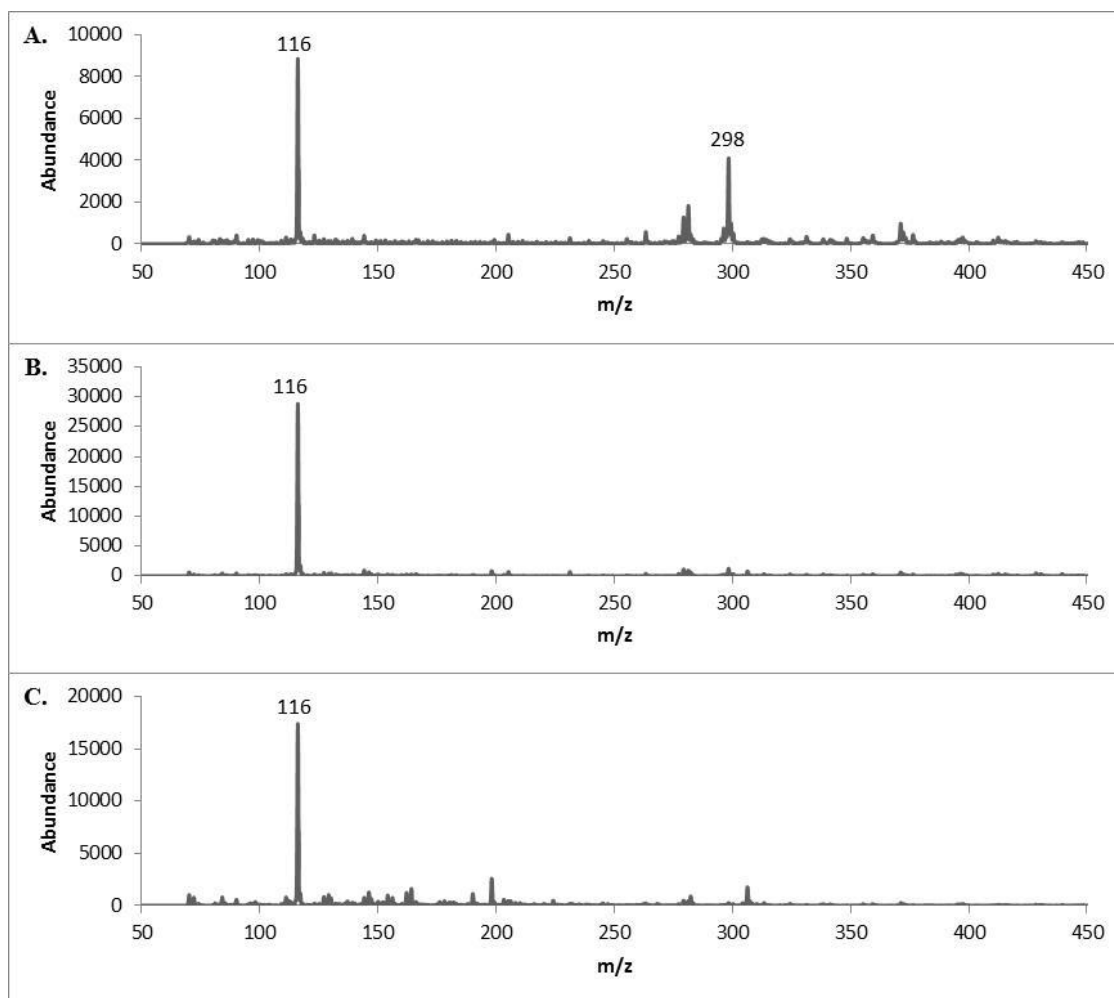


**Figure 27. Mass spectral data collected during DART source temperature profiles for the analysis of crushed Cowage seeds at A) 250°C, B) 300°C, and C) 350°C.**

Henbane seeds reportedly contain atropine and hyoscyamine which would result in a  $[M+H]^+$  peak at  $m/z$  290. Although this method would not differentiate between atropine and hyoscyamine, detection of either compound is important in the preliminary identification of the henbane seed. At all three source temperatures, other peaks are present at high abundances. As the temperature was increased, the number of other ions decreased, but the peak at  $m/z$  308 remained relatively abundant in comparison to the ion

of interest at  $m/z$  290, as shown in Figure 28. The other peaks are likely due to other compounds present in henbane seeds due to the lack of chromatographic separation by DART. The identification of all peaks present in the spectra was outside the scope of this thesis, although it may be an area of interest to aid in identification of unknown samples when the amount of the target drug analyte is found in lower abundances.

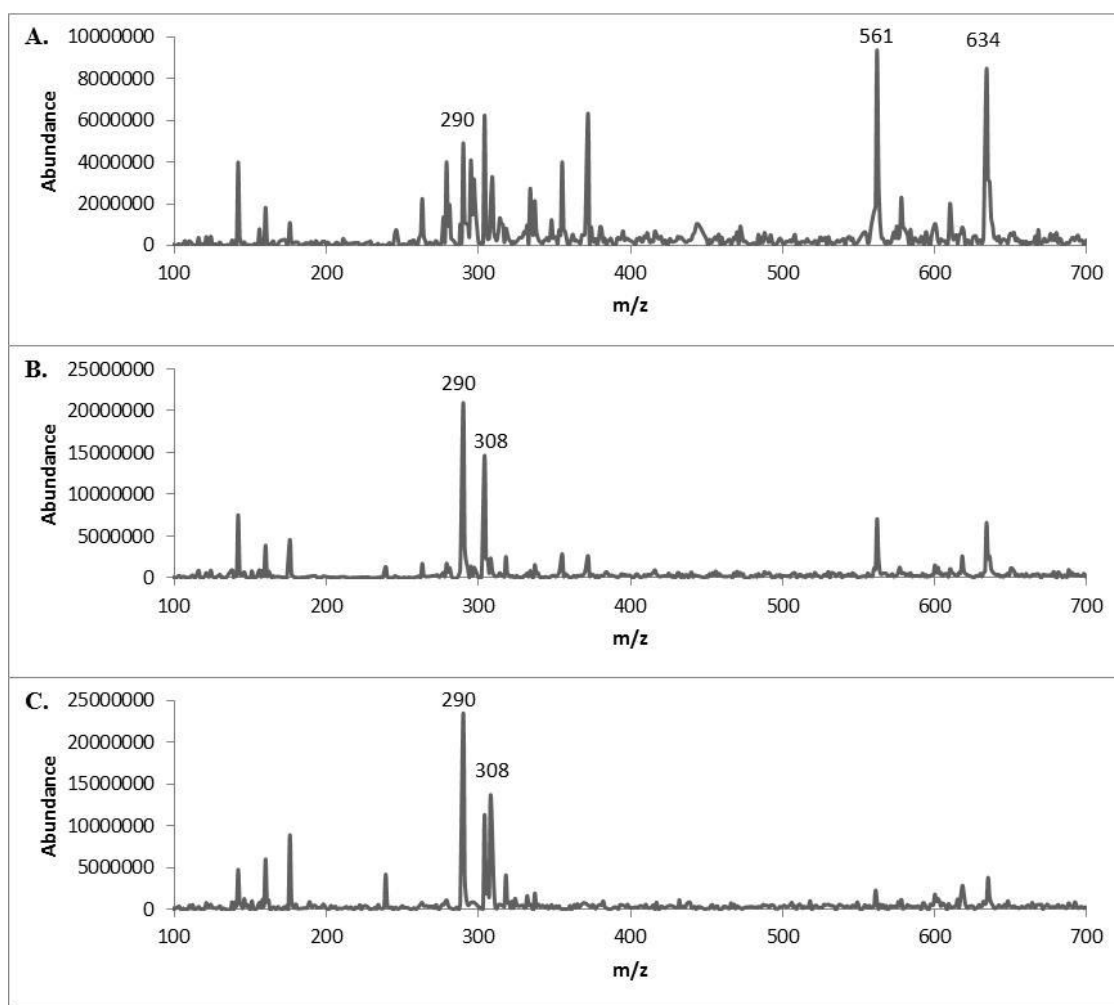


**Figure 28.** Mass spectral data collected during DART source temperature profiles for the analysis of crushed Henbane seeds at A) 250°C, B) 300°C, and C) 350°C.

Hawaiian Baby Woodrose seeds are reported to contain ergine and ergometrine (ergonovine) which would result in  $[M+H]^+$  peaks at  $m/z$  268 and 326, respectively. As can be seen in Figure 29, the spectrum for the Hawaiian strain lacked clearly defined peaks when the source temperature was 250°C. As the source temperature was increased, the ions of interest become distinguishable from the baseline. Both analytes of interest ( $m/z$  268 and 326) were present in high abundances at source temperatures of both 300°C and 350°C. However, the abundance was significantly higher at 350°C, which was determined to be the optimal source temperature for the analysis of Hawaiian Baby Woodrose seeds - Hawaiian strain. Similar to the data for other seeds, ions were present that were not associated with the drug analytes and were unable to be identified.

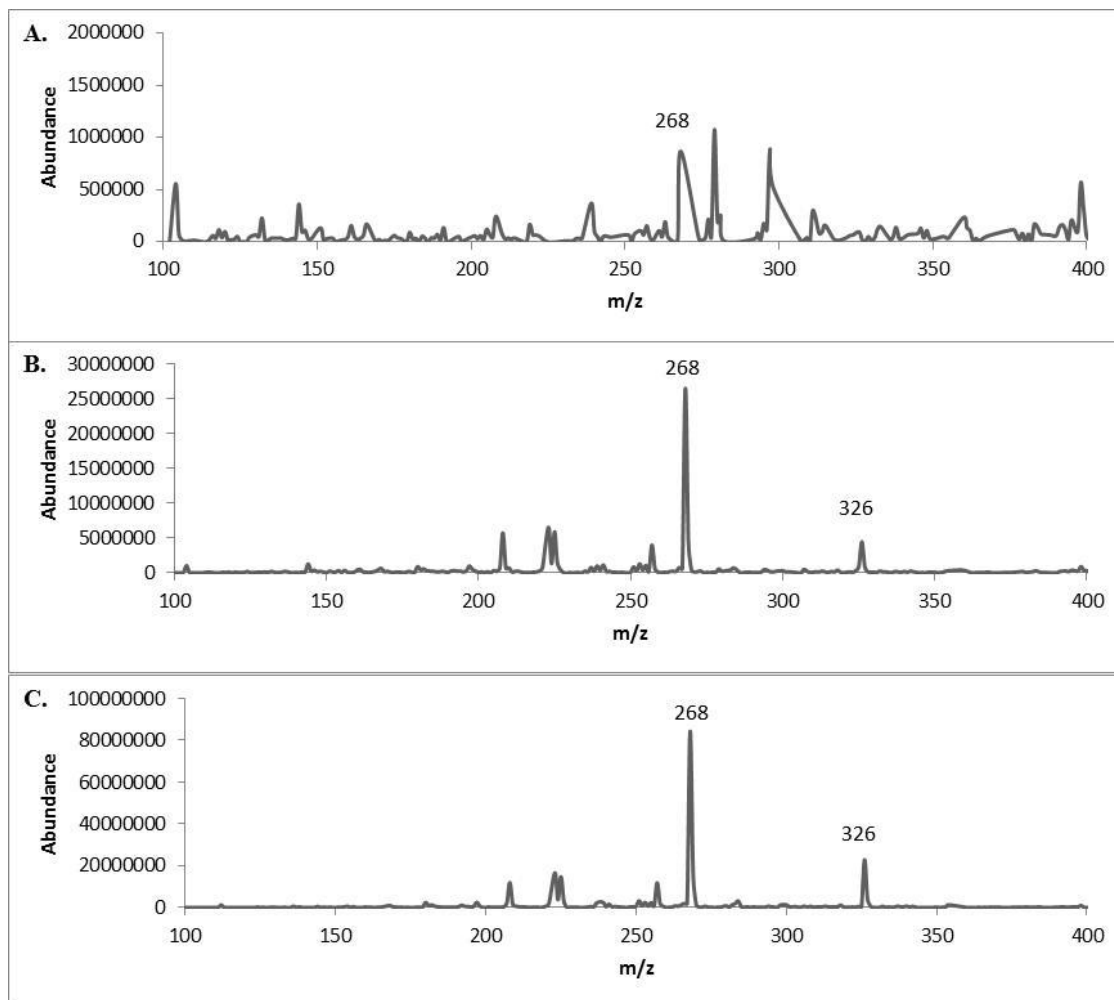


**Figure 29. Mass spectral data collected during DART source temperature profiles for the analysis of crushed Hawaiian Baby Woodrose Hawaiian strain seeds at A) 250°C, B) 300°C, and C) 350°C.**

The analysis of the Hawaiian Baby Woodrose seeds - Indian strain did not show any significant differences as the source temperature was increased, as shown in Figure 30. At 250°C, the ions of interest at  $m/z$  268 and 326 were abundant and no other peaks interfered with the spectrum. As the source temperature was increased, the abundance of the peaks almost doubled and no additional peaks were observed. Because a source

temperature of 300°C and 350°C provided results that were essentially equal, either source temperature would be ideal for the analysis of the Indian strain.

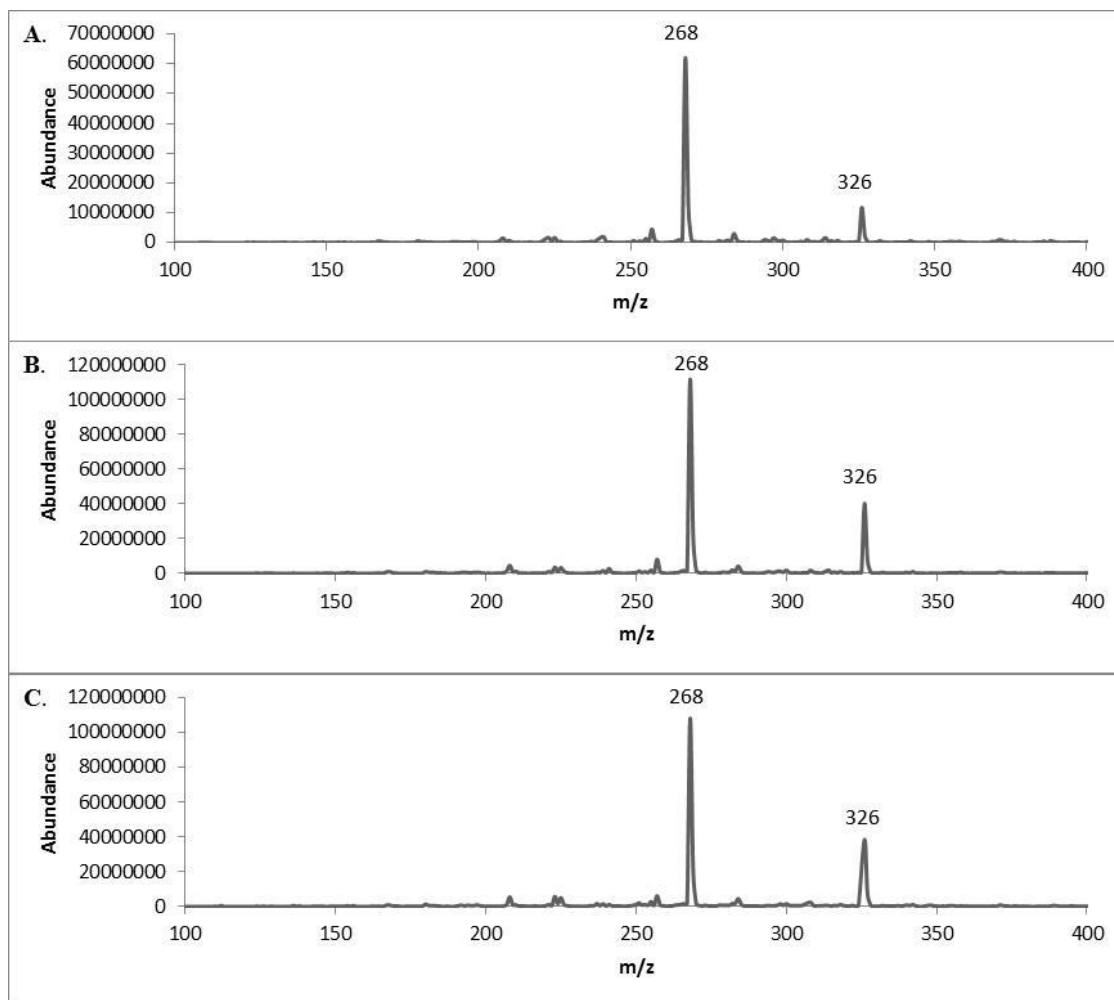


**Figure 30. Mass spectral data collected during DART source temperature profiles for the analysis of crushed Hawaiian Baby Woodrose Indian Strain seeds at A) 250°C, B) 300°C, and C) 350°C.**

The analysis of the Hawaiian Baby Woodrose seeds - Ghana strain provided results that were significantly different than the other two strains. As seen in Figure 31, numerous ions were present in addition to the ion of interest ( $m/z$  268). A peak at  $m/z$  326 was not apparent in any of the spectra, which may indicate that ergometrine is either not

present in the seeds or is present in concentrations below the limit of detection, or that ion suppression is occurring. In addition, the spectra obtained showed more significant baseline noise than was detected for the Hawaiian or Indian strains, which may be due to the nature of the sample and/or the concentration of the analytes of interest in this particular strain of seeds. Although, extraction and concentration procedures may have been helpful in detecting the analyte of interest, no further steps were performed as one of the goals was to reduce or eliminate the need to perform any extensive sample preparation measures and to decrease the time required for complete analysis. A source temperature of 350°C was used when analyzing the Ghana strain in subsequent tests.

All three of the Hawaiian Baby Woodrose seed samples were expected to exhibit the same analytes of interest when analyzed under similar conditions, but this was not the case, as can be seen in Figure 32 comparing the data collected for each of the strains at 350°C.



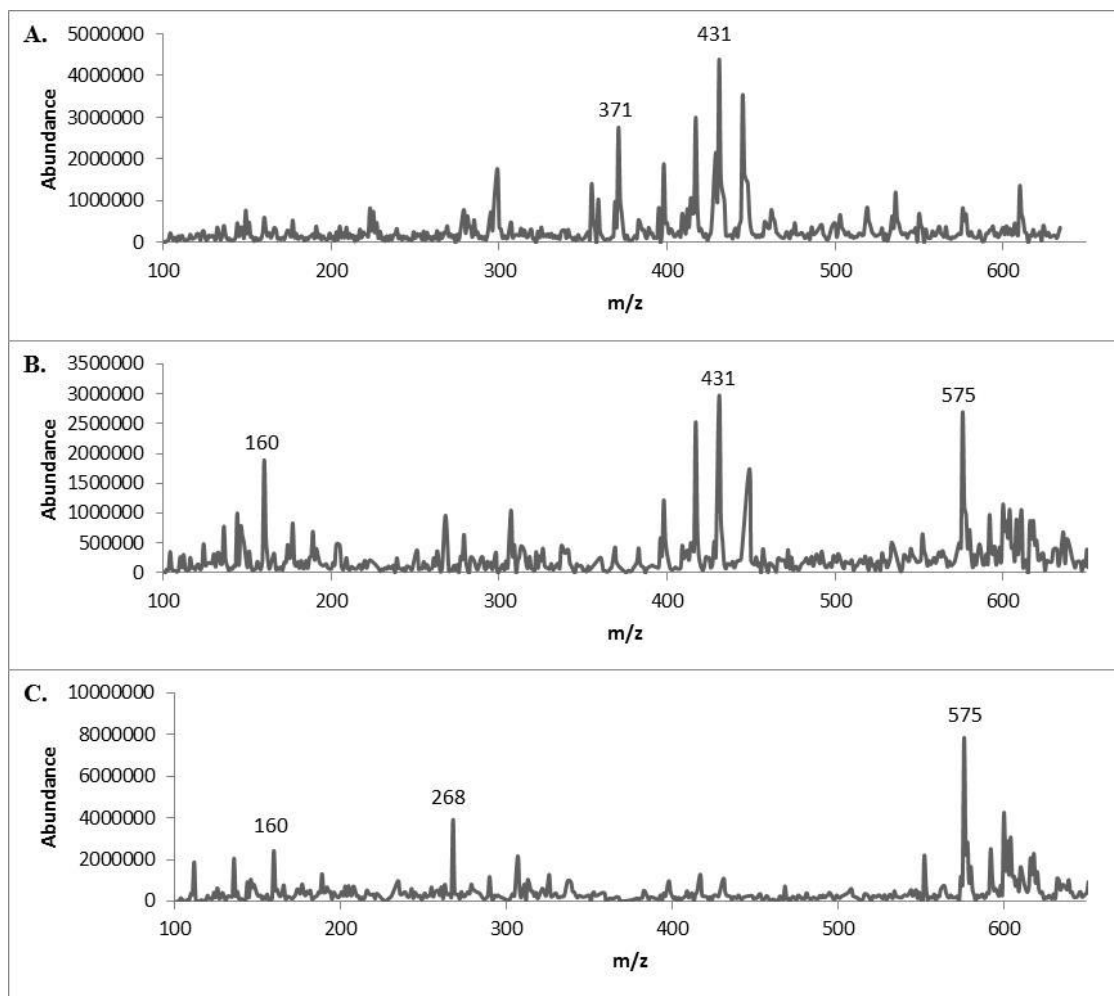


**Figure 31. Mass spectral data collected during DART source temperature profiles for the analysis of crushed Hawaiian Baby Woodrose Ghana Strain seeds at A) 250°C, B) 300°C, and C) 350°C.**

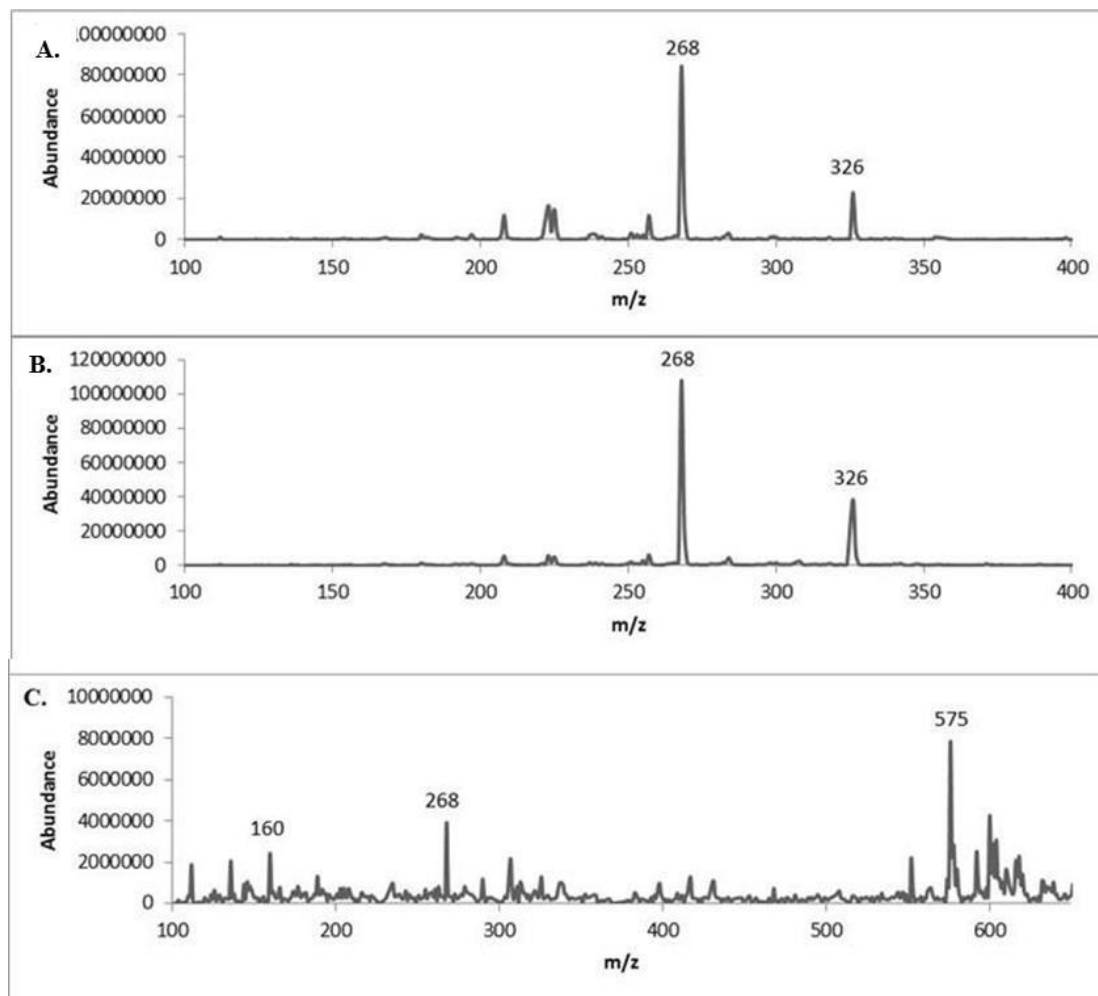


**Figure 32. Mass Spectral data collected with a DART source temperature 350°C for Hawaiian Baby Woodrose A) Hawaiian Strain, B) Indian Strain, and C) Ghana Strain.**

Intellect Tree seeds are reported to contain celastrine and paniculatin. Each of these compounds have two to three times more mass than the previously tested analytes, making them harder to ionize by DART, as DART is ideal for small, polar compounds. Celastrine would result in  $[M+H]^+$  of  $m/z$  573, and paniculatin would result in a  $[M+H]^+$  peak at  $m/z$  595. Both of these compounds are relatively unknown in terms of their chemical properties and pharmacokinetics. The analysis of the seeds with varying source

temperature can be seen in Figure 33. The analytes of interest were not observed at any of the source temperatures. Based on the structures (Figure 12) and molecular weights of the two analytes of interest, the compounds may not be ionized by DART and that the ions observed at  $m/z$  524 and 534 may be associated with other compounds present in the seeds or are fragments of larger unknown compounds. No resources were found to suggest any other compounds present in the seeds.

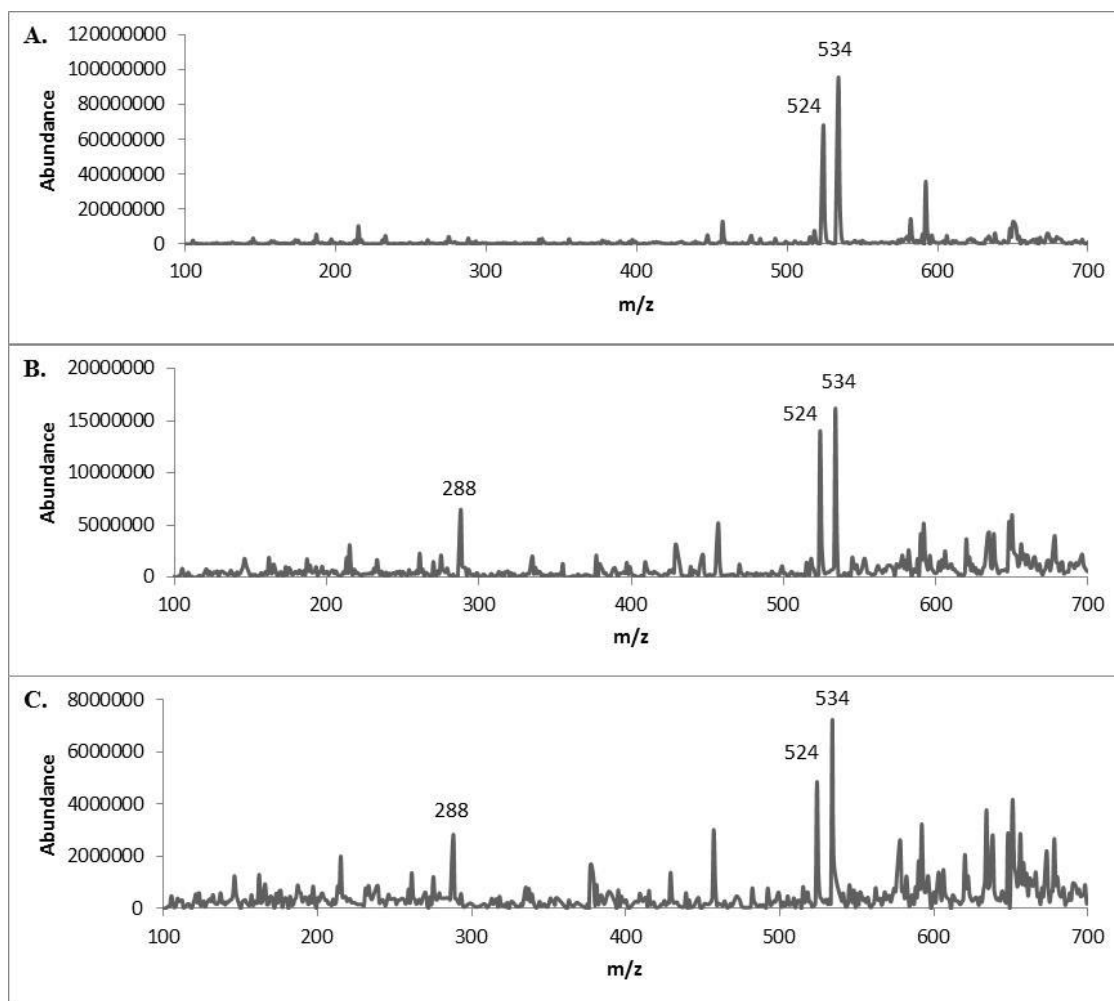


**Figure 33.** Mass spectral data collected during DART source temperature profiles for the analysis of crushed Intellect Tree seeds at A) 250°C, B) 300°C, and C) 350°C.

*Ephedra sinica* plant material is reported to contain a variety of compounds including ephedrine, pseudoephedrine, and norephedrine. Ephedrine and pseudoephedrine are diastereomers and cannot be differentiated from one another using mass spectrometry techniques alone. However, for the purposes of this study, detection and identification of either one was sufficient without knowing whether one or both compounds was being detected. Either ephedrine or pseudoephedrine would result in a  $[M+H]^+$  peak at  $m/z$  166. Norephedrine would result in a  $[M+H]^+$  peak at  $m/z$  152. As shown in Figure 34, neither of the analytes of interest were detected. The most abundant peak occurs at  $m/z$  128. The analyte of interest may not be present in the *Ephedra sinica* seeds, which would be consistent with other reports that state that the psychoactive properties are present in the leaves and stems of the plants rather than the seeds.

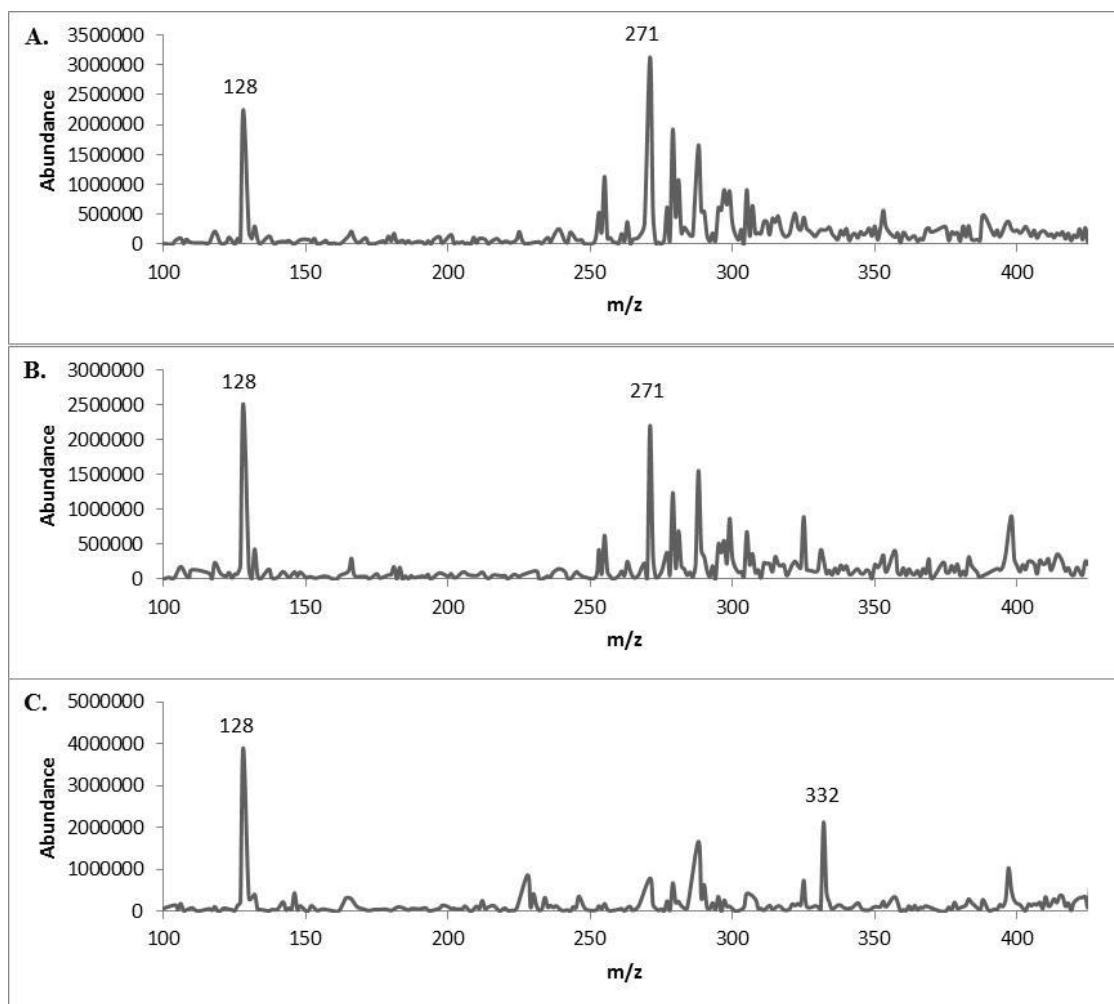


**Figure 34. Mass spectral data collected during DART source temperature profiles for the analysis of crushed *Ephedra Sinica* seeds at A) 250°C, B) 300°C, and C) 350°C.**

Mexican poppy seeds are reported to contain sanguinarine, dihydrosanguinarine, berberine and protopine. Sanguinarine and dihydrosanguinarine are the two most abundant compounds reportedly found in the seeds of the Mexican poppy. These compounds would result in  $[M+H]^+$  peaks at  $m/z$  333 and 334 respectively. Berberine would result in a  $[M+H]^+$  peak at  $m/z$  337 and protopine would be detected at  $m/z$  354. As

can be seen in Figure 35, the most abundant peak is observed at  $m/z$  334. The peak at  $m/z$  319 may be due to another analyte that is readily ionizable in the sample, or it may be a product of fragmentation due to the loss of a methyl group from the analyte at  $m/z$  334. Additional fragmentation information is necessary to draw any conclusions. Based on the abundance of the two peaks, it was determined that the optimal source temperature for the analysis of Mexican poppy seeds was 300°C.

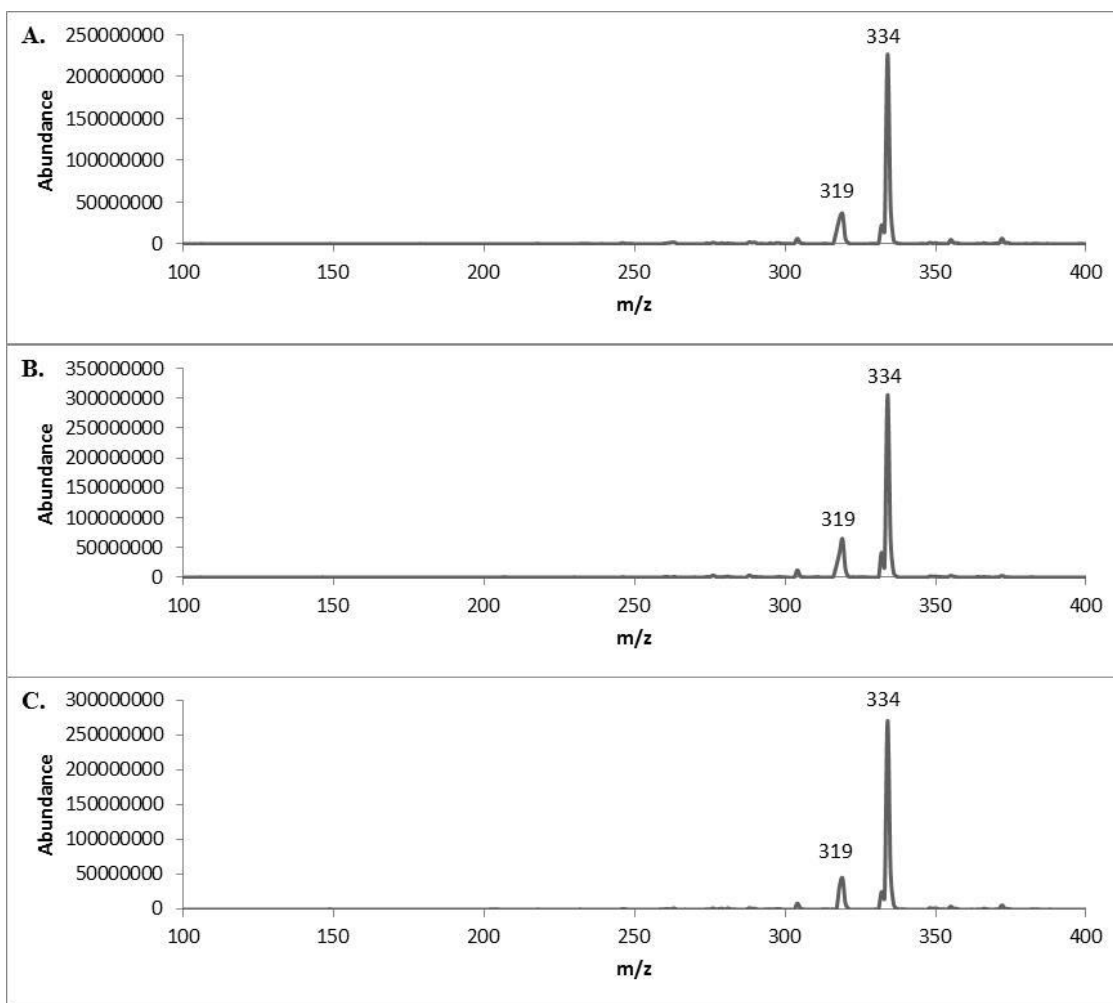


**Figure 35.** Mass spectral data collected during DART source temperature profiles for the analysis of crushed Mexican Poppy seeds at A) 250°C, B) 300°C, and C) 350°C.

### 3.3 MS<sup>2</sup> Fragmentation Data

After the source temperatures were optimized for the analytes of interest, the next step in identifying the compounds found in each of the seed samples was to perform MS<sup>n</sup> fragmentation using a quadrupole ion trap. Each ion of interest was fragmented at the optimized source temperatures, while adjusting the percent collision energy (CE) to maximize fragmentation, in order to provide as much unique structural information as possible. Fragmentation patterns were determined for each of the analytes and compared to the literature for each specific compound.

For the cebil seeds, analysis was performed at 300°C and the ion of interest was  $m/z$  205, which was preliminarily associated with bufotenine. The fragment at  $m/z$  205 was imparted with 20%, 23%, and 25% collision energy. At 23% CE, the ion at  $m/z$  205 is still present, but is reduced in abundance almost to the baseline noise as the CE is increased to 25%. A CE of 25% was ideal for fragmentation of the  $m/z$  205 peak, as is seen in Figure 36.

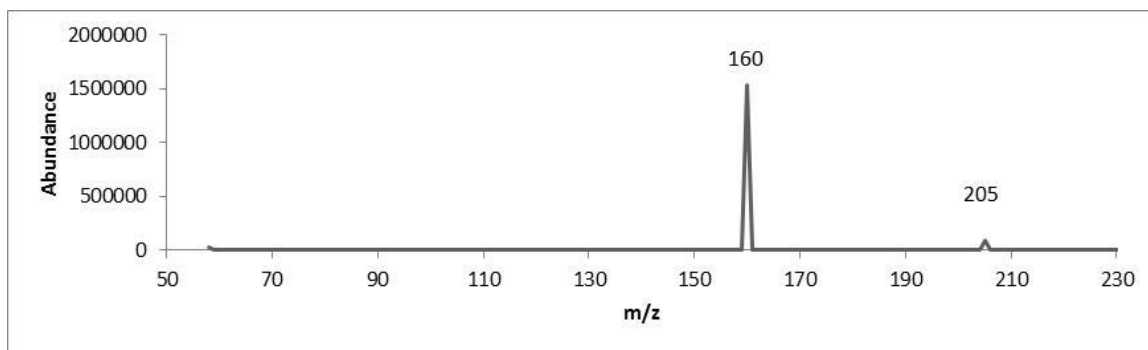


**Figure 36. MS<sup>2</sup> fragmentation data of  $m/z$  205 for crushed cebil seeds with a normalized collision energy of 25%.**

The main fragment produced was at  $m/z$  160, which can be explained due to the loss of the  $-(\text{CH}_3)_2\text{NH}$  side chain. Based on previous research, bufotenine, like most compounds, behaves in a specific manner when exposed to various ionization and fragmentation conditions. McClean et al. proposed the fragmentation pattern of bufotenine for electrospray ionization/ion trap mass spectrometry as shown in Figure 37<sup>23</sup>. When compared to other studies that involve the fragmentation of bufotenine, the peak at  $m/z$  160 further fragments to form a fragment at  $m/z$  132, but the pattern was not observed using this method.

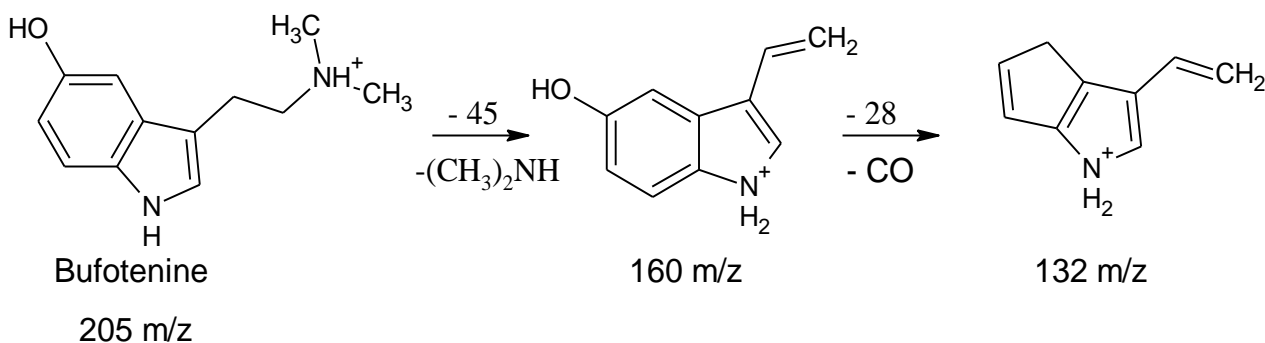


**Figure 37. Suggested fragmentation pattern of bufotenine by electrospray ionization – ion trap mass spectrometry as suggested by McClean et al.<sup>23</sup>**

Analysis of *Voacanga africana* seeds was performed at 250°C and the ions of interest were  $m/z$  337, 353, and 369, which were preliminarily associated with tabersonine, akuammidine, and voacangine, respectively. The peak at  $m/z$  337 was imparted with 28%, 30%, and 32% CE. At a CE of 30% the peak at  $m/z$  337 was still present, but other fragments became more abundant. As the CE was increased to 32%, the abundance of the peak at  $m/z$  337 decreased and was only slightly above the baseline



noise, as shown in Figure 38. In both cases, the most abundant fragment peaks occur at  $m/z$  305 and 228. No studies could be found that documented the fragmentation patterns for tabersonine to support the identification. The peak at  $m/z$  353 was imparted with 20%, 25%, and 30% collision energy. At a CE of 20% and 25%, no fragmentation occurred. When the CE was increased to 30% the peak at  $m/z$  353 was still apparent, but other fragments became more abundant, as shown in Figure 39. The most abundant fragment peaks occurred at  $m/z$  321, 228, 210, and 144. No studies could be found that documented the fragmentation patterns for akuammidine to support a positive identification. The peak at  $m/z$  369 was bombarded with a CE of 30%, which resulted in fragment peaks at  $m/z$  337, 325, 309, and 210 as shown in Figure 40. No studies were found that documented the fragmentation patterns for voacangine to support identification. The fragment resulting in a loss of 60 mass units to produce  $m/z$  309 may be the result of the loss of the protonated  $\text{COOCH}_3$  substituent. Additionally, all three parent ions produced a fragment that was the result of a loss of 32 mass units, suggesting that the same fragmentation mechanism is occurring with each compound.

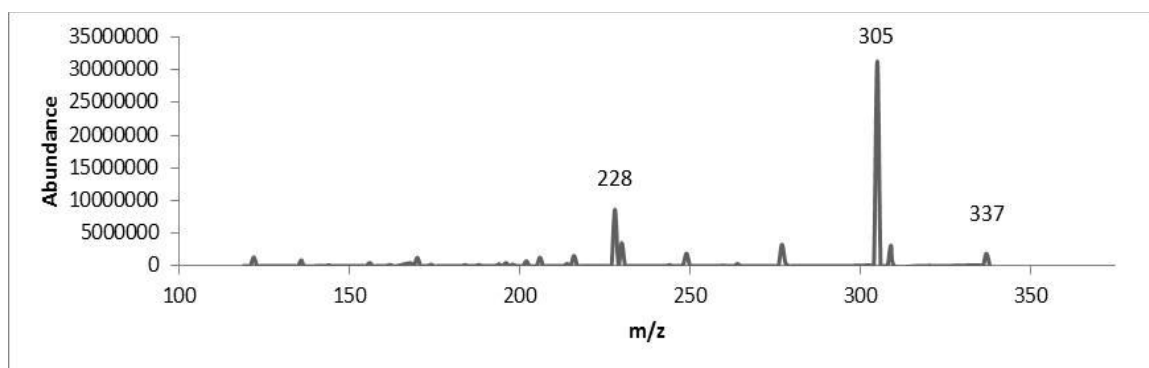


**Figure 38. MS<sup>2</sup> fragmentation data of  $m/z$  337 for crushed *Voacanga africana* seeds with a normalized collision energy of 32%.**

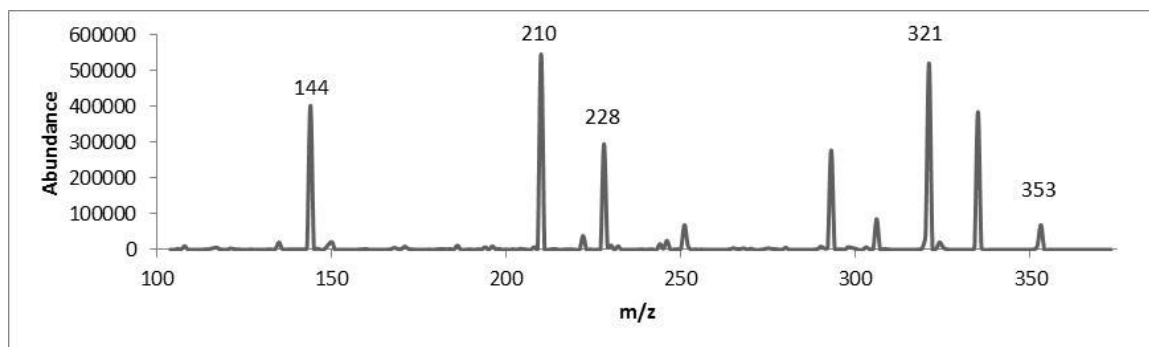


**Figure 39.** MS<sup>2</sup> fragmentation data of *m/z* 353 for crushed *Voacanga africana* seeds with a normalized collision energy of 30%.

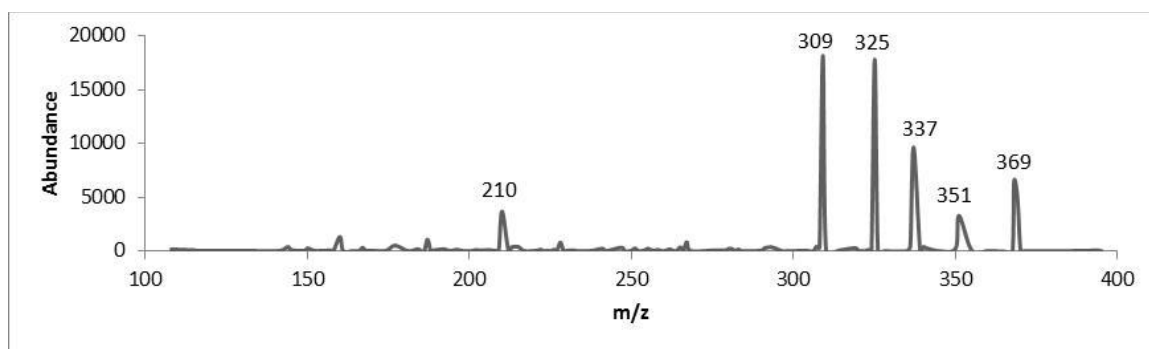


**Figure 40.** MS<sup>2</sup> fragmentation data of *m/z* 369 for crushed *Voacanga africana* seeds with a normalized collision energy of 30%.

The analytes of interest in ololiuqi seeds were ergot alkaloids, specifically ergine and ergometrine which have  $[M+H]^+$  values of *m/z* 268 and 326. However, no peaks associated with ergometrine were detected in the initial experiments. Only the peak at *m/z* 268 was investigated in this part of the experiment, in an attempt to further identify it as ergine. Normalized collision energies of 30% and 38% were used to fragment the analyte. At a CE of 30%, the peak at *m/z* 268 was still abundant, although a significant fragment peak at *m/z* 223 was present. As the CE was increased to 38%, the abundance of the fragment ion increased and the ion at *m/z* 268 significantly decreased almost into the baseline noise, as expected (Figure 41). In addition, a peak at *m/z* 208 becomes apparent.

Based on known fragmentation patterns, the ion at  $m/z$  268 can be identified as ergine. The fragment at  $m/z$  223 can be explained by the loss of the amide side chain, and the fragment at  $m/z$  208 is due to the loss of the methyl attached to the amine, as shown in Figure 42.

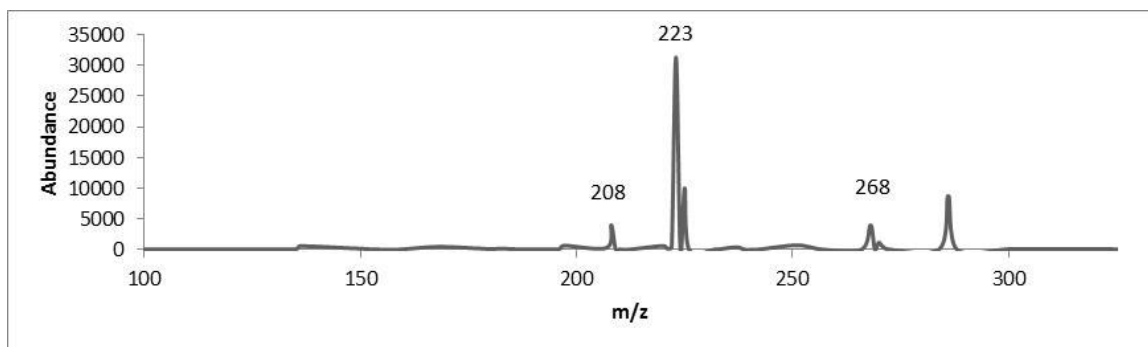


**Figure 41. MS<sup>2</sup> fragmentation data of  $m/z$  268 for crushed ololiuqui seeds with a normalized collision energy 38%.**

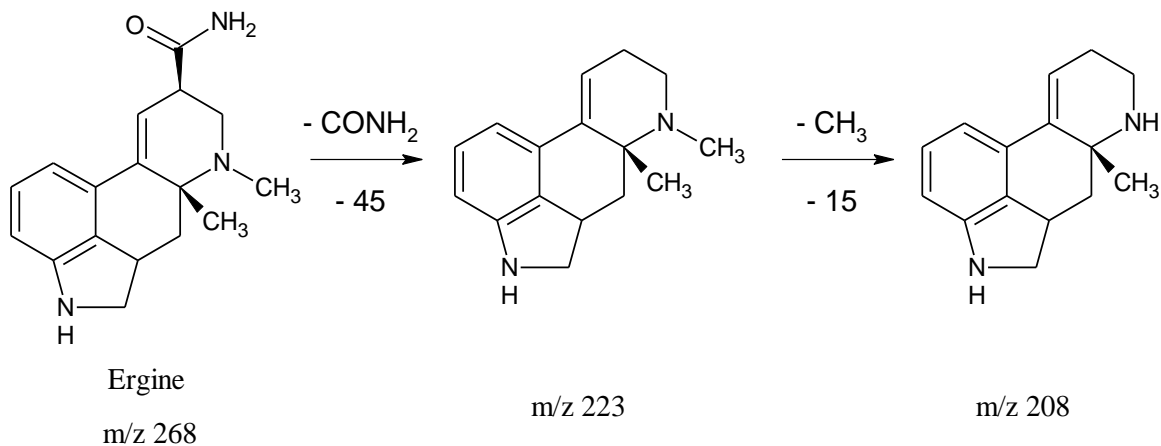


**Figure 42. Suggested fragmentation of ergine as reported by Lehner et al. <sup>70</sup>.**

Similar to the ololiuqui seeds, the analytes of interest in morning glory seeds were ergine and ergometrine. The peaks at  $m/z$  268 and 326 were investigated in this part of the experiment, in an attempt to further identify the analytes as ergine and ergometrine,

respectively. At a normalized CE of 30%, the peak at  $m/z$  268 was not very abundant and a significant fragment peak at  $m/z$  223 was present, as seen in Figure 43. A fragment at  $m/z$  208 was also observed. Since it is the same compound, the fragmentation pattern observed for ergine in morning glory seeds was expected to be very similar to that of the compound in ololiuqui seeds (Figure 42). The fragmentation of the analyte at  $m/z$  326 was most prevalent with a CE of 32%, and produced fragment ions at  $m/z$  308, 283, 265, 251, 223, and 208 (Figure 44). The ions produced were consistent with past reports on fragmentation patterns of ergometrine. The peak at  $m/z$  223 is due to the loss of the side chain, and the peak at 208 is the result of the loss of the methyl group attached to the amine, as shown in Figure 45<sup>70</sup>. Although identification of all peaks in the spectra was outside the scope of this thesis, some predictions can be offered based on the structure and what is known about ergot alkaloids. The fragment seen at  $m/z$  308 may be due to the loss of water from the end of the compound, which is common in the fragmentation of ergot alkaloids<sup>70</sup>. The peak at  $m/z$  197 may be due to the 223 fragment losing an alkyne, as suggested by Lehner et al.<sup>70</sup>.

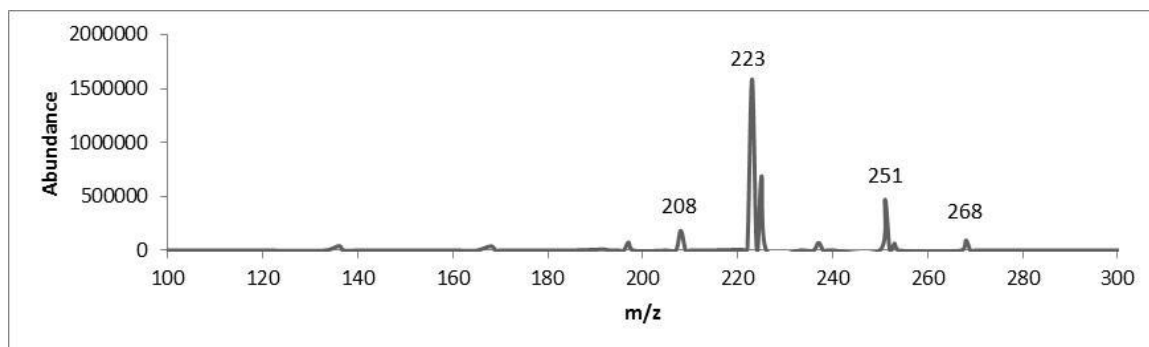


**Figure 43. MS<sup>2</sup> fragmentation data of  $m/z$  268 for crushed morning glory seeds with a normalized collision energy of 30%.**

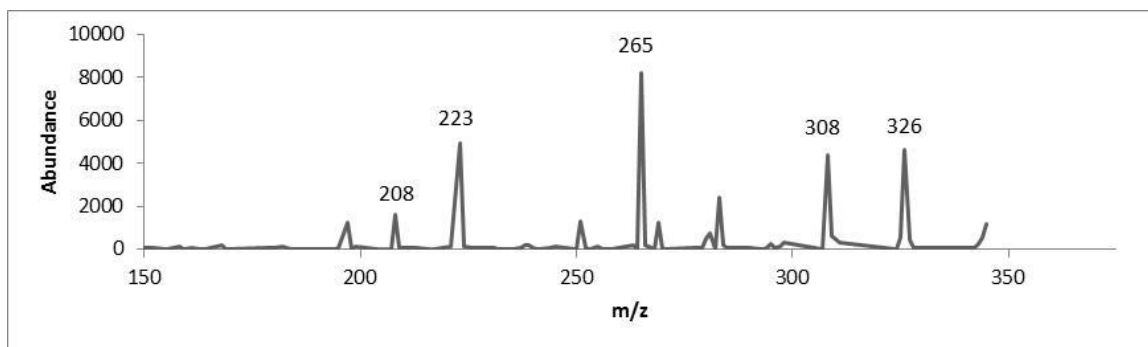


**Figure 44.** MS<sup>2</sup> fragmentation data of *m/z* 326 for crushed morning glory seeds with a normalized collision energy of 32%.

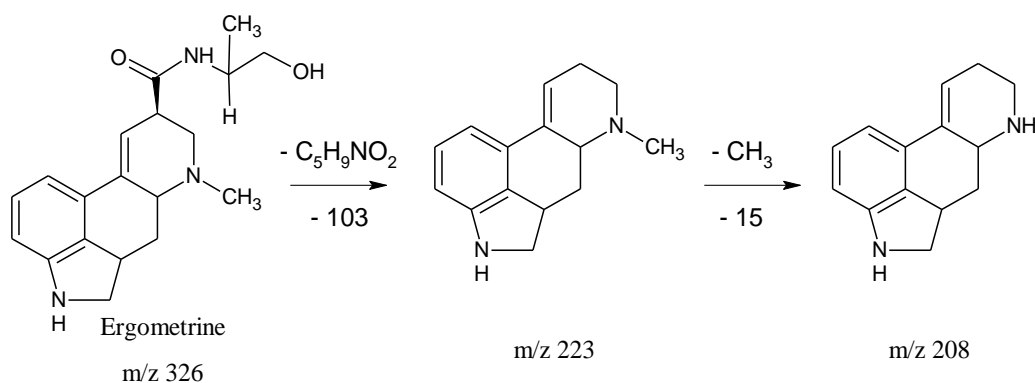


**Figure 45.** Suggested fragmentation pattern for ergometrine (*m/z* 326) to form fragments at *m/z* 223 and 208.

Syrian rue seeds are reported to contain harmine and harmaline, which produce peaks at *m/z* 213 and 215, respectively. A source temperature of 250°C was proven sufficient to ionize both compounds, as shown in the previous experiments, and was used for MS<sup>2</sup> experiments. Harmine was fragmented with normalized collision energy of 55% and 60%, as seen in Figure 46. At 55%, the peak at *m/z* 213 remained the most abundant and showed very little fragmentation, although a small fragment at *m/z* 198 was present. As the CE was increased to 60%, the fragment peak at *m/z* 198 became abundant and the peak at *m/z* 213 decreased into the baseline. A CE between 55% and 60% is ideal for the fragmentation of harmine. Based on the structure of harmine, the fragment observed can

be associated with the loss of the terminal methyl of the ether functional group, as shown in Figure 47. Studies have shown that harmine is often metabolized to form harmol, which results in a peak at  $m/z$  198<sup>37,77,78</sup>. Due to the similarities in the data collected in this study and the data collected in other studies, the analytes can be confidently identified as harmine.

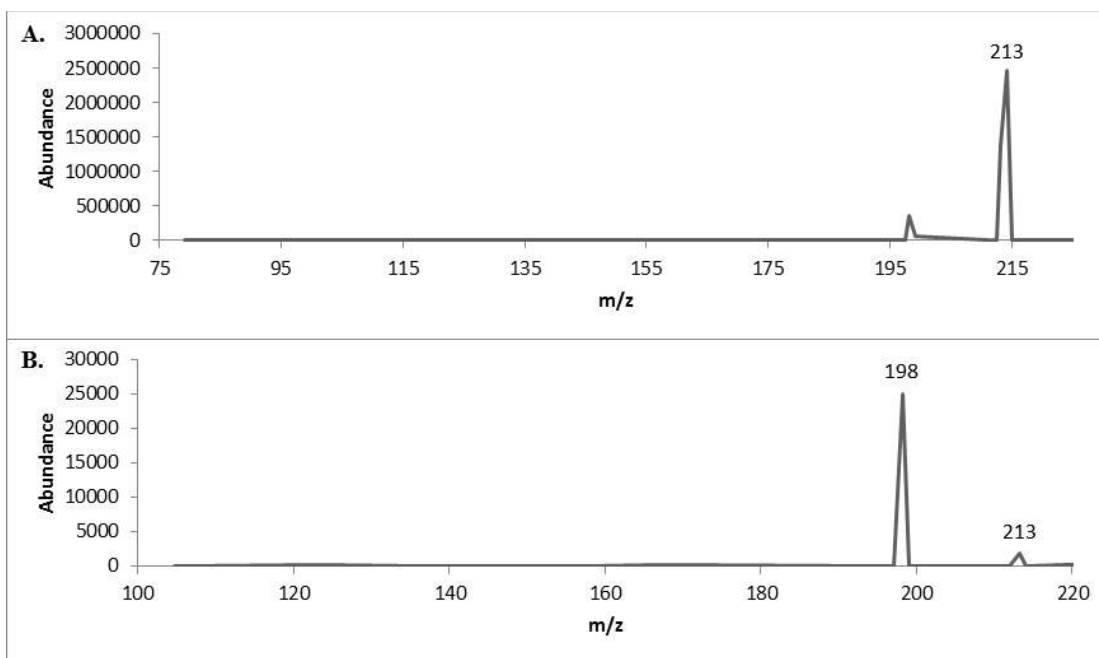


**Figure 46.** MS<sup>2</sup> fragmentation data of  $m/z$  213 for crushed Syrian rue seeds with normalized collision energy of A) 55% and B) 60%.

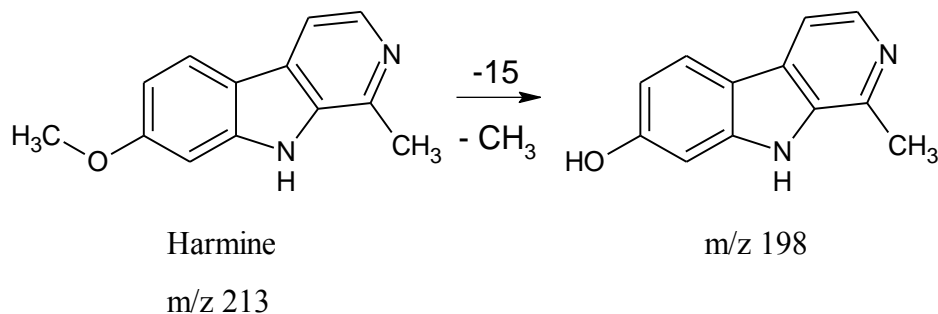


**Figure 47.** Suggested fragmentation of harmine. The loss of the methyl group to form a hydroxyl substituent would result in a fragment at  $m/z$  198, likely associated with the formation of harmol through demethylation.

Harmaline was fragmented with normalized collision energy of 55% and 60%, as seen in Figure 48. At 55%, the peak at  $m/z$  215 remained the most abundant and showed some fragmentation, to form peaks at  $m/z$  200 and 174. As the CE was increased to 60%, the fragment peak at  $m/z$  198 became more abundant and the peak at  $m/z$  215 decreased into the baseline. Similar to harmine, a CE between 55% and 60% was ideal for the fragmentation of harmaline. Due to the similarities between the structures of harmine and harmaline, the fragments produced would likely be due to similar fragmentation mechanisms. The loss of the terminal methyl of the ether group to form either a ketone or hydroxyl substituent would result in the fragment at  $m/z$  200. In addition, a rearrangement and loss of a carbon and nitrogen would result in the formation of the fragment at  $m/z$  174. Although the exact fragmentation mechanism was outside the scope of this study, the pattern observed is consistent with past studies on the metabolism of harmaline into harmalol<sup>37,77,78</sup>. The suggested fragmentation of harmaline is shown in Figure 49. Additionally, harmaline is often metabolized to harmine<sup>37</sup>, although no peak is observed at  $m/z$  213.

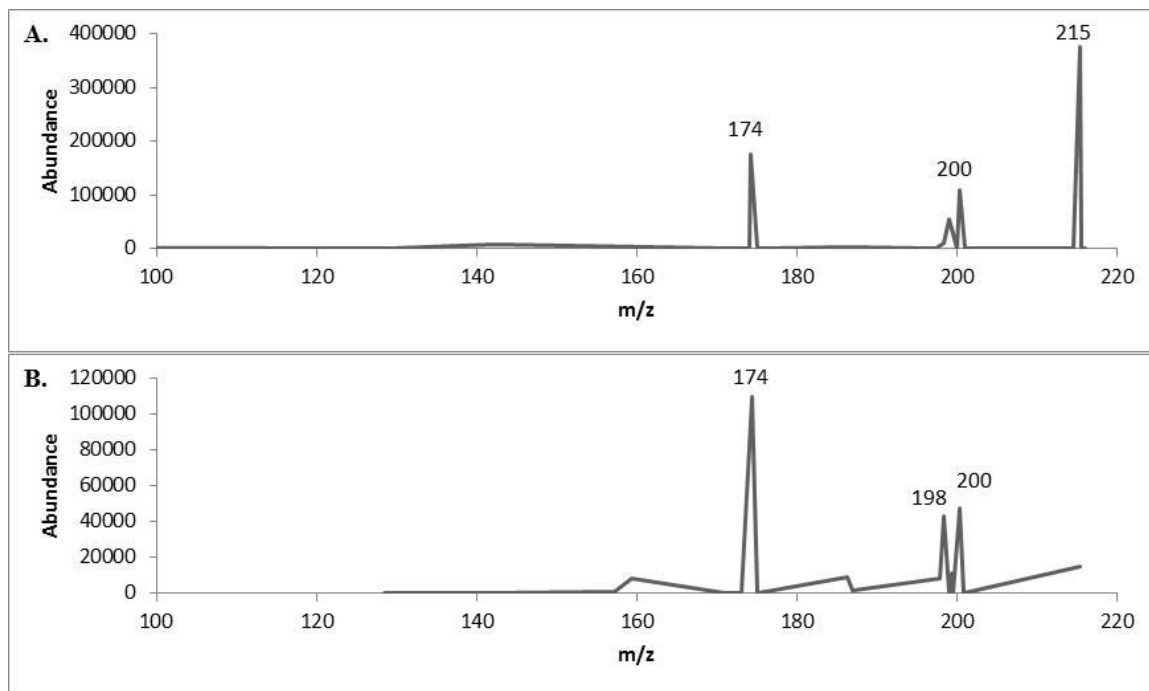


**Figure 48.** MS<sup>2</sup> fragmentation data of *m/z* peak at 215 for crushed Syrian rue seeds with normalized collision energy of A) 55% and B) 60%.

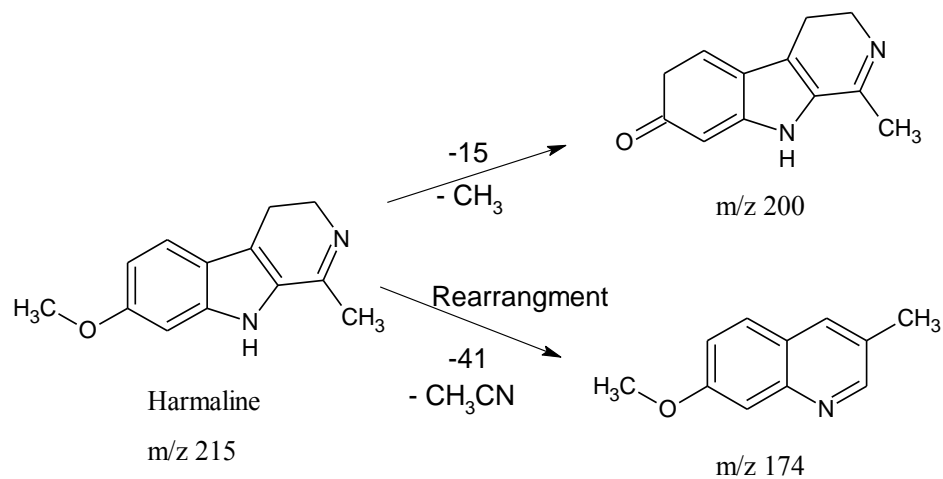


**Figure 49.** Suggested fragmentation of harmaline. The loss of the methyl group to form a ketone would result in a fragment at *m/z* 200. Alternatively, rearrangement resulting in the loss of a CH<sub>3</sub>CN would result in a compound responsible for *m/z* 174. Both fragments have been shown in previous studies to be related to the metabolism of harmaline.



The African Dream herb was unique in this study in that there were no known psychoactive ingredients present in the seeds. The approach to analysis of these seeds was slightly different, in that there were no analytes of interest to focus on or optimize the method for. Based on the data from the source temperature profile experiments, the peaks at  $m/z$  116 and 142 were the peaks of interest and further attempts were made to identify the analytes. Figure 50 shows the fragmentation of  $m/z$  116 with a CE of 45% and 50% with a source carrier gas temperature of 300°C. At CE 45%, there was minimal fragmentation, although peaks at  $m/z$  88 and 98 were present. As the CE was increased to 50%, the parent peak decreased into the baseline and the fragments at  $m/z$  88 and 98 increased. Also, a small fragment at  $m/z$  70 was present. Due to limitations of the instrument, further fragmentation of these peaks was unable to be done as the instrument is unable to reliably detect small fragments below  $m/z$  55. Through a search of general compounds present in plant materials, it was suggested that proline may be present in high concentrations within seeds<sup>75</sup>. Although no references were found to suggest the fragmentation pattern specific to proline, it was shown that  $m/z$  70 is a fragment commonly associated with amino acids<sup>69</sup>. Based on the ions observed and the known structure of proline, there were only two options as to how the compound would fragment to produce the given results<sup>79</sup>. The suggested fragmentation pattern is shown in Figure 51. It is possible that the peak at  $m/z$  98 was due to the loss of  $H_2O$ <sup>79</sup> from the parent peak of proline, likely from the carboxyl substituent. Additionally, the species observed at  $m/z$  98 could be due to the loss of 28 mass units in the form of CO or  $CH_2N$ <sup>79</sup>.

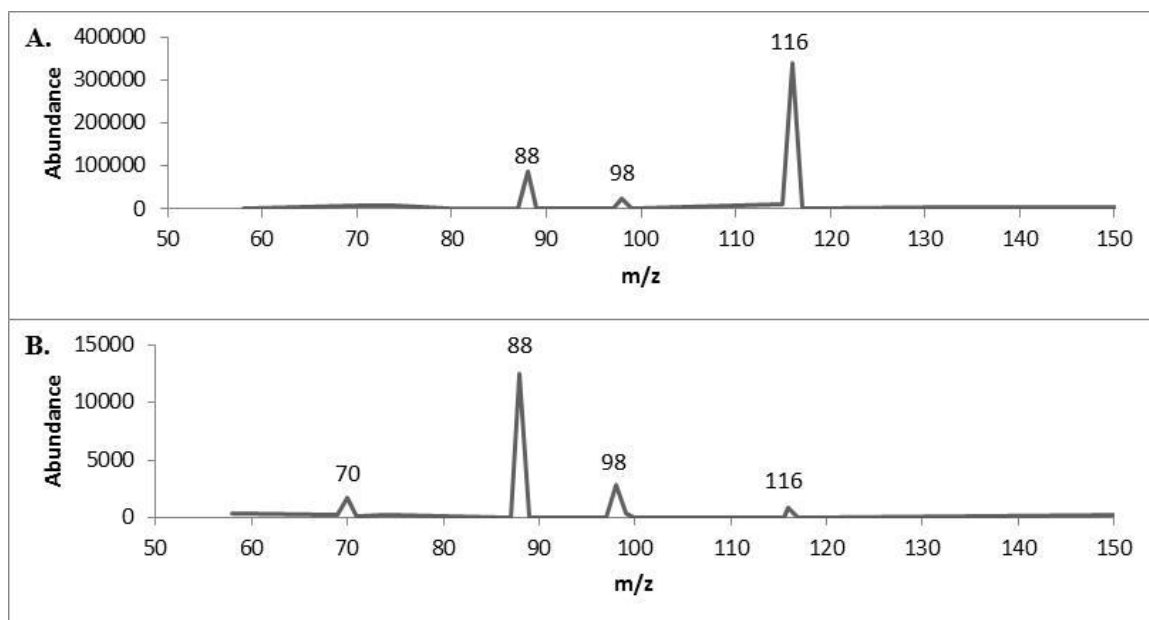


**Figure 50. MS<sup>2</sup> fragmentation data of  $m/z$  116 for crushed African Dream herb seeds with normalized collision energy of A) 45% and B) 50%.**

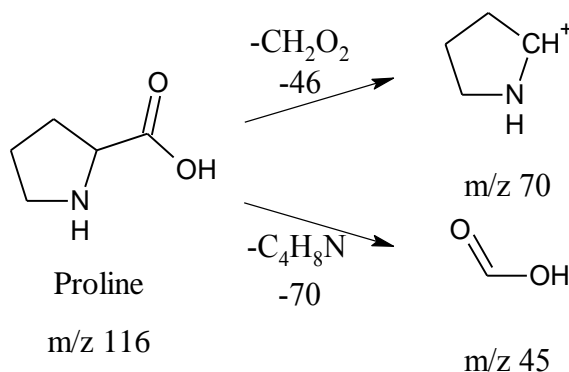


**Figure 51. Suggested fragmentation pattern of proline ( $m/z$  116) to form fragments at  $m/z$  70 and 46.**

The peak at  $m/z$  142 was fragmented with normalized CE of 40%, 45% and 50%. At CE 40%, there was no apparent fragmentation of the parent peak. As the CE was increased to 45% and 50%, the parent peak decreased and the fragment at  $m/z$  124 became more abundant. Normalized CE of 50% produced the maximum fragmentation

while still maintaining the presence of the parent peak at  $m/z$  142, as shown in Figure 52. Based on the loss of  $m/z$  18, a terminal hydroxyl group may be a part of the molecular structure that is being protonated and fragmented. Up to this point, no studies have been found to support the identification of this peak as any known compound present in the seeds. Further research would be necessary to draw any conclusions.

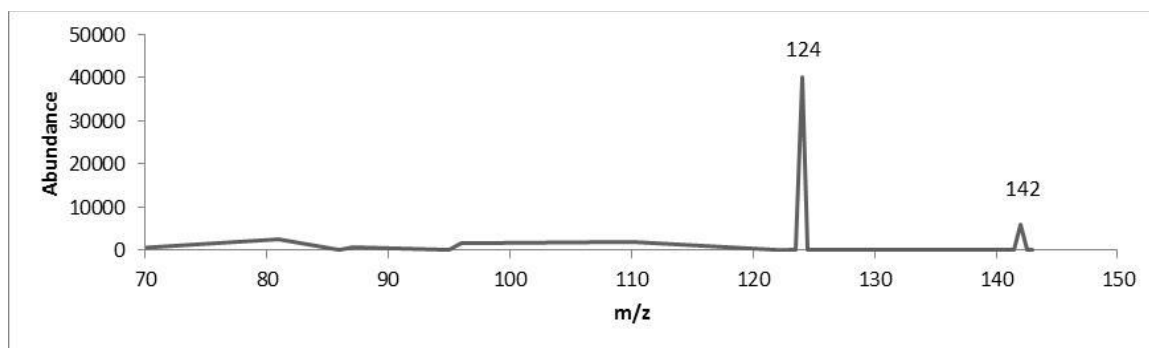


**Figure 52. MS<sup>2</sup> fragmentation data of  $m/z$  142 for crushed African Dream herb seeds with normalized collision energy of 50%.**

Cowage seeds were fragmented with a source temperature of 300°C. Based on the temperature profiles obtained in the first part of the experiment, the analytes of interest for fragmentation were L-dopa ( $m/z$  198) and potentially proline ( $m/z$  116). An additional peak at  $m/z$  298 was observed in low abundances as well. The peak at  $m/z$  116 was fragmented with a CE of 40% and 45%. At 40% CE, there was very minimal fragmentation observed. As it was increased to 45%, the fragment at  $m/z$  70 became more abundant, as shown in Figure 53. Further fragmentation of the analyte with  $m/z$  70 was not done due to limitations of the instrument to detect small fragment ions.

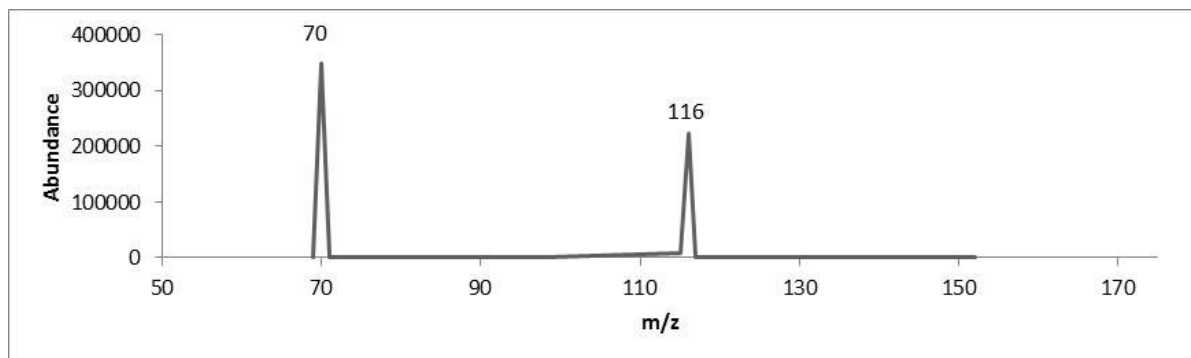


**Figure 53. MS<sup>2</sup> fragmentation data of *m/z* 116 for crushed cowage seeds with normalized collision energy of 45%.**

The peak at *m/z* 198, which was suspected of being L-dopa, was fragmented with CE 50% and 55%. At a CE of 50%, the parent ion was the most abundant and a low abundance of fragments at *m/z* 181 and 152 were present. As the energy was increased to 55%, the parent ion abundances decreased almost into the baseline, while the fragment peaks at 181 and 152 increased, as shown in Figure 54. It was determined that 55% CE was ideal for obtaining the most information about the fragmentation pattern of the compound. When compared with known fragmentation patterns of L-dopa, peaks at *m/z* 181 and 152 have been observed previously<sup>80-82</sup>. It is suggested that the peak at *m/z* 181 is due to the loss of NH<sub>2</sub> and the peak at *m/z* 152 is the result of fragmentation H<sub>2</sub>O and CO from the side chain<sup>81,82</sup>. The suggested fragmentation patterns are shown in Figure 55. Although the analysis only provides a presumptive identification, it is very likely that the parent ion is the result of the ionization of L-dopa.

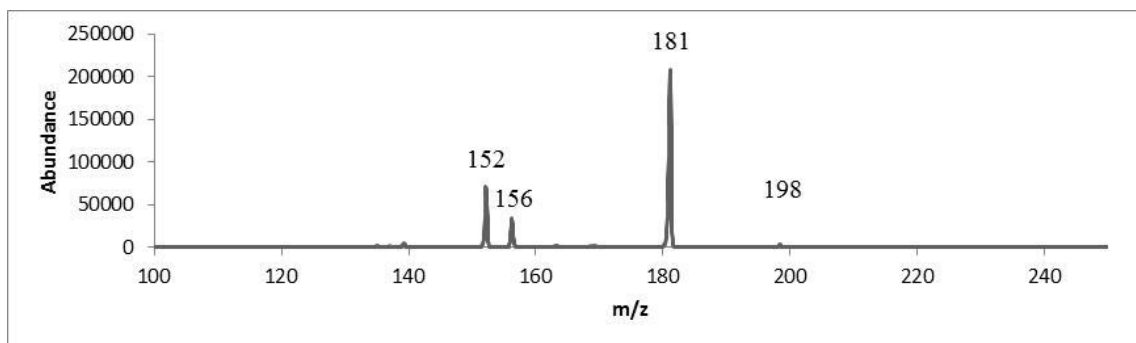


**Figure 54. MS<sup>2</sup> fragmentation data of *m/z* 198 for crushed cowage seeds with normalized collision energy of 55%.**

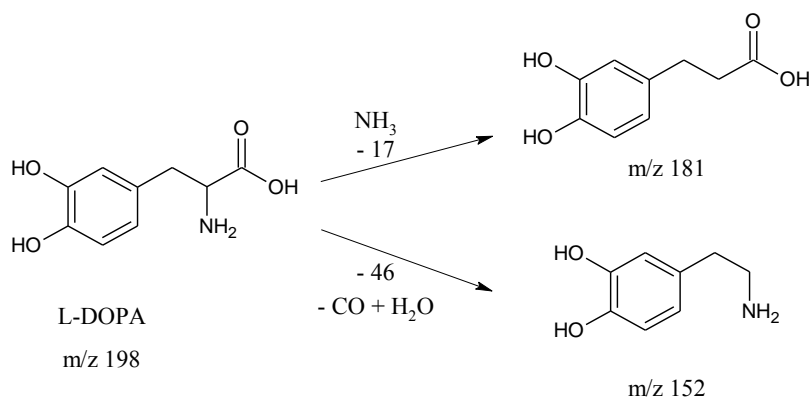


**Figure 55. Suggested fragmentation of L-dopa, resulting in  $[\text{M}+\text{H}]^+$  fragments of *m/z* 181 and 152.**

When analysis was conducted using the DART/ion trap MS, an additional ion was present at *m/z* 298 that was only seen with a source temperature of 250°C in the temperature profile experiments. This ion was not able to be preliminarily associated with any known compound present in the seed. Fragmentation was performed in an effort to identify the analyte. The ion was fragmented with a normalized CE of 45% and 50%. At 45% CE, very little fragmentation was observed, and no ions were abundant in comparison to the baseline. When the CE was increased to 50%, multiple fragments were produced (Figure 56), making it difficult to distinguish where the fragments may be

coming from. Some of the ions observed had masses that were greater than the parent peak. The ion observed at  $m/z$  316 may be due to a water adduct forming ( $[(M+H)+H_2O]^+$ ), since the ionization is performed in the open air, which would result in an addition of 18 mass units. In previous studies, water adducts have sometimes been observed as the most abundant peaks in the mass spectra<sup>83,84</sup>. However, this cannot be concluded with absolute certainty as no tests were done as confirmation. In addition, when the CE was increased to 50%, the abundance of the ions seen significantly decreased. Identification was unable to be made for the analyte responsible for the peak at  $m/z$  298. Further experimentation utilizing MS<sup>n</sup> would be necessary to elucidate additional structural information.

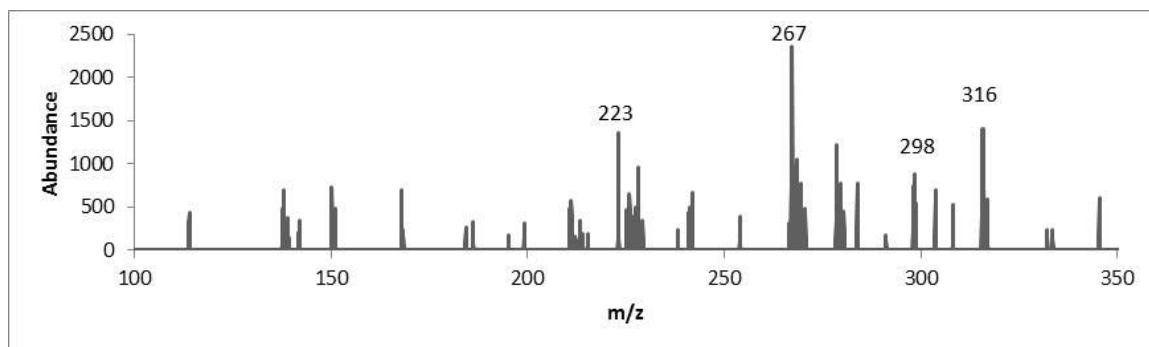


**Figure 56. MS<sup>2</sup> fragmentation data of  $m/z$  298 for crushed cowage seeds with normalized collision energy of 50%.**

Based on data from the temperature profile analysis of henbane seeds, the fragmentation experiments were conducted with a source temperature of 350°C. The ions present were  $m/z$  290 and 308. The ion at  $m/z$  290 was determined to likely be associated with atropine or hyoscyamine. The ion was fragmented with at 45%, 55%, and 57% CE. At 45% CE, minimal fragmentation was observed and a small peak at  $m/z$  124 began to

form. As the CE was increased, the abundance of the fragment ions increased, and the parent ion decreased, as expected. Additionally, a fragment at  $m/z$  160 became apparent. A 57% CE was ideal, based on the abundance of the fragment ions relative to the parent ion, as shown in Figure 57. Previous research has found that atropine/ hyoscyamine fragments to form an ion at  $m/z$  124, as shown in Figure 58<sup>85</sup>.

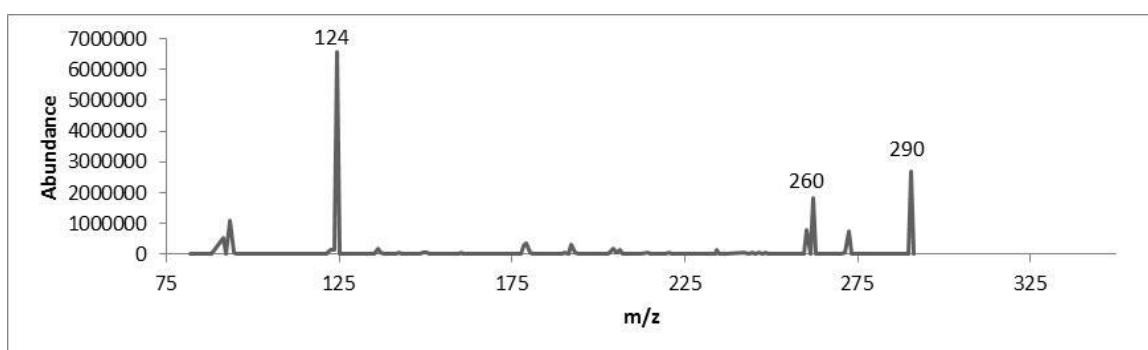


**Figure 57. MS<sup>2</sup> fragmentation data of  $m/z$  290 for crushed henbane seeds with normalized collision energy of 57%.**

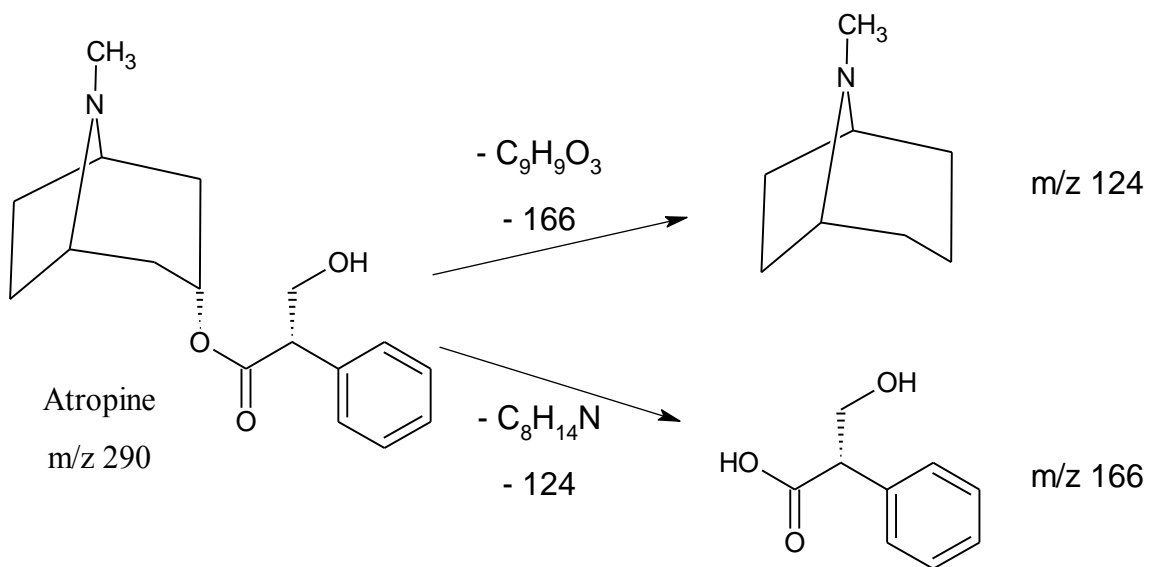


**Figure 58. Suggested fragmentation of atropine to form fragments at  $m/z$  124 and 166. Only the fragment at  $m/z$  124 is observed in this study.**

When the peak at  $m/z$  308 was fragmented with a CE of 45%, 55%, and 57% the only species observed was  $m/z$  290, indicating that the ion may be due to the loss of a water molecule that was forming the adduct (Figure 59), which is a phenomenon sometimes observed in DART-MS analyses<sup>83,84</sup>. A confirmative identification was unable to be made for the analyte responsible for the peak at  $m/z$  308. Further experimentation would be necessary.

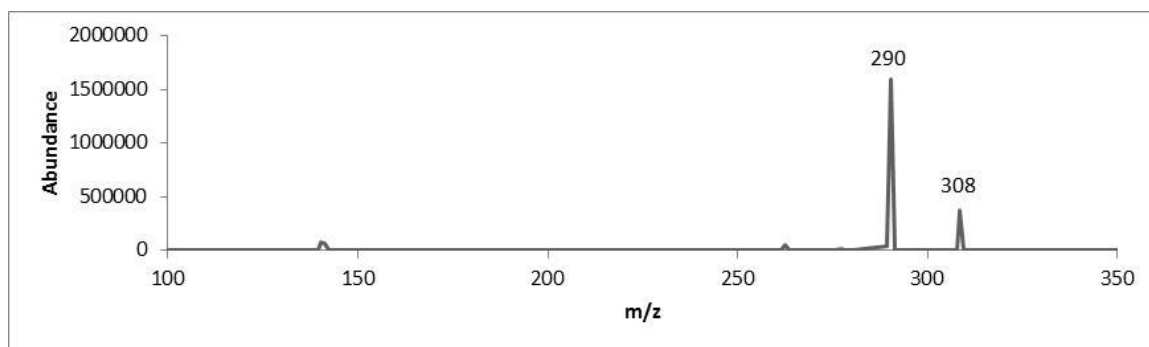


**Figure 59. MS<sup>2</sup> fragmentation data of  $m/z$  308 for crushed henbane seeds with normalized collision energy of 57%.**

*Ephedra sinica* plants were reported to contain ephedrine and norephedrine. Based on results of the source temperature profiles, neither of the analytes of interest were detected in the seeds using this method. Instead, ions with  $m/z$  128 and 332 were the most abundant. Fragmentation was performed on each of the ions in an attempt to provide identification for the compounds observed. The peak at  $m/z$  128 was fragmented with 55% and 57% CE. At 55% CE, there was very minimal fragmentation. When the CE was increased to 57%, a large fragment ion was produced at  $m/z$  82, as shown in Figure 60. No further fragmentation was performed on the fragment due to limitations of the



instrument at low mass values. Because there was no preliminary identification of the parent ion, no fragmentation patterns resulting in a loss of 46 mass units were suggested.

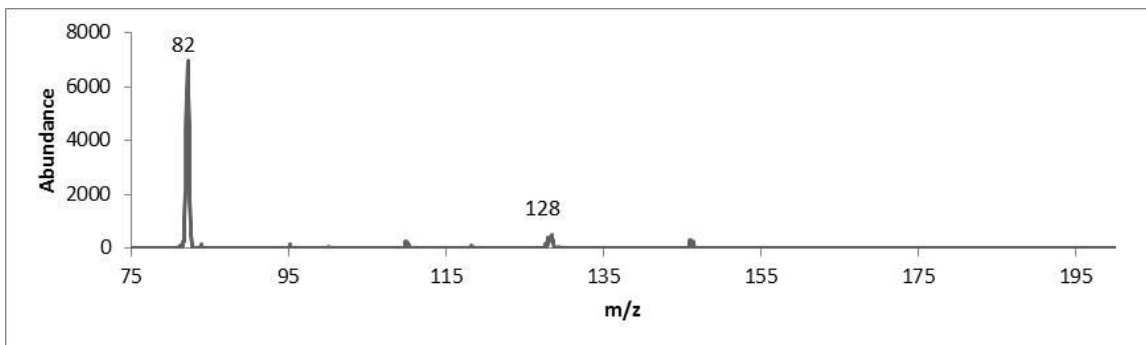


**Figure 60. MS<sup>2</sup> fragmentation data of *m/z* 128 for crushed ephedra seeds with normalized collision energy of 57%.**

The second ion observed in the source temperature profiles for *Ephedra sinica* seeds was *m/z* 332. This ion was fragmented with normalized CE of 50% and 55%. As shown in Figure 61, a 55% CE resulted in three main fragment ions, *m/z* 272, 183, and 142. Because the parent ion was not associated with any known compounds, no fragmentation mechanisms were suggested.

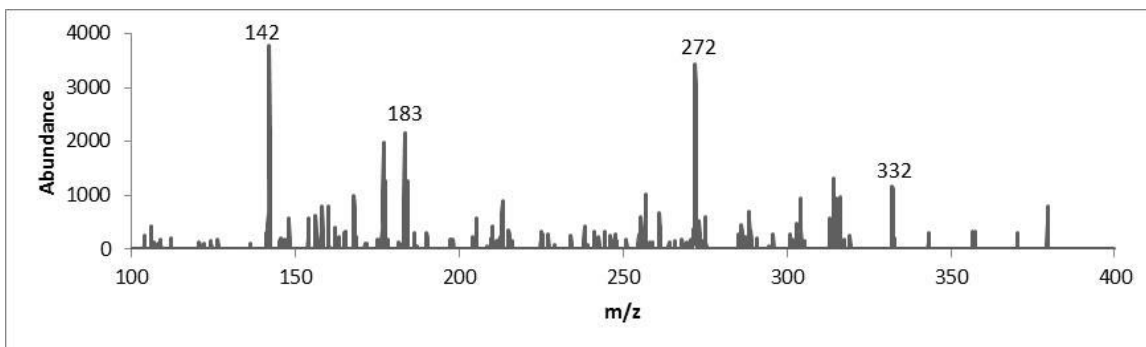


**Figure 61. MS<sup>2</sup> fragmentation data of *m/z* 332 for crushed ephedra seeds with normalized collision energy of 55%.**

Mexican poppy seeds were reported to contain two main compounds sanguinarine and dihydrosanguinarine, only one of which was observed in the temperature profile experiments. Although the two compounds may not have been completely differentiated from one another due to the lack of separation and the vast similarities between the compounds, only dihydrosanguinarine ( $m/z$  334) was studied in this section. Upon fragmentation with a normalized CE of 50%, the analyte fragmented to form ions at  $m/z$  319 and 304, as shown in Figure 62. The fragment at  $m/z$  319 can be explained by the loss of a methyl group as shown in Figure 63. Based on the loss of 15 from the  $m/z$  319 fragment, the fragment is likely the result of a demethylation reaction. However, no methyl groups are present that would likely be cleaved. The fragment may be a result of the loss of  $\text{CH}_2\text{O}$  (-30 mass units) from one of the terminal rings of the parent compound to form a hydroxyl or ketone. Further experimentation would be necessary to determine the structure of the peak at  $m/z$  304.

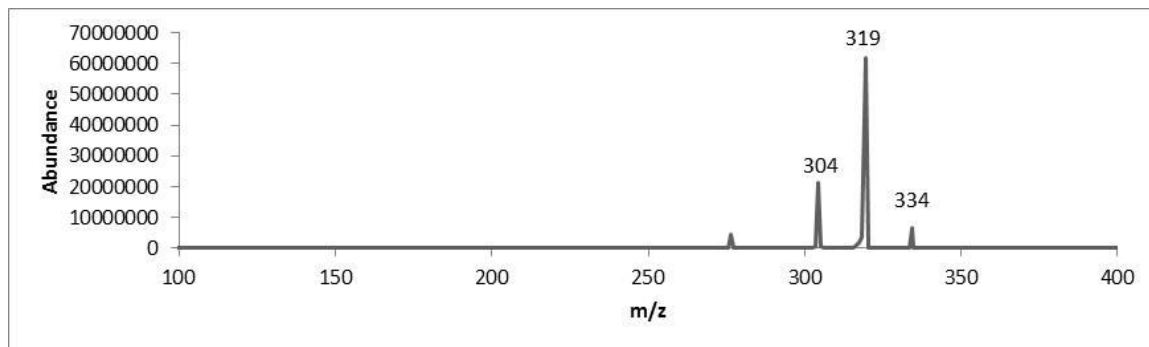


**Figure 62. MS<sup>2</sup> fragmentation data of  $m/z$  peak at 334 for crushed Mexican poppy seeds with normalized collision energy of 50%.**

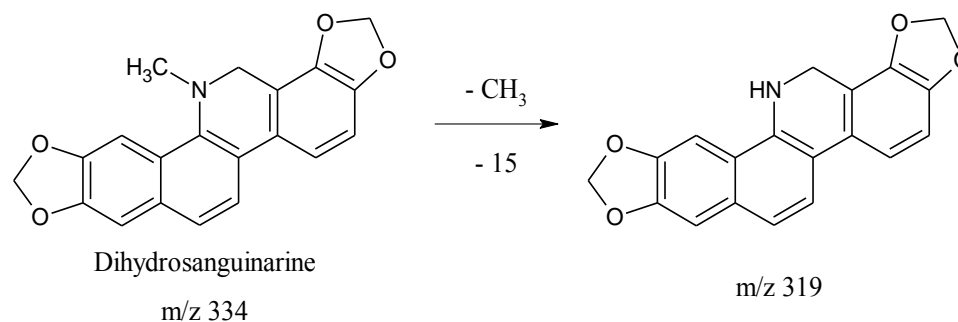


**Figure 63. Suggested fragmentation of dihydrosanguinarine to form a fragment with  $m/z$  319 through the loss of a methyl group.**

In addition, the peak at  $m/z$  319 was fragmented with normalized CE of 45%, 48%, and 55%. At 45% and 48% CE, the abundance of the parent peak remained more prominent than either fragment at  $m/z$  290 and 260. At 55% CE, the abundance of the fragments increased, as shown in Figure 64.

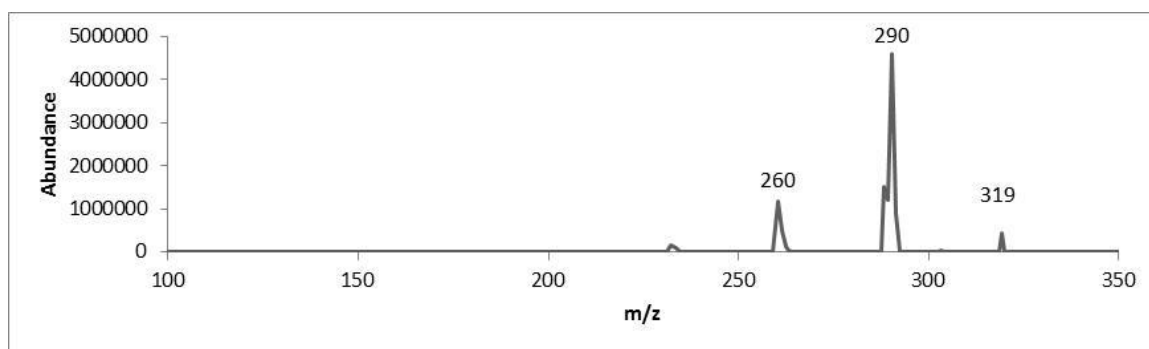


**Figure 64. MS<sup>2</sup> fragmentation data of  $m/z$  319 for crushed Mexican poppy seeds with normalized collision energy of 55%.**

Limited research has been done on Intellect tree seeds. Based on the data collected from carrier gas temperature profiles, the major ions produced with this method were  $m/z$  534 and 524. However, these ions did not correlate to any of the compounds reported to be present in the seeds, and fragmentation of these ions did not aid in

identification. The ion at  $m/z$  534 fragmented to form  $m/z$  515, 473, and 399, as shown in Figure 65, which was a loss of 19, 61, and 135 mass units, respectively. No research was found to support the identification of the compound based on the fragmentation pattern obtained. More research would be necessary to draw conclusions about the identity or ideal conditions for analysis of the analytes and the seeds as a whole. Similarly, the peak at  $m/z$  524 was fragmented with 45%, 50%, and 55% CE. At 50% and 55%, multiple fragment ions were produced, resulting in a loss of 19, 61, and 75 mass units (Figure 66), although none of them were able to be associated with known compounds. Based on the similarities in fragmentation patterns obtained for the ions of interest, it is likely that the two parent compounds are similar in structure to one another.

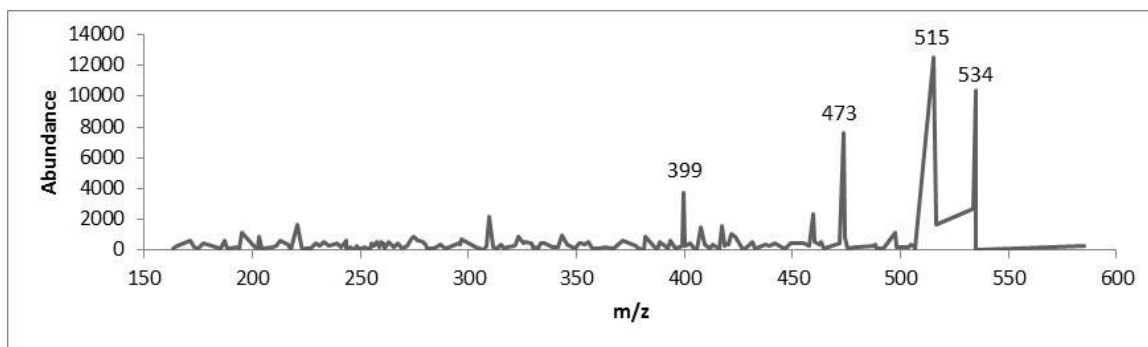


**Figure 65. MS<sup>2</sup> fragmentation data of  $m/z$  534 for crushed Intellect tree seeds with normalized collision energy of 50%.**

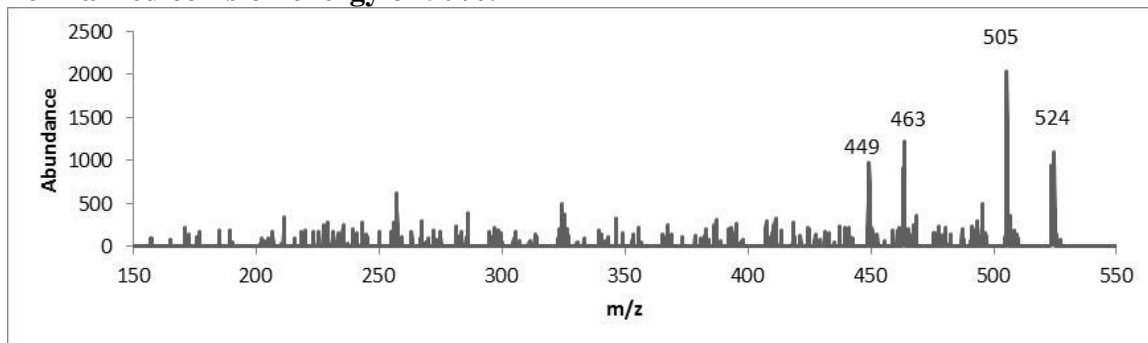


**Figure 66. MS<sup>2</sup> fragmentation data of  $m/z$  524 for crushed Intellect tree seeds with normalized collision energy of 55%.**

Hawaiian baby Woodrose seeds are reported to contain various ergot alkaloids. Based on the source temperature profiles, ergine and ergometrine ( $m/z$  268 and 326) were being detected and preliminarily identified in the Hawaiian and Indian strains. The fragmentation of  $m/z$  268 for the Hawaiian strain can be seen in Figure 67. Normalized CE of 50% resulted in a significant amount of fragmentation, producing fragments with  $m/z$  251, 223, and 208. Each of these fragments was consistent with previous research on the chemical behavior of ergine.<sup>70</sup> The fragment at  $m/z$  223 is due to the loss of the -CONH<sub>3</sub> side chain. The remaining fragment is further fragmented to form  $m/z$  208 through the loss of a methyl group. The fragmentation pattern is shown in Figure 42. Although not specifically reported, the fragment at  $m/z$  251 may be due to the loss of -NH<sub>3</sub> from the end of the compound.

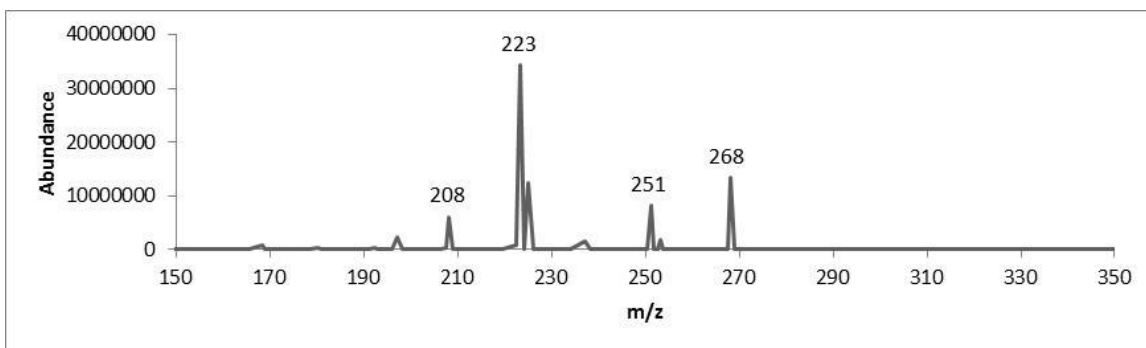


**Figure 67. MS<sup>2</sup> fragmentation data of  $m/z$  268 for crushed Hawaiian Baby Woodrose (Hawaiian strain) seeds with normalized collision energy of 50%.**

The fragmentation of  $m/z$  326 for the Hawaiian strain can be seen in Figure 68. Normalized CE of 50% and 55% resulted in a significant amount of fragmentation. Both conditions produced fragments at  $m/z$  308, 283, 265, 251, 223, 208, and 197. Because ergometrine is very similar in structure to ergine, some of the same fragments were

expected to be under similar conditions. The peak at 223 is due to the loss of the side chain, and the peak at 208 is the result of the loss of a methyl group, as shown in Figure 45<sup>70</sup>.

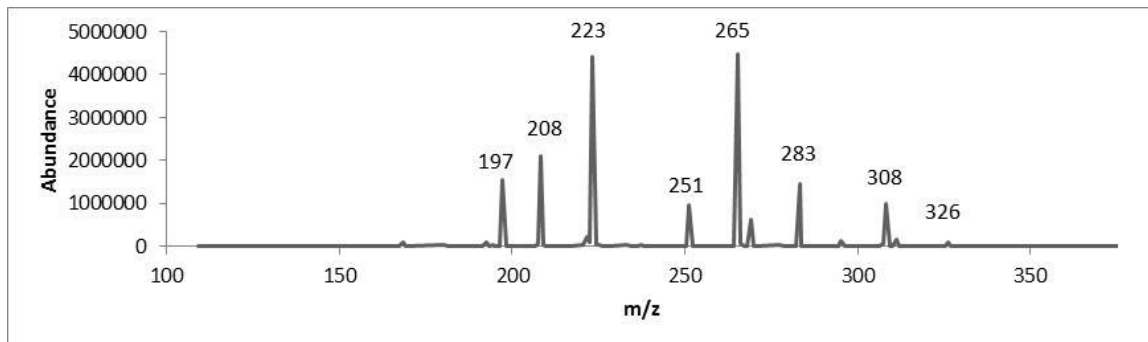


**Figure 68. MS<sup>2</sup> fragmentation data of *m/z* 326 for crushed Hawaiian Baby Woodrose (Hawaiian strain) seeds with normalized collision energy of 55%.**

Similar to the Hawaiian strain, the Indian strain of Hawaiian baby woodrose was identified as containing ergine and ergometrine (*m/z* 268 and 326, respectively). The fragmentation was performed at slightly higher collision energies; however the same fragments (*m/z* 251, 223, and 208) were produced, as shown in Figure 69. The suggested fragmentation can be seen previously in the discussion on the analysis of the Ololiuqui seeds. (Figure 42) The compound being detected at *m/z* 268 can be positively identified as ergine.

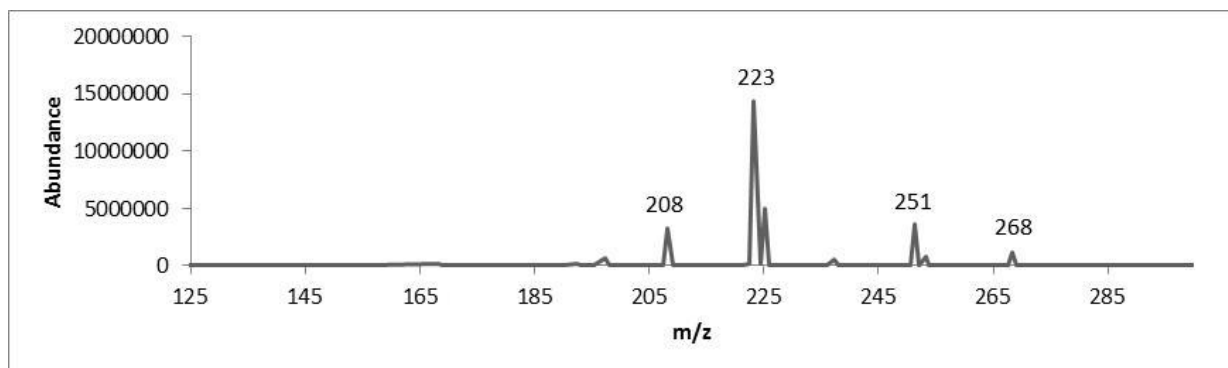


**Figure 69. MS<sup>2</sup> fragmentation data of *m/z* 268 for crushed Hawaiian Baby Woodrose (Indian strain) seeds with normalized collision energy of 53%.**

The fragmentation of what was preliminarily identified as ergometrine was performed in the same manner as the fragmentation of the Hawaiian strain. In both cases, the same fragmentation occurred, resulting in *m/z* 308, 283, 265, 251, 223, 208, and 197, as shown in Figure 70. The suggested fragmentation pattern can be seen previously in the discussion on the analysis of the morning glory seeds (Figure 45). The compound being detected at *m/z* 326 can be positively identified as ergometrine.

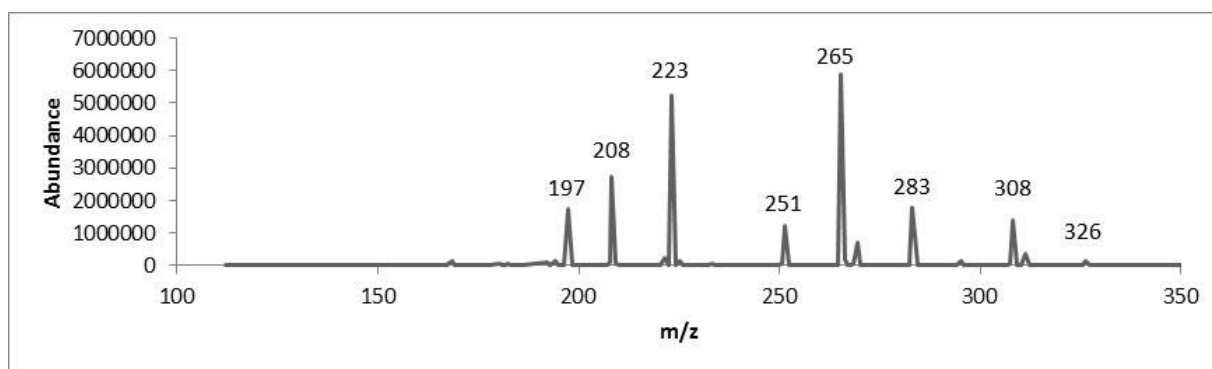


**Figure 70. MS<sup>2</sup> fragmentation data of *m/z* 326 for crushed Hawaiian Baby Woodrose (Indian strain) seeds with normalized collision energy of 55%.**

Analysis of the Ghana strain revealed the presence of what was suspected to be ergine, but lacked any mass spectral data that could be associated with the presence of ergometrine. When fragmenting the peak at  $m/z$  268 (Figure 71), the same fragments were produced as with the Hawaiian and Indian strains.

In comparison to the other strains of Hawaiian baby Woodrose, the lack of ergometrine is a significant difference in the chemical composition. The lack of ergometrine may be because the Ghana strain has a low concentration of ergometrine in comparison to the other strains, so it is not detected within the plant matrix using this method. A peak representative of ergometrine may have been absent due to ion suppression effects caused by other compounds within the plant matrix that are not present in the other two strains. No further testing was done as part of this study.

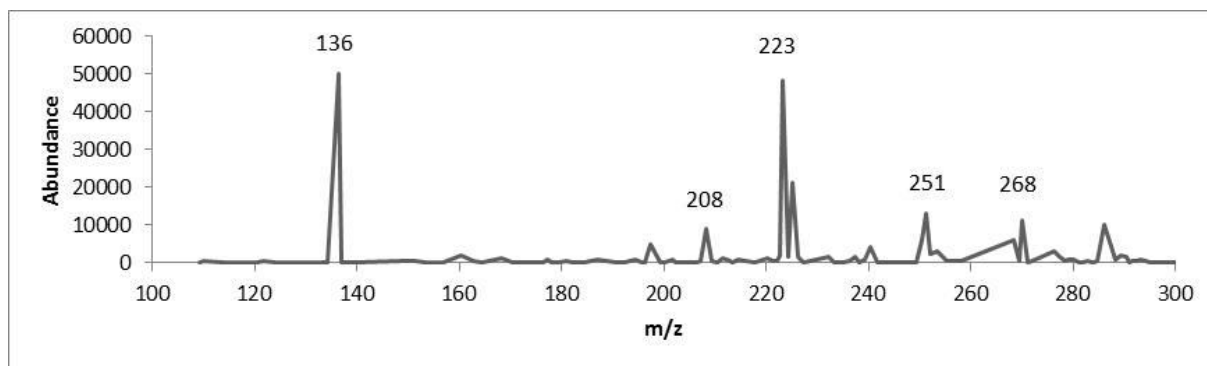


**Figure 71. MS<sup>2</sup> fragmentation data of  $m/z$  268 for crushed Hawaiian Baby Woodrose (Ghana strain) seeds with normalized collision energy of 55%.**

A summary of the data collected throughout this study, including the carrier gas temperature, normalized collision energy, fragments observed, and analyte identification is contained in Table 4.



**Table 4. Summary of data collection and conclusions for each seed type.**

Seed Sample	Source Temperature (°C)	Ions (m/z)	Collision Energy (%)	Fragment Ions (m/z)	Possible Identification
Cebil	300	205	25	160	Bufotenine
Voacanga	250	337	32	305, 228	Tabersonine
		353	30	3221, 228, 210, 144	Akuammidine
		369	30	337, 305, 309, 210	Voacangine
Ololiuqui	350	268	38	223, 208	Ergine (LSA)
Morning Glory	350	268	30	251, 223, 208	Ergine (LSA)
		326	32	308, 283, 265, 251, 223, 208, 197	Ergometrine
Syrian Rue	250	213	55 - 60	198	Harmine
		215	55 - 60	200, 198, 174	Harmaline
African Dream Herb	300	116	50	98, 88, 70	Proline
		142	50	124	---
Cowage	300	116	45	70	Proline
		198	55	181, 152	Levodopa
		298	50	316, 267, 223	---
Hawaiian Baby Woodrose - Hawaii	350	268	50	251, 223, 208	Ergine (LSA)
		326	55	308, 283, 265, 251, 223, 208, 197	Ergometrine
Hawaiian Baby Woodrose - Indian	300 or 350	268	53	251, 223, 208	Ergine (LSA)
		326	55	308, 283, 265, 251, 223, 208, 197	Ergometrine
Hawaiian Baby Woodrose - Ghana	350	268	55	251, 223, 208, 136	Ergine (LSA)
Henbane	350	290	57	260, 124	Atropine/Hyoscyamine
		308	57	290	Atropine/Hyoscyamine + H <sub>2</sub> O
Intellect Tree	350	524	55	505, 463, 449	---
		534	50	515, 473, 399	---
Ephedra Sinica	300	128	57	82	---
		332	55	272, 183, 142	---
Mexican Poppy	250	319	55	290, 260	Dihydrosanguinarine – CH <sub>3</sub>
		334	50	319, 304	Dihydrosanguinarine

#### **4. Conclusion**

DART proved to be an effective technique in tentatively identifying many different compounds present within several complex plant matrices. Limited sample preparation was done prior to analysis of the samples. Analysis was able to be performed in a manner that was significantly faster than the traditional gas chromatography-mass spectrometry (GC-MS) methods employed in routine drug analysis. On average, a set of twelve samples could be collected in approximately 2-3 minutes, unlike a typical 20-30 GC-MS method. The ability to rapidly analyze samples would be extremely important in a forensic drug laboratory where increasing case backlogs and increasing caseloads is an issue.

Methods were determined for the successful analysis and identification of at least one analyte of interest for eleven of the thirteen samples that had known compounds with psychoactive properties. *Ephedra sinica* and Intellect tree seeds contained compounds that were not detected through DART-MS techniques. The inability to detect the analytes may be due to other compounds present in the plant matrix suppressing the ionization and subsequent detection, or that the compounds are present in such low concentrations that other analytes within the matrix are preferentially analyzed and detected. The African Dream herb seeds had no compounds known to be responsible for the psychoactive effects experienced by users. Although two ions were able to be detected, there were no reports to support the findings of either ion within the seeds and no confirmatory identification was determined.

Initial findings suggested that there may be detectable differences between different strains of Hawaiian baby Woodrose seeds. Although the same compounds were expected to be present in each of the strains, ergometrine was not detected in the Ghana strain, representing a significant difference when compared to both the Hawaiian and Indian strains. Differences in the mass spectral data may indicate that the concentration of ergometrine in the Ghana strain is below the limit of detection or that there are other compounds present that are causing the ergometrine to remain unionized or undetected. Further studies would be necessary to determine the cause.

Overall, DART-MS is an easy to use, effective technique that allows for rapid analysis of a wide variety of compounds within a complex plant matrix. DART-MS should be considered in laboratories where case backlog is an increasing area of concern. A typical GC-MS analysis of a suspected drug of abuse and a correlating blank may take an hour or more to analyze, while a DART-MS analysis can be completed in a matter of minutes including set-up, sample analysis, and the analysis of blanks or control samples.

## **5. Future Directions**

Further research should be done to optimize other aspects of DART analysis for the plant seeds utilized in this study, including possible analysis of the seed material as a whole rather than ground up. Overall, further research should be performed to reduce and eliminate the need for any sample preparation in order to obtain the most time efficient and accurate analysis of the samples. Additionally, a standard procedure that would allow for the analysis and identification on any unknown seed would be very useful in a

forensic setting. The standard procedure should include one set of instrumental parameters that would be successful with the analysis of a wide variety of samples, which may include a temperature profile analysis of each sample rather than selecting a single optimum source temperature to be used with each individual sample.

More research should be done to confirm the preliminary identifications of the compounds being detected throughout this study. Confirmatory analysis could include the use of high resolution instrumentation, analysis of standards, or subsequent analysis by GC-MS which would allow for the use of a spectral library database, assuming the analytes of interest are a part of the library.

Analysis of the Hawaiian Baby Woodrose seeds in an attempt to differentiate between the different strains should be continued. If more data was collected, statistical modeling software could be used to more confidently determine whether the differences observed in the mass spectral data were significant or not. Statistical modeling may also be able to detect small variations in the spectra of the different strains that are not obvious to the naked eye.

The analysis of plant based drugs of abuse by DART-MS should be continued to include plant leaves, stems, and flowers that are reported to contain psychoactive compounds. Expanding this type of analysis to the identification of poisonous compounds contained within plant materials and in the identification of synthetic cannabinoids that have been incorporated into a plant matrix may also be beneficial.

## **LIST OF ABBREVIATED JOURNAL TITLES**

Afr J Pharm Pharmacol	African Journal of Pharmacy and Pharmacology
Am J Pharm Educ	The American Journal of Pharmaceutical Education
Am J Public Health	American Journal of Public Health
Am Lab	American Laboratory
Anal Bioanal Chem	Analytical and Bioanalytical Chemistry
Anal Chem	Analytical Chemistry
Anal Chim Acta	Analytical Chimica Acta
Chromatogr B Biomed Sci App	Journal of Chromatography B: Biomedical Sciences and Applications
Clin Toxicol	Journal of Clinical Toxicology
Curr Sports Med Rep	Current Sports Medicine Reports
Drug Alcohol Depend	Drug and Alcohol Dependence
Drug Metab Dispos	Drug Metabolism and Disposition
Eur J Pharmacol	European Journal of Pharmacology
Food Addit Contam Part A	Food Additives and Contaminants: Part A
Food Chem	Food Chemistry
Forensic Sci Int	Forensic Science International
J Am Soc Mass Spectrom	Journal of the American Society for Mass Spectrometry
J Chem Soc Trans	Journal of the Chemical Society, Transactions

J Chromatogr B	Journal of Chromatography B: Biomedical Sciences and Applications
J Crim Criminol	Journal of Criminal Law and Criminology
J Emerg Med	Journal of Emergency Medicine
J Ethnopharmacol	Journal of Ethnopharmacology
J Food Sci Technol	Journal of Food Science and Technology
J Forensic Sci	Journal of Forensic Science
J Mass Spectrom	Journal of Mass Spectrometry
J Mex Chem Soc	Journal of the Mexican Chemical Society
J Neurol Neurosurg Psychiatry	Journal of Neurology, Neurosurgery, and Psychiatry
J Pharm Biomed Anal	Journal of Pharmaceutical and Biomedical Analysis
J Pharmacol Exp Ther	Journal of Pharmacology and Experimental Therapeutics
J Plant Biol	Journal of Plant Biology
J Psychoactive Drugs	Journal of Psychoactive Drugs
J Subst Abuse Treat	Journal of Substance Abuse Treatment
Lat Am Antiq	Latin American Antiquity
Nat Prod Rep	Natural Product Reports
Pharm Biol	Pharmaceutical Biology
Pharm Chem J	Pharmaceutical Chemistry Journal
Phytother Res	Phytotherapy Research
Rapid Commun Mass Spectrom	Rapid Communications in Mass Spectrometry

Subst Abuse Rehabil

Journal of Substance Abuse and Rehabilitation

Toxicol Sci

Journal of Toxicological Sciences

TrAC Trends Anal Chem

Trends in Analytical Chemistry

## REFERENCES

1. Furst PT. Hallucinogens and culture. San Francisco: Chandler & Sharp, 1976.
2. Robins LN. The natural history of adolescent drug use. *Am J Public Health* [Internet] 1984 [cited 2014 Mar 24];74(7):656–7. Available from: <http://ajph.aphapublications.org/doi/pdf/10.2105/AJPH.74.7.656>
3. Substance Abuse and Mental Health Services Administration. Results from the 2012 National Survey on Drug Use and Health: Summary of National Findings [Internet]. Rockville, MD: U.S. Department of Health and Human Services, 2013; Available from: <http://www.samhsa.gov/data/NSDUH/2012SummNatFindDetTables/NationalFindings/NSDUHresults2012.htm#ch1.1>
4. National Forensic Laboratory Information System. NFLIS 2012 Annual Report. U.S. Department of Justice, 2012.
5. Mumola CJ, Karberg JC. Drug use and dependence, state and federal prisoners, 2004 [Internet]. US Department of Justice, Office of Justice Programs, Bureau of Justice Statistics Washington, DC, 2006 [cited 2014 Mar 26]; Available from: <http://proxychi.baremetal.com/csdp.org/research/dudsfp04.pdf>
6. Tina L. Dorsey, Priscilla Middleton. Drugs and Crime Facts.pdf [Internet]. U.S. Department of Justice, 2007 [cited 2014 Mar 26]; Available from: <http://www.ojp.usdoj.gov/bjs>
7. National Forensic Laboratory Information System. 2013 Survey of Crime Laboratory Drug Chemistry Sections [Internet]. 2013 [cited 2014 Mar 26]; Available from: <https://www.nflis.deadiversion.usdoj.gov/Reports.aspx>
8. Schneir AB, Cullen J, Ly BT. “Spice” Girls: Synthetic Cannabinoid Intoxication. *J Emerg Med* [Internet] 2011 [cited 2014 Mar 24];40(3):296–9. Available from: <http://linkinghub.elsevier.com/retrieve/pii/S0736467910008802>
9. Rojek S, Kłys M, Strona M, Maciów M, Kula K. “Legal highs”—Toxicity in the clinical and medico-legal aspect as exemplified by suicide with bk-MBDB administration. *Forensic Sci Int* [Internet] 2012 [cited 2014 Mar 24];222(1-3):e1–e6. Available from: <http://linkinghub.elsevier.com/retrieve/pii/S0379073812002058>
10. Controlled Substances Analogue Enforcement Act of 1986. 1986.



11. U.S. Government Information. Drug Enforcement Administration 21 CFR Part 1308. Fed Regist 2013;78(3):664–6.
12. Chiarotti M, Fucci N. Comparative analysis of heroin and cocaine seizures. J Chromatogr B Biomed Sci App [Internet] 1999 [cited 2014 Mar 24];733(1):127–36. Available from: <http://www.sciencedirect.com/science/article/pii/S0378434799002406>
13. Samuel Contreras. The Chemistry of Seeds [Internet]. [cited 2014 Jun 11]; Available from: [seedbiology.osu.edu/HCS631\\_files/7B%20Seed%20Chemistry.pdf](http://seedbiology.osu.edu/HCS631_files/7B%20Seed%20Chemistry.pdf)
14. Fakjri A, Bazzaz, David D, Ackerly, Edward G, Reekie. Reproductive Allocation in Plants. New York: CABI, 2000.
15. Lange JE, Reed MB, Croff JMK, Clapp JD. College student use of Salvia divinorum. Drug Alcohol Depend [Internet] 2008 [cited 2014 Apr 1];94(1-3):263–6. Available from: <http://linkinghub.elsevier.com/retrieve/pii/S0376871607004310>
16. Shultes RE, Hofmann A, Rätsch C. Plants of the Gods Their sacred, Healing, and Hallucinogenic Powers. Rochester, Vermont: Healing Arts Press, 2001.
17. González D, Riba J, Bouso JC, Gómez-Jarabo G, Barbanoj MJ. Pattern of use and subjective effects of Salvia divinorum among recreational users. Drug Alcohol Depend [Internet] 2006 [cited 2014 Apr 1];85(2):157–62. Available from: <http://linkinghub.elsevier.com/retrieve/pii/S0376871606001396>
18. Wu L-T, Woody G, Yang C, Li J-H, Blazer. Recent national trends in Salvia divinorum use and substance-use disorders among recent and former Salvia divinorum users compared with nonusers. Subst Abuse Rehabil [Internet] 2011 [cited 2014 Mar 26];53. Available from: <http://www.dovepress.com/recent-national-trends-in-salvia-divinorum-use-and-substance-use-disor-peer-reviewed-article-SAR>
19. Hoover V, Marlowe DB, Patapis NS, Festinger DS, Forman RF. Internet access to Salvia divinorum: Implications for policy, prevention, and treatment. J Subst Abuse Treat [Internet] 2008 [cited 2014 Mar 26];35(1):22–7. Available from: <http://linkinghub.elsevier.com/retrieve/pii/S0740547207002243>
20. Patricia J. Knobloch. Wari Ritual Power at Conchopata An Interpretation of Anadenanthera Colubrina Iconography.pdf. Lat Am Antiq [Internet] 2000 [cited 2014 Apr 1];11(4):387–402. Available from: <http://www.jstor.org/stable/972003> .
21. De Smet PA. Ritual enemas and snuffs in the Americas [Internet]. Centre for Latin American Research and Documentation, 1985 [cited 2014 Apr 3]; Available from: [http://www.samorini.it/doc1/alt\\_aut/ad/de%20smet%20enemas.pdf](http://www.samorini.it/doc1/alt_aut/ad/de%20smet%20enemas.pdf)

22. Rätsch C. *The Encyclopedia of Psychoactive Plants: Ethnopharmacology and Its Applications*. Rochester, Vermont: Park Street Press, 2005.
23. McClean S, Robinson RC, Shaw C, Smyth WF. Characterisation and determination of indole alkaloids in frog-skin secretions by electrospray ionisation ion trap mass spectrometry. *Rapid Commun Mass Spectrom* [Internet] 2002 [cited 2013 Nov 25];16(5):346–54. Available from: <http://doi.wiley.com/10.1002/rcm.583>
24. Zuba D. Identification of cathinones and other active components of “legal highs” by mass spectrometric methods. *TrAC Trends Anal Chem* [Internet] 2012 [cited 2014 Apr 4];32:15–30. Available from: <http://linkinghub.elsevier.com/retrieve/pii/S0165993611003761>
25. Costa TOG, Morales RAV, Brito JP, Gordo M, Pinto AC, Bloch C. Occurrence of bufotenin in the *Osteocephalus* genus (Anura: Hylidae). *Toxicon* [Internet] 2005 [cited 2014 Apr 4];46(4):371–5. Available from: <http://linkinghub.elsevier.com/retrieve/pii/S0041010105000346>
26. Michael C. McBride. *Bufotenine-Toward an Understanding of Possible Psychoactive Mechanisms.pdf*. *J Psychoactive Drugs* [Internet] 2000 [cited 2014 Apr 4];32(3):321–31. Available from: <http://search.proquest.com.ezproxy.bu.edu/docview/207959544/8994DA425A734414PQ/1?accountid=9676>
27. Hussain H, Hussain J, Al-Harrasi A, Green IR. Chemistry and biology of the genus *Voacanga*. *Pharm Biol* [Internet] 2012 [cited 2014 Apr 9];50(9):1183–93. Available from: <http://informahealthcare.com/doi/abs/10.3109/13880209.2012.658478>
28. Leeuwenberg AJM. *Series of revisions of Apocynaceae. XV XV*. Wageningen, the Netherlands: Agricultural University Wageningen, 1985.
29. Saxton JE. Recent progress in the chemistry of indole alkaloids and mould metabolites. *Nat Prod Rep* [Internet] 1989 [cited 2014 Apr 22];6(1):1–54. Available from: <http://pubs.rsc.org/en/content/articlepdf/1989/np/np9890600001>
30. Deshmukh R, Sharma V, Mehan S, Sharma N, Bedi KL. Amelioration of intracerebroventricular streptozotocin induced cognitive dysfunction and oxidative stress by vinpocetine — a PDE1 inhibitor. *Eur J Pharmacol* [Internet] 2009 [cited 2014 Apr 22];620(1-3):49–56. Available from: <http://linkinghub.elsevier.com/retrieve/pii/S0014299909007146>
31. Schiff Jr PL. Ergot and its alkaloids. *Am J Pharm Educ* [Internet] 2006 [cited 2014 Apr 11];70(5). Available from: <http://search.ebscohost.com/login.aspx?direct=true&profile=ehost&scope=site&auth>

ype=crawler&jrnl=00029459&AN=23185534&h=%2By6UfnjPfs9bsxciSj6k5tUFgh  
q78hjEplJyFnN5pI%2BVwyEowqMi4Ei%2Fftl2IFSOz8DMcZp09DFGNGNiHkHp  
xQ%3D%3D&crl=c

32. John K. Brown, Marvin H. Malone. "Legal Highs" - Constituents, Toxicology, and Herbal Folklore. *Clin Toxicol* 1978;12(1):1–31.
33. Klinke HB, Müller IB, Steffenrud S, Dahl-Sørensen R. Two cases of lysergamide intoxication by ingestion of seeds from Hawaiian Baby Woodrose. *Forensic Sci Int* [Internet] 2010 [cited 2014 Apr 23];197(1-3):e1–e5. Available from: <http://linkinghub.elsevier.com/retrieve/pii/S0379073809004745>
34. Nzowa LK, Teponno RB, Tapondjou LA, Verotta L, Liao Z, Graham D, et al. Two new tryptophan derivatives from the seed kernels of *Entada rheedii*: Effects on cell viability and HIV infectivity. *Fitoterapia* [Internet] 2013 [cited 2014 Apr 23];87:37–42. Available from: <http://linkinghub.elsevier.com/retrieve/pii/S0367326X13000749>
35. Dai J, Kardono L, Tsauri S, Padmawinata K, Pezzuto JM, Kinghorn AD. Phenylacetic acid derivatives and a thioamide glycoside from *Entada phaseoloides*. *Phytochemistry* [Internet] 1991 [cited 2014 Apr 23];30(11):3749–52. Available from: <http://www.sciencedirect.com/science/article/pii/0031942291801027>
36. Nzowa LK, Barboni L, Teponno RB, Ricciutelli M, Lupidi G, Quassinti L, et al. Rheediiinosides A and B, two antiproliferative and antioxidant triterpene saponins from *Entada rheedii*. *Phytochemistry* [Internet] 2010 [cited 2014 Apr 23];71(2-3):254–61. Available from: <http://linkinghub.elsevier.com/retrieve/pii/S0031942209004300>
37. Zhao T, Zheng S-S, Zhang B-F, Li Y-Y, Bligh SWA, Wang C-H, et al. Metabolic pathways of the psychotropic-carboline alkaloids, harmaline and harmine, by liquid chromatography/mass spectrometry and NMR spectroscopy. *Food Chem* [Internet] 2012 [cited 2014 Apr 7];134(2):1096–105. Available from: <http://linkinghub.elsevier.com/retrieve/pii/S0308814612004840>
38. Jinous Asgarpanah. Chemistry, pharmacology and medicinal properties of *Peganum harmala* L. *Afr J Pharm Pharmacol* [Internet] 2012 [cited 2014 Apr 15];6(22). Available from: <http://www.academicjournals.org/ajpp/abstracts/abstract%202012/15%20June/Asgarpanah%20and%20Ramezanloo.htm>
39. Kevseroglu K, Sağlam B. Physical and physiological dormancy in black henbane (*Hyoscyamus niger* L.) seeds. *J Plant Biol* [Internet] 2004 [cited 2014 Apr

- 16];47(4):391–5. Available from:  
<http://link.springer.com/article/10.1007/BF03030556>
40. Ramoutsaki IA, Askitopoulou H, Konsolaki E. Pain relief and sedation in Roman Byzantine texts:< i> Mandragoras officinarum</i>,< i> Hyoscyamos niger</i> and< i> Atropa belladonna</i> [Internet]. In: International Congress Series. Elsevier, 2002 [cited 2014 Apr 23]; 43–50. Available from:  
<http://www.sciencedirect.com/science/article/pii/S0531513102006994>
  41. Geis G. In scopolamine veritas. J Crim Criminol [Internet] 1959 [cited 2014 Apr 16];50:347. Available from: [http://heinonlinebackup.com/hol-cgi-bin/get\\_pdf.cgi?handle=hein.journals/jclc50&section=76](http://heinonlinebackup.com/hol-cgi-bin/get_pdf.cgi?handle=hein.journals/jclc50&section=76)
  42. M.K Lee, B. W. H. Cheng, C. T Che, D. P. Hsieh. Cytotoxicity Assessment of Ma-huang (ephedra) under different conditions of preparation.pdf. Toxicol Sci 2000;(56):424–30.
  43. Rothman RB. In Vitro Characterization of Ephedrine-Related Stereoisomers at Biogenic Amine Transporters and the Receptorome Reveals Selective Actions as Norepinephrine Transporter Substrates. J Pharmacol Exp Ther [Internet] 2003 [cited 2014 Apr 16];307(1):138–45. Available from:  
<http://jpet.aspetjournals.org/cgi/doi/10.1124/jpet.103.053975>
  44. Bohn AM, Khodae M, Schwenk TL. Ephedrine and other stimulants as ergogenic aids. Curr Sports Med Rep [Internet] 2003 [cited 2014 Apr 16];2(4):220–5. Available from: <http://www.springerlink.com/index/R53335RT80421376.pdf>
  45. Katzenschlager R. Mucuna pruriens in Parkinson’s disease: a double blind clinical and pharmacological study. J Neurol Neurosurg Psychiatry [Internet] 2004 [cited 2014 Apr 16];75(12):1672–7. Available from:  
<http://jnnp.bmj.com/cgi/doi/10.1136/jnnp.2003.028761>
  46. Bhat R, Sridhar KR, Young C-C, Bhagwath AA, Ganesh S. Composition and functional properties of raw and electron beam-irradiated *Mucuna pruriens* seeds. Int J Food Sci Technol [Internet] 2008 [cited 2014 Apr 16];43(8):1338–51. Available from: <http://doi.wiley.com/10.1111/j.1365-2621.2007.01617.x>
  47. Columbia B. Monoamine oxidase inhibitors in south american hallucinogenic plants: tryptamine and p-carboline constituents of a yahuasca. J Ethnopharmacology [Internet] 1984 [cited 2014 Apr 16];10:195–223. Available from:  
<http://fii.fi.tartu.ee/~helle/kool/AYA/Aya/McKenna1984.pdf>

48. Manyam BV, Dhanasekaran M, Hare TA. Neuroprotective effects of the antiparkinson drug *Mucuna pruriens*. *Phytother Res* [Internet] 2004 [cited 2014 Apr 16];18(9):706–12. Available from: <http://doi.wiley.com/10.1002/ptr.1514>
49. Oliver-Bever B. Medicinal plants in tropical West Africa I. Plants acting on the cardiovascular system. *J Ethnopharmacol* 1982;5(1):1–72.
50. Guízar-González C, Trujillo-Villanueva K, Monforte-González M, Vázquez-Flota F. Sanguinarine and Dihydrosanguinarine Accumulation in *Argemone mexicana* (L) Cell Suspension Cultures Exposed to Yeast Extract. *J Mex Chem Soc* [Internet] 2012 [cited 2014 Apr 8];56(1):19–22. Available from: [http://www.scielo.org.mx/scielo.php?pid=S1870-249X2012000100005&script=sci\\_arttext&tlng=en](http://www.scielo.org.mx/scielo.php?pid=S1870-249X2012000100005&script=sci_arttext&tlng=en)
51. Bhanumathy M, Harish MS, Shivaprasad HN, Sushma G. Nootropic activity of *Celastrus paniculatus* seed. *Pharm Biol* [Internet] 2010 [cited 2014 Apr 16];48(3):324–7. Available from: <http://informahealthcare.com/doi/abs/10.3109/13880200903127391>
52. K. Nalini, K.S. Karanth, A. Rao, A.R. Aroor. Effects of *Celastrus paniculatus* on passive avoidance performance and biogenic amine turnover in albino rats. *J Ethnopharmacol* 1995;47:101–8.
53. A. Russo, A. Izzo, V. Cardile, F. Borrelli, A. Vanella. Indian medicinal plants as antiradicals and DNA cleavage protectors. *Phytochemistry* 2001;8(2):125–32.
54. Ahmad F, Khan RA, Rasheed S. Preliminary screening of methanolic extracts of *Celastrus paniculatus* and *Tecomella undulata* for analgesic and anti-inflammatory activities. *J Ethnopharmacol* [Internet] 1994 [cited 2014 Apr 16];42(3):193–8. Available from: <http://www.sciencedirect.com/science/article/pii/037887419490085X>
55. *Celastrus Paniculatus* - *Celastrus* Seeds [Internet]. *Entheology Preserv. Anc. Sacred Knowl.* [cited 2014 Apr 16]; Available from: <http://www.entheology.org/edoto/anmviewer.asp?a=391>
56. Steiner RR, Larson RL. Validation of the Direct Analysis in Real Time Source for Use in Forensic Drug Screening. *J Forensic Sci* [Internet] 2009 [cited 2012 Apr 18];54(3):617–22. Available from: <http://doi.wiley.com/10.1111/j.1556-4029.2009.01006.x>
57. Chernetsova E, Bochkov P, Zatonskii G, Abramovich R. New approach to detecting counterfeit drugs in tablets by DART mass spectrometry. *Pharm Chem J* [Internet] 2011;45(5):306–8. Available from: <http://dx.doi.org/10.1007/s11094-011-0622-y>

58. Lesiak AD, Musah RA, Domin MA, Shepard JRE. DART-MS as a Preliminary Screening Method for “Herbal Incense”: Chemical Analysis of Synthetic Cannabinoids. *J Forensic Sci* [Internet] 2014 [cited 2014 Apr 17];59(2):337–43. Available from: <http://doi.wiley.com/10.1111/1556-4029.12354>
59. Laramée JA, Durst H., Connell TR, Nilles JM. Detection of Chemical Warfare Agents on Surfaces Relevant to Homeland Security by Direct Analysis in Real-Time Spectrometry. *Am Lab* [Internet] 2008;40:16–20. Available from: <http://www.americanlaboratory.com/913-Technical-Articles/757-Detection-of-Chemical-Warfare-Agents-on-Surfaces-Relevant-to-Homeland-Security-by-Direct-Analysis-in-Real-Time-Spectrometry/>
60. Nilles JM, Connell TR, Durst HD. Quantitation of Chemical Warfare Agents Using the Direct Analysis in Real Time (DART) Technique. *Anal Chem* [Internet] 2009 [cited 2012 Apr 18];81(16):6744–9. Available from: <http://pubs.acs.org/doi/abs/10.1021/ac900682f>
61. Crawford E, Musselman B. Evaluating a direct swabbing method for screening pesticides on fruit and vegetable surfaces using direct analysis in real time (DART) coupled to an Exactive benchtop orbitrap mass spectrometer. *Anal Bioanal Chem* [Internet] 2012 [cited 2014 Apr 17];403(10):2807–12. Available from: <http://link.springer.com/10.1007/s00216-012-5853-6>
62. Schurek J, Vaclavik L, Hooijerink H, Lacina O, Poustka J, Sharman M, et al. Control of Strobilurin Fungicides in Wheat Using Direct Analysis in Real Time Accurate Time-of-Flight and Desorption Electrospray Ionization Linear Ion Trap Mass Spectrometry. *Anal Chem* 2008;80(24):9567–75.
63. Vaclavik L, Cajka T, Hrbek V, Hajslova J. Ambient mass spectrometry employing direct analysis in real time (DART) ion source for olive oil quality and authenticity assessment. *Anal Chim Acta* 2009;645(1-2):56–63.
64. Cody RB, Laramée JA, Durst HD. Versatile New Ion Source for the Analysis of Materials in Open Air under Ambient Conditions. *Anal Chem* 2005;77(8):2297–302.
65. Cody RB. The Observation of Molecular Ions and Analysis of Nonpolar Compounds with the Direct Analysis in Real Time Ion Source. *Anal Chem* 2009;81(3):1101–7.
66. Cody RB. Method of surface ionization with solvent spray and excited-state neutrals [Internet]. 2010 [cited 2014 Apr 17]; Available from: <http://www.google.com/patents/US20120006983>

67. IonSense, Inc. [Internet]. IonSense Inc Prod. 2014 [cited 2014 Apr 17]; Available from: <http://www.ionsense.com/products>
68. Howlett SE, Steiner RR. Validation of Thin Layer Chromatography with AccuTOF-DART™ Detection for Forensic Drug Analysis\*: VALIDATION OF TLC-DART. *J Forensic Sci* [Internet] 2011 [cited 2014 Apr 17];56(5):1261–7. Available from: <http://doi.wiley.com/10.1111/j.1556-4029.2011.01881.x>
69. Tejero R, Rossbach P, Keller B, Anitua E, Reviakine I. Time-of-Flight Secondary Ion Mass Spectrometry with Principal Component Analysis of Titania–Blood Plasma Interfaces. *Langmuir* [Internet] 2013 [cited 2014 Apr 23];29(3):902–12. Available from: <http://pubs.acs.org/doi/abs/10.1021/la303360f>
70. Lehner AF, Craig M, Fannin N, Bush L, Tobin T. Fragmentation patterns of selected ergot alkaloids by electrospray ionization tandem quadrupole mass spectrometry. *J Mass Spectrom* [Internet] 2004 [cited 2014 Mar 24];39(11):1275–86. Available from: <http://doi.wiley.com/10.1002/jms.678>
71. A. Goldblatt, C. Hootlet, J. Pecher. The alkaloids of voacanga thouarsii var obtusa.pdf. *Phytochemistry* 1970;9:1293–8.
72. Ryan Bonfiglio, Richard C. King, Timothy V. Olah, Kara Merkle. The Effects of Sample Preparation Methods on the Variability of the Electrospray Ionization Response for Model Drug Compounds. *Rapid Commun Mass Spectrom* 1999;(13):1175–85.
73. Sterner JL, Johnston MV, Nicol GR, Ridge DP. Signal suppression in electrospray ionization Fourier transform mass spectrometry of multi-component samples. *J Mass Spectrom* [Internet] 2000 [cited 2014 Apr 24];35(3):385–91. Available from: [http://onlinelibrary.wiley.com/doi/10.1002/\(SICI\)1096-9888\(200003\)35:3%3C385::AID-JMS947%3E3.0.CO;2-O/full](http://onlinelibrary.wiley.com/doi/10.1002/(SICI)1096-9888(200003)35:3%3C385::AID-JMS947%3E3.0.CO;2-O/full)
74. Henry Perkin W. CXC.—Harmine and harmaline. Part I. *J Chem Soc Trans* [Internet] 1912 [cited 2014 Apr 22];101:1775–87. Available from: <http://pubs.rsc.org/EN/content/articlepdf/1912/ct/ct9120101775>
75. Verbruggen N, Hermans C. Proline accumulation in plants: a review. *Amino Acids* [Internet] 2008 [cited 2014 Mar 19];35(4):753–9. Available from: <http://link.springer.com/10.1007/s00726-008-0061-6>
76. Schlichtherle-Cerny H, Affolter M, Cerny C. Hydrophilic Interaction Liquid Chromatography Coupled to Electrospray Mass Spectrometry of Small Polar Compounds in Food Analysis. *Anal Chem* [Internet] 2003 [cited 2014 Apr 23];75(10):2349–54. Available from: <http://pubs.acs.org/doi/abs/10.1021/ac026313p>

77. Zhang L, Teng L, Gong C, Liu W, Cheng X, Gu S, et al. Simultaneous determination of harmine, harmaline and their metabolites harmol and harmalol in beagle dog plasma by UPLC–ESI-MS/MS and its application to a pharmacokinetic study. *J Pharm Biomed Anal* [Internet] 2013 [cited 2014 Apr 13];85:162–8. Available from: <http://linkinghub.elsevier.com/retrieve/pii/S0731708513003257>
78. D.J. Tweedie, M.D. Burke. Metabolism of the beta-carbolines, harmine and harmol, by liver microsomes from Phenobarbitone or 3-methylcholanthrene treated mice.pdf. *Drug Metab Dispos* 1987;15(1):74–81.
79. Silverstein RM, Webster FX. *Spectrometric Identification of Organic Compounds*. Sixth. New York: John Wiley & Sons, Ltd., 1998.
80. Igarashi K, Hotta K, Kasuya F, Abe K, Sakoda S. Determination of cabergoline and L-dopa in human plasma using liquid chromatography–tandem mass spectrometry. *J Chromatogr B* [Internet] 2003 [cited 2014 Apr 13];792(1):55–61. Available from: <http://www.sciencedirect.com/science/article/pii/S1570023203002794>
81. Micheal B. Clark, Jr., Joseph A Gardella, Jr. Quantitative Static Secondary Ion Mass Spectrometry of Molecular Ions from 1-B-3-4-Dihydroxyphenylalanine (L-DOPA) and Indolic Derivatives.pdf. *Anal Chem* 1990;62(8):870–5.
82. Kotiaho T, Eberlin MN, Vainiotalo P, Kostianen R. Electrospray mass and tandem mass spectrometry identification of ozone oxidation products of amino acids and small peptides. *J Am Soc Mass Spectrom* [Internet] 2000 [cited 2014 Apr 23];11(6):526–35. Available from: <http://www.sciencedirect.com/science/article/pii/S1044030500001161>
83. Self RL. Direct analysis in real time-mass spectrometry (DART-MS) for rapid qualitative screening of toxic glycols in glycerin-containing products. *J Pharm Biomed Anal* [Internet] 2013 [cited 2014 Jul 17];80:155–8. Available from: <http://linkinghub.elsevier.com/retrieve/pii/S0731708513001052>
84. Ackerman LK, Noonan GO, Begley TH. Assessing direct analysis in real-time-mass spectrometry (DART-MS) for the rapid identification of additives in food packaging. *Food Addit Contam Part A* [Internet] 2009;26(12):1611–8. Available from: <http://dx.doi.org/10.1080/02652030903232753>
85. Steenkamp PA, Harding NM, van Heerden FR, van Wyk B-E. Fatal Datura poisoning: identification of atropine and scopolamine by high performance liquid chromatography/photodiode array/mass spectrometry. *Forensic Sci Int* [Internet] 2004 [cited 2014 Apr 7];145(1):31–9. Available from: <http://linkinghub.elsevier.com/retrieve/pii/S0379073804001719>



## CURRICULUM VITAE

# Crystal Hart

Current Address: 93 Watertown St. Watertown, MA 02472  
Permanent Address: 2130 SW 195<sup>th</sup> Ave. Aloha, OR 97006  
Phone Number: (503) 679-5960  
E-mail Address: hartcr@bu.edu

Place of Birth: Portland, Oregon  
Year of Birth: 1989

### **Education:**

2012 Southern Oregon University Ashland, OR  
**GPA: 3.59**  
Bachelor of Science in Chemistry (Emphasis in Forensics)  
*Anticipated* Boston University School of Medicine Boston, MA  
2014 **Current GPA: 3.68**  
Master of Science in Biomedical Forensic Sciences  
**Thesis: "Rapid Analysis of Plant Based Drugs of Abuse by DART-MS"**  
Advisor: Adam Hall Ph.D., D-ABC

### **Research and Relevant Work Experience:**

2013 – Present Thesis research at *IonSense* in Saugus, MA. Performing research and developing methods for the analysis of plant based drugs of abuse using Direct Analysis in Real Time (DART) attached to an Agilent MSD. Advisor Dr. Adam Hall, Ph.D., D-ABC.

2013 Research intern at *Boston Police Department Latent Print Unit* in Boston, MA. Conducted research on the use of an infrared camera for photographing latent fingerprints in blood on a variety of surfaces. Shadowed analysts in evaluation of evidence in the latent print unit.

2011 Summer research assistant at *U.S. Fish and Wildlife Forensic Laboratory* in Ashland, OR. Performed research under guidance of Dr. Edgard Espinoza and Dr. Michael Scanlan on the chemical characteristics of plastic tipped bullets to create a database for future forensic use. Relied on analyses using Video Spectral Comparator (VSC), X-ray Fluorescence Spectroscopy (XRF), and Attenuated Total Reflectance Fourier Transform Infrared Spectroscopy (ATR-FTIR).

2010 - 2011 Undergraduate research assistant at *Southern Oregon University* in Ashland, OR. Performed research under guidance of Dr. Mary Carrabba into the use of fluorescence spectroscopy as a method of detection for counterfeit pharmaceutical labels and packaging.

### **Publications:**

2012 “Chemical Properties of Selected Plastic-Tipped Bullets” in *Association of Firearm and Toolmark Examiners Journal (AFTE)* January issue.  
The chemical properties of a variety of plastic-tipped bullets were studied and characterized through the use of a video spectral comparator, x-ray fluorescence spectrophotometry, and Fourier transform infrared spectroscopy coupled with discriminate analysis.

### **Presentations:**

2014 Poster entitled “Profiling Beer: Solid Phase Micro-Extraction (SPME) Analysis via Direct Analysis in Real Time HRMS” at ASMS in Baltimore, MD with Joseph LaPointe, Robert Goguen, and Brian Musselman of IonSense, Inc. (Saugus, MA, USA)

2014 Poster entitled “Enabling Direct Sample Analysis of Sorbent-based Microextraction Fibers with DART-MS for Rapid Generation of Unique Chemical Attribute Signatures” at ASMS in Baltimore, MD with Robert Goguen and Brian Musselman of IonSense, Inc. (Saugus, MA, USA)

2013 Presentation entitled “Infrared Photography of Bloody Latent Prints” at the Boston Police Department Latent Print Unit.

2012 Poster presentation entitled “Chemical Properties of Selected Plastic-Tipped Bullets” at Southern Oregon Arts and Research seminar held annually at Southern Oregon University.

### **Professional Conferences:**

2014 Attended the American Academy of Forensic Scientists (AAFS) Conference in Seattle, WA.

2013 Attended the Northeastern Association of Forensic Scientists (NEAFS) Conference in Cromwell, CT.